GEM TN-92-203


# Limited Streamer Drift Tubes for the GEM Muon System

R. Sumner - LeCroy Corp.

R. McNeil, W. Metcalf - Louisianna State University

W. Busza, H. W. Kendall, A. Korytov, J. Kelsey, L. S. Osborne, L. Rosenson, D. Ross, F. E. Taylor, R. Verdier, B. Wadsworth - Massachusetts Institute of Technology

October 2, 1992

Abstract:

A review of the Limited Streamer Drift Tube (LSDT) technology option for the GEM muon system.

# LIMITED STREAMER DRIFT TUBES FOR THE GEM MUON SYSTEM

**LSDT R & D Group**

**R. Sumner**

*LeCroy Corp., Chestnut Ridge, NY*

**R. McNeil, W. Metcalf**

*Louisiana State Univ., Baton Rouge, LA*

**W. Busza, H. W. Kendall, A. Korytov, J. Kelsey, L. S. Osborne, L. Rosenson, D. Ross, F. E. Taylor, R. Verdier, B. Wadsworth**

*Massachusetts Institute of Technology*

*Cambridge, MA*

**We expect that whatever technologies are chosen most of the present GEM muon group will coalesce around the chosen one(s). Many groups have expressed a definite interest in pursuing LSDT's were they selected. Among them:**

**Joint Institute for Nuclear Research, Dubna, Russia**

**Institute of High Energy Physics, Beijing, P. R. China**

**Superconducting Super Collider Lab, Dallas, Texas**

**University of Houston, Houston, Texas**

## Table of Contents

Appendix VII: Hardware implementation of the level 1 trigger

Appendix VIII: Neutron Sensitivity of LSDT Chambers; GEM Note GEM TN-92-122

## The GEM Limited Streamer Drift Tube Muon System

### I. Description of chamber and its operation

### A. Desiderata

The GEM muon system must cover over $10^4$ $m^2$ of sensitive area and yet must measure sagittas in muon trajectories which can be as low as hundreds of microns. We list here some of the major desiderata that any such system should be:

1.) Fast; events must be related to their proper collision bunch. A drift system such as we propose should keep delays well below the microsecond level.

2.) Accurate; the per wire measuring error should be kept to 100 $\mu$m or better.

3.) Able to measure longitudinal position; this measurement must be in the cm range, 1) for particle mass reconstruction, 2) to disentangle multiple particle outputs from the layers after the calorimeter.

4.) Robust; it must be relatively insensitive to electronic and particle noise. Residual neutrons from the calorimeter are an example of the latter.

5.) Locatable to 25 $\mu$m's; the wires must be spatially referenced to this accuracy independent of external conditions such as temperature variations, magnet on/off, wire tension variations, etc.

6.) Usable with non-flammable gas; though at this time a flammable gas has not been arbitrarily excluded, prudence would indicate that it will eventually be found too dangerous.

7.) Ammenable to mass production; this not only keeps costs down but will give rise to uniformity of product.

8.) Minimal in material; this is particularly important for the middle superlayer where multiple scattering can contribute to the momentum measurement error. Should be <10% rad. lengths.

9.) Minimally sensitive to backgrounds such as gamma rays and neutrons.

## B. Principle of operation

We have selected a technology based on a drift tube system operating in the streamer mode. This mode of operation has been used widely in many contemporary detectors, SLD, Aleph, Delphi, etc.[1-4]. It has the merit of giving pulses of large amplitude (~100mV) and fast rise time (~10 nsecs); both properties result in a small time jitter in measuring drift times. A further merit is obtained by streamer initiation on first electron arrival; this results in about a factor of 2 better time measurement over proportional mode operation[5]. These properties respond to items 1, 2, and 4 above. A demerit to the system comes from the higher avalanche gains which can result in faster degradation of tube operation; this latter is much dependent on the gas being used and will be discussed later.

As in the applications mentioned above, the open cathode tubes allow the placement of pick-up strips facing the wires thereby allowing a measurement of streamer longitudinal position along the wire. We make use of this feature by having pick-up strips perpendicular to the wire. The time correlation with the wire pulse allows an unambiguous x-y measurement of each streamer (item 3).

Several gas mixtures, including non-flammable ones, are available to operate in this limited streamer drift tube mode (LSDT). See item 5.

## C. Mechanical description

We wish to make use of the general manufacturing technology used in previous large systems[1-4]. This calls for manufacturing multiple tubes in layers and multiple layers in each gas box. Our basic detector unit has 4 staggered layers of tubes. The gas box varies in width between 0.7 m and 1.2 m in width and 3.7 m and 7.65 m in length. to fit the dimensions called for in each superlayer. We are making the cathode tube layers as complete units; the prototype chambers have such layers made from 10 mil Al. Similar constuction is envisaged for the final system although a simpler and/or cheaper

manufacturing method may be found in the future. Note that the positional tolerances for the cathodes is not critical($\pm$ 0.5 mm, typical).

The positioning of the wires is critical. The wires are supported by Mycalex bridges that have been grooved accurately to receive the wires; the bridges are, in turn, accurately positioned to an outside reference point. Details of this are related in Sect. X.III.A below.

## II. Laser and Fermilab tests

We have made various test of our proposed technique; the detailed description and results have been, or will be published[6,7,8,10,11]. We summarize these:

1.) An aluminum tube, 2.5 cm x 2.5 cm in cross section with a central 100 $\mu$m wire was made with a slit window on two opposing sides to allow passage of a laser beam. The laser beam intensity was adjusted to give ionization density comparable to a minimum ionizing particle. The laser beam could be moved with respect to the wire. In this way we could obtain both distance vs. drift time curves for each gas used and each high voltage and, also, a measure of the spatial resolution. The latter gives the contribution to measuring error from electron diffusion and electronic jitter. The results are summarized in Table X.1. This setup was also used to measure the tube behaviour in a magnetic field.

2.) A 0.5 m long prototype chamber was made of four layers, each of four channels of 2.5 cm square aluminum tubes; a schematic cross section is shown in Fig. 1. In addition, a layer of pick-up strips, orthogonal to the wire direction was placed over one layer to allow an x-y measurement of the pulses. The correlation could be done unambiguously by matching pulse times on wire and strip. The chamber was exposed to 0.5 TeV muons in the Fermilab E665 beam. By fitting muon tracks to the four point measured tracks we obtained the effective single wire measuring resolution; this is listed in Table

X.1. Details of the results can be found in references 6 and 7.

In the same 0.5 Tev beam we placed various materials in front of our chamber to examine the muon induced shower production and to find the degree to which this disrupts the finding of the muon track. Details of the results can be found in reference 8. We can summarize our findings grossly by stating the reduction of track finding efficiency from ~7% to ~17% with insertion of 10 cm of Pb.

3.) We studied another technology suggested by a Dubna group[9] based on charge interpolation using cathode strips. The apparatus is described in this reference. This technology is essentially the same as later suggested by the CSC GEM group for use as the muon detector in the end cap region. Details of our results are published in references 6 and 7; a summary of these is shown in Table X.2.

4. We also studied the behaviour of small tubes, as in item 1.) above, again illuminated with a laser beam but operating in a magnetic field. The details of our results can be found in reference 10. A summary of these results is shown in Table X.1. Essentially both resolution and drift times are little affected by the field, whether parallel or perpendicular to the wire.

5. A demerit of operation in the streamer mode is that the large amplification in the streamer avalanche gives rise to UV radiation which can reach the tube walls in spite of the quenching gases used giving rise to secondary electrons which, in turn, give a second pulse. This second pulse is recognizable since it occurs at the drift time from wall to wire after the first pulse.

   We have made tubes with different coatings on the inside wall; namely Al, Al with carbon coating, Ni, Cu, and Ag. We measure the number and pulse height distribution of these secondary pulses as a function of this coating, the high voltage, and the gas composition. Our results can be found in refernce 11. In summary, we found, as expected, that the secondary pulse probability increased with high voltage i.e. with

avalanche gain. It was greater with Isobutane, $CO_2$, and $CF_4$, in that order. It was relatively independent of the metallic coatings we tried- Al, Cu, Ni, and Ag. However, we found that a carbon coating considerably suppresed the secondary pulses. The reason for this is still unclear; the work function for carbon is not much different from those of the metals. We are continuing to investigate this.

## III. Tecnology Evaluations

Looking at the results of our measurements at Fermilab as shown in Tables I and II it appears that one gets comparable resolutions from either drift or strip system. One may ask, then, why we pursued the drift system. The answer lies in our assurances with respect to the drift system with only the mechanical wire placement accuracy to consider; however, we felt, given modern mechanical technologies, that this would not be a problem. On the other hand we had the following worries about a strip system:

1.) Measuring to 100 $\mu$m with 1 cm strips requires a 1% measurement.
   a.) Superb amplifiers would be needed on a mass scale.
   b.) Very accurately made strips with accurate placement in large areas would be required.
2.) Thermal noise requires long ($\sim$ 1 $\mu$sec) integrating times.
3.) Thermal noise places upper limits on the size of the strips and, therefore, the chambers.
   a.) Needs many small chambers.
   b.) Needs large number of electronics channels.
4.) Man made noise will be present to some extent; this will not be known quantitatively until turn on day.

In view of these worries we elected to pursue the more assured route, namely, a drift system. A more thorough and quantitative analysis comparing the two systems is done in Appendix II.

## IV. Full chamber

## A. Design

A cross sectional view of a full sized chamber is shown in Figure 2. The chambers are supported and their positions monitored at the points along their length where the bridges holding the wires in place are located. An L-shaped strong back will fasten to the support structure; the position monitor (presumed, at this time to be an optical alignment method) is located in the holes provided on the upright of the strong back; a second hole is provided on the other end of the horizontal bar for vertical monitoring of the other side. The slot against which the ends of the wire bridges are mounted are precision machined with respect to the optical hole; the upright part of the L which bears the optical hole has been welded to the side wall before the machining. We have, then, only one transfer surface. The grooves in the bridge which hold the wires are precision machined with respect to the reference edge of the bridge. We have tested the machining capabilities of a CNC on a Mycalex bridge and find that it can locate the grooves in absolute position to less than 10 $\mu$m's.

The other side of the bridge is held by a slip pin which controls the height of the bridge (less tolerance required ($\pm 150\mu$m's) but is not constrained by any "breathing" of the Al box. The bridges are not in contact with the cathodes, and suffer bending only under their own weight. This would be excessive in a 1 meter span; a central post is provided to eliminate this sag.

The cathodes are stacked in four layers resting ultimately on the Hexcel bottom. The cathode placement is not critical. The present method for making the cathode planes involves attaching L-shaped beams of 10 mil Al to a substrate of 10 mil Al with thermosetting films. The result is a layer of U-shaped tubes, which, when covered with the next layer on top give our required layer of square cross section cathodes with minimal material.

The space over the fourth layer contains the pick-up strip plane for measurements in the longitudinal direction.

With our design the seperation distance between bridges may be selected. We have chosen to place them at such a seperation that the droop under gravity is always below the desired measuring error rather than trust in making a correction for this, assuming the tension is as planned. This does require more bridges and more optical alignment points and thereby more cost. If one wishes to relax this requirement it can, of course, be done.

Summing all the material in the chamber, excluding the sides, a particle traverses 6.4% of a radiation length.

**B. Tests**

We have built a 1.0x4.0 $m^2$ chamber. The purpose was to confront some of the mechanical, electrical, gas handling, and software problems; it was not built with the ultimate mechanical precision required. We have taken cosmic ray data and analyzed it. A cosmic ray event is shown in Fig. 3.; the radius of the circles shown around each wire represent the calculated distance of the closest ionization. The wires are connected to one another with short delay lines in pairs at the end opposite the electronics. By measuring time differences in each pair one may get a coarse ($\pm$ 15 cm) measure of the longitudinal position of the track along the wire. The figure shows both the direct pulse and its delayed counterpart on the adjacent wire. Shown also is a straight line fit made to the direct pulses.

Finally, we have taken data with this full scale chamber. A cosmic ray telescope was placed over and under the chamber with 10 cm of lead filtering. Straight line fits were made to the tracks so detected. From these fits we computed the residuals a single wire would have to give these results. A distribution in these residuals is shown in Figures 4 and 5. The first is for a $CO_2$ based gas and the second is for a 1 to 3, Argon-Isobutane mixture. The rms widths of these distributions are 108 $\mu$m and 69 $\mu$m, respectively. We have left tests with the $CF_4$ based gas to residence at the SSCLab TTR; we would expect it to be intermediate between the two gases above.

**C. Electronics**

The electronics for the chambers is described in greater detail in Appendix III of this report. It is a straight forward application of, and improvement over present day techniques. We use, at present, a discriminator based on the LeCroy MVL407 and a multichannel TDC Camac module, LeCroy 2277. A block diagram of the future electronics for one channel is shown in Figure A.III.1.

We have devised and tested a system which would use the LSDT chambers in a level 1 trigger. This system is described and the results of its tryout given in Appendix IV. We simply state that it appears quite feasible and works.

## V. Full system

### A. Layout in GEM detector

The layout of the chambers in the GEM detctor is shown in Figures 5 (side view) and 6 (end view). We have assumed the 8-8-4 configuration for measurement number in successive layers. It appears prudent to keep the full 8 layers in the chambers just outside the calorimeter in view of the particle disentanglement which will probably be necessary to find the muon track within the punch thorough and shower tracks expected at this point.

The chambers have been overlapped wherever possible to maximize efficiency for getting at least some measurement on every track. In order to get inter-sector overlap we propose splitting the central layer between its two component chambers. Alternate sectors have small-large then large-small two chamber layers in width. A structural plate must be placed at both z-ends of the sector and, at least, one penetration in between. A similar structure has been analyzed at Draper for rigidity with two such penetrations for the PDT scheme. It remains to be seen whether we one plate is sufficient. If not, we would have to trisect the middle layer in z. We would probably bring the electronics feed through a bulkhead at the top and bottom of the chambers rather than at the end (as done in the prototypes) to minimize dead space; this is always possible with no more than 2 chambers

to a superlayer. This would occur at the inner junction between two chambers so that the outter, particle sensitve, ends would extend as far as possible.

### B. Inventory of chambers

Table X.3 gives an inventory of the chambers with dimensions and number of wires and bridges. The totals for the whole system is also shown.

### C. Outline of manufacture

1. Parts procurement

The philosophy behind the LSDT chamber design is that the parts, from which the chambers are assembled and which represent a fair fraction of the cost, are based on a common technology. In this way we can expect the benefits from competitive bidding, common technology, and multiple sources were production times a problem. The work is also accessible to foreign participation though much of it depends on modern machining tecnology i.e. the availability of a CNC machine.

The one technology which is unusual is the production of thin cathode planes. This is being done for our prototype chambers at Lincoln Laboratory of MIT. They have also taken on the responsibility of locating outside manufacturers who are capable of, and interested in, mass producing such cathode planes. It is from these that we also get cost estimates for the work.

2. Wiring factory

Ultimately the parts must be brought together, the wires strung, and the finished chambers tested. We have had experience in this; the MIT Counter, Spark Chamber group which forms part of the GEM LSDT group operated the factory which built the modules for the SLD WIC system. It required laying down a comparable number of wires as required here ($\sim 10^5$). We have also had the help of R. Weinstein of the U. of Houston who operates a factory for making Iarocci tubes (SCARF)[4]. Our projected factory makes use of this experience. In order to explain and estimate times and cost we have broken down the steps in the manufacture and testing of chambers; this is illustrated in Fig. 7.

We wish to make as much use of mass production methods as possible both to minimize costs and to assure a more homogeneous product. Thus, a fair fraction of the total effort is placed into designing and building specialized apparatus for wiring, soldering, checking, and testing the chambers. The details of all this can be found in the back-up material submitted with our cost analysis[13].

## VI. Costing of full system

The detailed costing of this proposed system is covered in another section of this report, Appendix V. We can summarize the total costs by breaking them down into the following 6 categories coresponding to the 6 "worksheets" found in that Appendix. The figures are in k$'s.

| Title | Material | Labor | Contingency |
|---|---|---|---|
| Shipping | 153 | 65 | 30% |
| Test | 360 | 689 | 30% |
| Assembly | 443 | 2931 | 30% |
| Factory prep. | 370 | 464 | 23% |
| Machining | 15514* | 3303 | 30% |
| Final design | 20 | 349 | 30% |
| Total | 16860 | 7801 | |

* this number is probably 4000 k$'s too high due to a misunderstanding on the part of the estimator. See Appendix I.

## VII. Performance

### A. Meeting the specifications

We list here some of the specifications which we have high lighted to be used in evaluating the technologies within the GEM muon group and the degree to which they are met

by this LSDT system.

1.) Alignment-chamber: This depends first on the alignment system. For transfer from this system to the wire bridge we expect $< 25\mu$m's.

2.) Alignment-wires: $< 25$ $\mu$m's.

3.) Single layer resolution: $< 100$ $\mu$m's and random. Could be $< 60$ $\mu$m's with Argon-Isobutane.

4.) Dead time per wire: determined by pulse duration, 100 nsec.

5.) Track measurement efficiency per layer: 96%. Loss is due to delta ray production. The efficiency for finding a vector in our 4 layer chamber-getting 3 out of 4 hits- is 98%.

6.) 2D capability: available (the wire and z-strips are time correlated).

7.) Temperature stability: 1 meter of Mycalex expands 10 $\mu$m's per $^{o}$C.

8.) Noise sensitivity: little-time measurements and the large streamer pulses are relatively immune to noise.

9.) Sensitivity to gas parameters: gas mixture, pressure, and temperature must be monitored.

10.) Safety: The use of Isobutane above the flammability point, 10%, is problematic. However, we can use non-flammable gases though these give poorer resolutions. In any case, the chambers would be run at low pressures ($\sim$ 0.5" of water).

11.) Multiple scattering probability: each 4 layer chamber presents 6.4% of a radiation length.

**B. Backgrounds**

1.) Punch through

The punch through rates have been calculated[14]. The main problem occurs when a muon is associated with a hadronic jet. These processes have been simulated. The results indicate that a minimum calorimeter thickness of 12 interaction lengths should be

used, that the first muon superlayer should have a full 8 measuring layers, and that a 2D measurement on tracks in this layer is desirable.

2.) Neutrons

The sensitivity of our tubes to neutrons has been measured and is reported in reference 15. This was measured both in the direct neutron spectrum from a $Cf^{252}$ source and the moderated spectrum after 30 cm of Boron loaded polyethylene. The "efficiency" was $5.2 \times 10^{-3}$ and $2.5 \times 10^{-3}$ per incident neutron respectively with an uncertainty of 50%. Roughly half of this arose from a conversion source which was not the gas; it is thought to be some deposit on the inside wall of the tube from insufficient cleaning or condensate from the flowing gas. If we take the neutron flux from the middle barrel region at 4 meters[12] , $.0115 \times 10^{12}$/n/SSC year (a moderated flux), we would get a typical counting rate of $\sim$ 1.8 kHz/wire with no moderator after the calorimeter and, possibly, a factor of ten less with a moderator. With no moderator this also amounts to $2.5 \times 10^{-3}$ Coulombs per cm of wire per year. One Coulomb per cm of wire is considered to be a danger point if no additives are added to the gas.

The above neutron rate estimate seems reassuring but certain cautions must be expressed. The neutron fluxes at smaller angles are larger; one must make sure that these larger fluxes do not rattle around in the magnet and affect the central angles. The neutron flux calculations should be refined beyond doubts. One must make sure that extra-calorimeter sources, e.g. the accelerator, do not contribute.

3.) Muon generated showers.

During the Fermilab tests (see Sect. II) we investigated the E-M showers produced by muons by measuring the track proliferation in our chambers produced by Pb in front of the chambers. The results were checked against a Monte Carlo simulation with reasonable agreement[14]. An extrapolation of these measurements with the Monte Carlo allows an estimate of track loss (not found); this is 3% for an 8-8-4 muon system but 9% for a 4-8-4 system.

## C. Robustness

1. Mechanical

The chamber (1x4 meter) is mechanically robust, to use that word in its true sense. When supported at its two 4 meter ends it sags less than 25 $\mu$m along its 1 meter dimension and 1/8 inch along its 16 cm dimension. It can be, and has been, rotated onto its edge; it survived a trip from Cambridge to Dallas without wire loss.

2. Wire loss

A wire break results in the loss of only one tube, a fractional solid angle of $2.5 \times 10^{-4}$. Naturally, this does not deaden that solid angle since each chamber has 4 layers of tubes.

3. Wire aging

see Sect. VII.B.@

## Summary

We feel that we have met the baseline requirements for the GEM muon system with our proposal for use of LSDT's. A full scale prototype has been built and tested and found to give the desired wire resolution, including bridge displacements, as well as measuring resolution. We have estimated costs in a relatively conservative way and find that a full scale system can be built within the expected guidelines. In addition, we have devised a level 1 triggering system and tested it on our chamber; it works satisfactorally as we expected. Such a triggering system would be needed were the RPC system not found acceptable or were one to desire the economies of having only one technology in the muon barrel.

We feel that the LSDT system has fewer questionable aspects over other technologies. Whatever system picked must be able to guarantee success, particularly if it finds itself in competition for funds over other detectors.

## References


1.) A. C. Benvenuti et al. "The Iron Calorimeter and Muon Identifier for SLD", SLAC-PUB-4677, July 1988; NIM **A276**, 94 (1989); NIM **A290**, 353 (1990); NIM **A289**, 463 (1990).

2.) Aleph Technical Report 1983, CERN/LEPC/83-2; LEPC/PI 15 May, 1983.

3.) Delphi Technical Proposal CERN/LEPC 83-3 (1983); NIM **A273** (1988) 841.

4.) K. Lau et al, NIM **A306**, 397 (1991); D. Hungerford et al, NIM **A286**, 155 (1990).

5.) A. H. Walenta, Proceedings of Summer Institute on Particle Physics, SLAC Report, July 1983.

6.) Yu. Bonyushkin et al., NIM **A315**, 55 (1992).

7.) Yu. Bonyushkin et al. (Toroidal Spectrometer Group), SSC Detector R & D Program, Progress Report No. 218, Sept. 1991.

8.) Studies of shower production with from muons passing through Pb, A. Korytov, private communication.

9.) G. Alekseev et al., "The Strip Readout for the EMPACT Muon System", EMPACT/TEXAS Note 242 (1990); Yu. Bonyshkin et al., "Readout for EMPACT Muon System Detectors: Strip Readout Studies", EMPACT/TEXAS Note 327 (1990).

10.) A. Korytov et al. "Studies of LSDT's in a Magnetic Field", GEM Note TN-92-123.

11.) A. Korytov et al, "Studies of Cathode Material for the LSDT", GEM Note TN-92-121.

12.) D. M. Lee, R. E. Prael, L. Waters, GEM Note TN-92-91; L. Waters, private communication.

13.) Cost analysis of the factory. See Appendix VI.

14.) R. McNeil, GEM Note Note TN-92-118.

15.) A. Korytov et al, "Neutron Sensitivity of LSDT Chambers", GEM Note TN-92-122.

## Figures

Fig. 1 A cross-sectional view of the prototype chamber used in the Fermilab tests.

Fig. 2 Cross sectional view of a typical full sized chamber

Fig. 3 Cosmic ray event from a 0.5 m x 4.0 m prototype chamber

Fig. 4 The distribution in effective single wire residuals from fits to cosmic ray tracks in the 1x4 meter chamber using a $CO_2$ based gas in the chamber. The spread includes errors in wire alignment and thus is an overall $\sigma$ for the chamber.

Fig. 5 The same as Fig. 4 but with a 1 to 3 mixture of Argon-Isobutane gas in the chamber.

Fig. 6 Chamber layout in the GEM detector;side view

Fig. 7 Chamber layout in the GEM detector ;end view

Fig. 8 Block diagram of the assembly procedure in the chamber factory

| Table X.1: Resolution* and $T_{max}$ for Drift Readout in 2.5 cm. cells | | | | | | | | |
|---|---|---|---|---|---|---|---|---|
| Gas⟶ | A-IB 25 – 75 | | A-IB-$CO_2$ 2.5 – 9.5 – 88 | | $CO_2$ – $CF_4$ – IB 20 – 69 – 11 | | $CO_2$ – $CF_4$ – IB 40 – 50 – 10 | |
| Ioniz. Source ↓ | $\sigma$ ($\mu m$) | $T_{max}$ (n sec) | $\sigma$ ($\mu m$) | $T_{max}$ (n sec) | $\sigma$ ($\mu m$) | $T_{max}$ (n sec) | $\sigma$ ($\mu m$) | $T_{max}$ (n sec) |
| Laser-no mag. field | 35 | 260 | 55 | 830 | 70 | 280 | 70 | 460 |
| Laser- mag. field(0.8 T) | 45 | 278 | 60 | 835 | 75 | 295 | | |
| 0.5 TeV Muons | 55 | | | | 95 | | 75 | |

* Averaged over all drift times

| Table X.2: Resolution* for Pick-up Strip Readout ( 1.0 cm. strips) | | |
|---|---|---|
| GasAmpl.Mode ⟶ Ioniz.Source ↓ | Proportional | Limited Streamer |
| Laser | 45 $\mu$m | 100 $\mu$m |
| 0.5 TeV Muons | 85 $\mu$m | |

* Averaged over all ionization positions

## Table X.3 Chamber Inventory: GEM LSTD System

for 8-8-4 system, 16 sectors

### Barrel

| Layer | r(m) | l(m) | w(m) | chmbrs. /sect | total chmbrs | wgt/sect (lbs.) | vol/sect litres | wires /chmbr | bridges /chmbr |
|---|---|---|---|---|---|---|---|---|---|
| 1A1a | 4.1 | 3.80 | 0.70 | 1 | 32 | 236 | 307 | 112 | 12 |
| 1A1b | 4.1 | 3.80 | 0.80 | 1 | 32 | 254 | 358 | 128 | 12 |
| 1A2a | 4.1 | 3.80 | 0.70 | 1 | 32 | 236 | 307 | 112 | 12 |
| 1A2b | 4.1 | 3.80 | 0.80 | 1 | 32 | 254 | 358 | 128 | 12 |
| 1B1a | 4.3 | 3.70 | 0.80 | 1 | 32 | 249 | 350 | 128 | 12 |
| 1B1b | 4.3 | 3.70 | 0.75 | 1 | 32 | 240 | 325 | 120 | 12 |
| 1B2a | 4.3 | 4.30 | 0.80 | 1 | 32 | 278 | 400 | 128 | 12 |
| 1B2b | 4.3 | 4.30 | 0.75 | 1 | 32 | 372 | 372 | 120 | 12 |
| 2A1a | 6.0 | 5.60 | 1.15 | 1 | 32 | 439 | 764 | 184 | 16 |
| 2A1b | 6.0 | 5.60 | 1.00 | 1 | 32 | 402 | 655 | 160 | 16 |
| 2A2a | 6.0 | 5.60 | 1.15 | 1 | 32 | 439 | 764 | 184 | 16 |
| 2A2b | 6.0 | 5.60 | 1.00 | 1 | 32 | 402 | 655 | 160 | 16 |
| 2B1a | 6.2 | 5.40 | 1.00 | 1 | 32 | 392 | 634 | 160 | 16 |
| 2B1b | 6.2 | 5.40 | 1.20 | 1 | 32 | 440 | 774 | 192 | 16 |
| 2B2a | 6.2 | 5.90 | 1.00 | 1 | 32 | 417 | 688 | 160 | 16 |
| 2B2b | 6.2 | 5.90 | 1.20 | 1 | 32 | 468 | 840 | 192 | 16 |
| 3A1 | 7.9 | 7.45 | 1.10 | 2 | 64 | 1091 | 1900 | 176 | 20 |
| 3A2 | 7.9 | 7.45 | 1.10 | 2 | 64 | 1091 | 1900 | 176 | 20 |
| 3B1 | 8.2 | 7.25 | 1.10 | 1 | 32 | 535 | 926 | 176 | 20 |
| 3B2 | 8.2 | 7.65 | 1.10 | 1 | 32 | 556 | 974 | 176 | 20 |
| Sect Totals | | | | 22 | | 8689 | 14,251 | 3,424 | 344 |
| Gnd Totals | | | | | 704 | 278,062 | 456,032 | 109,568 | 11,008 |

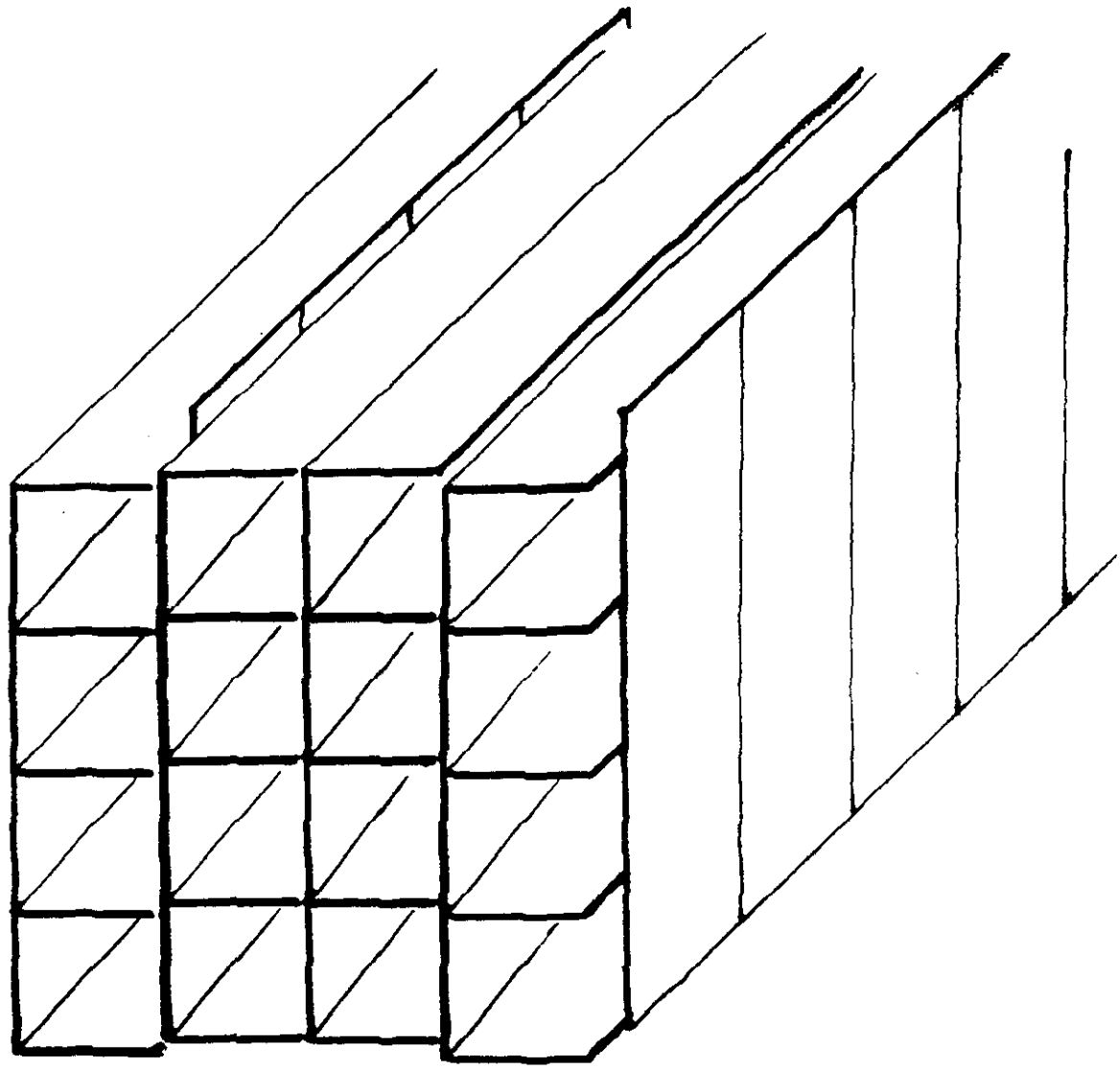


# Fermilab Muon Telescope

Fig. . 1 A cross-sectional view of the prototype chamber used in the Fermilab tests.

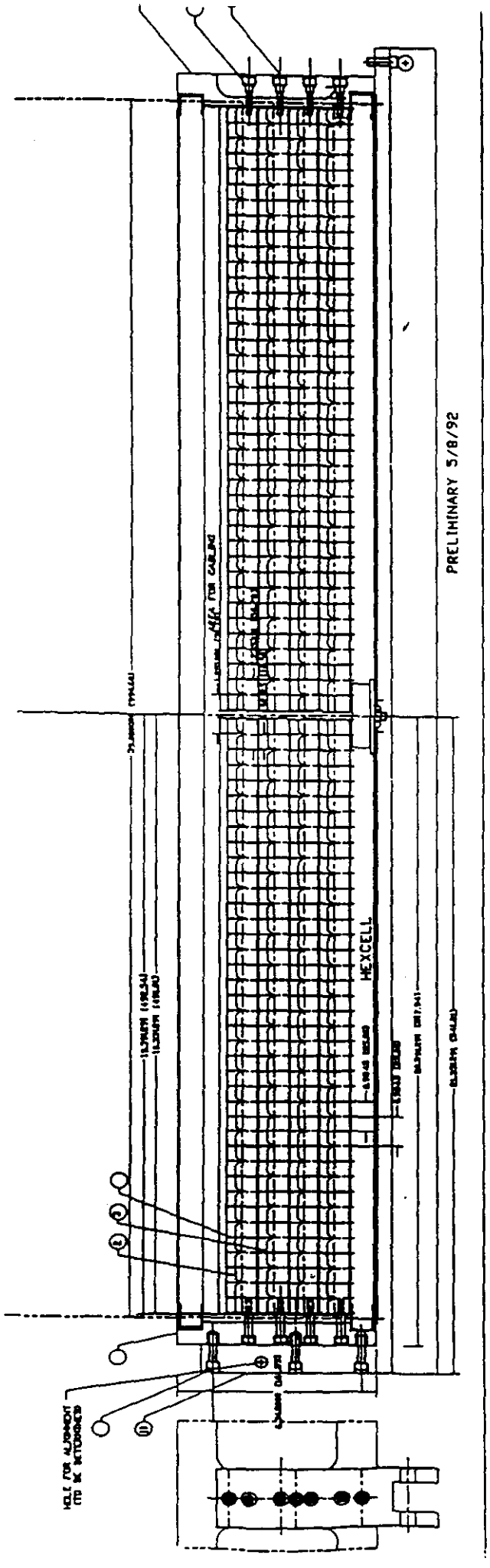


Fig. 2 Cross sectional view of a typical full sized chamber

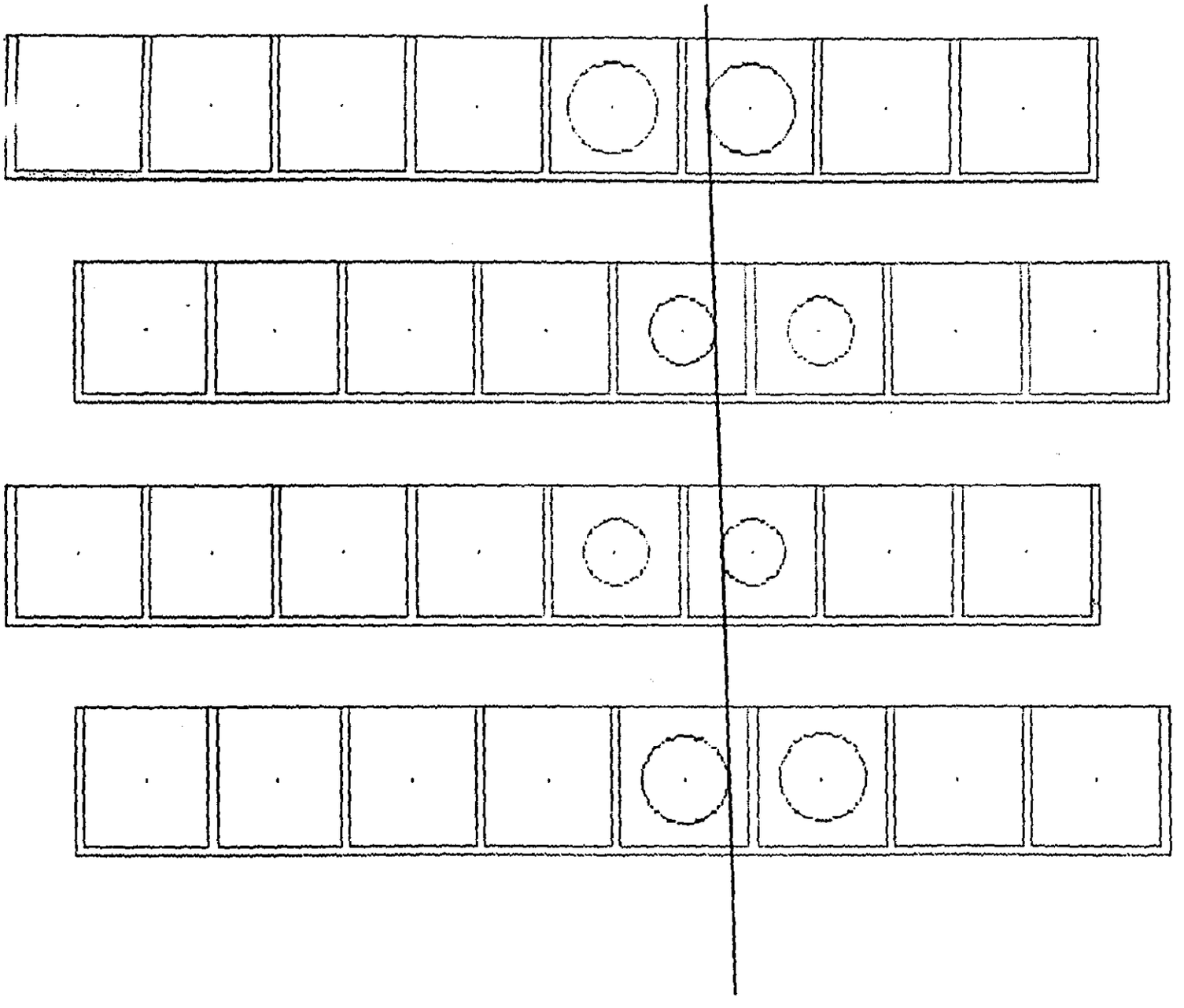

Fig. 3 Cosmic ray event from a 0.5 m x 4.0 m prototype chamber

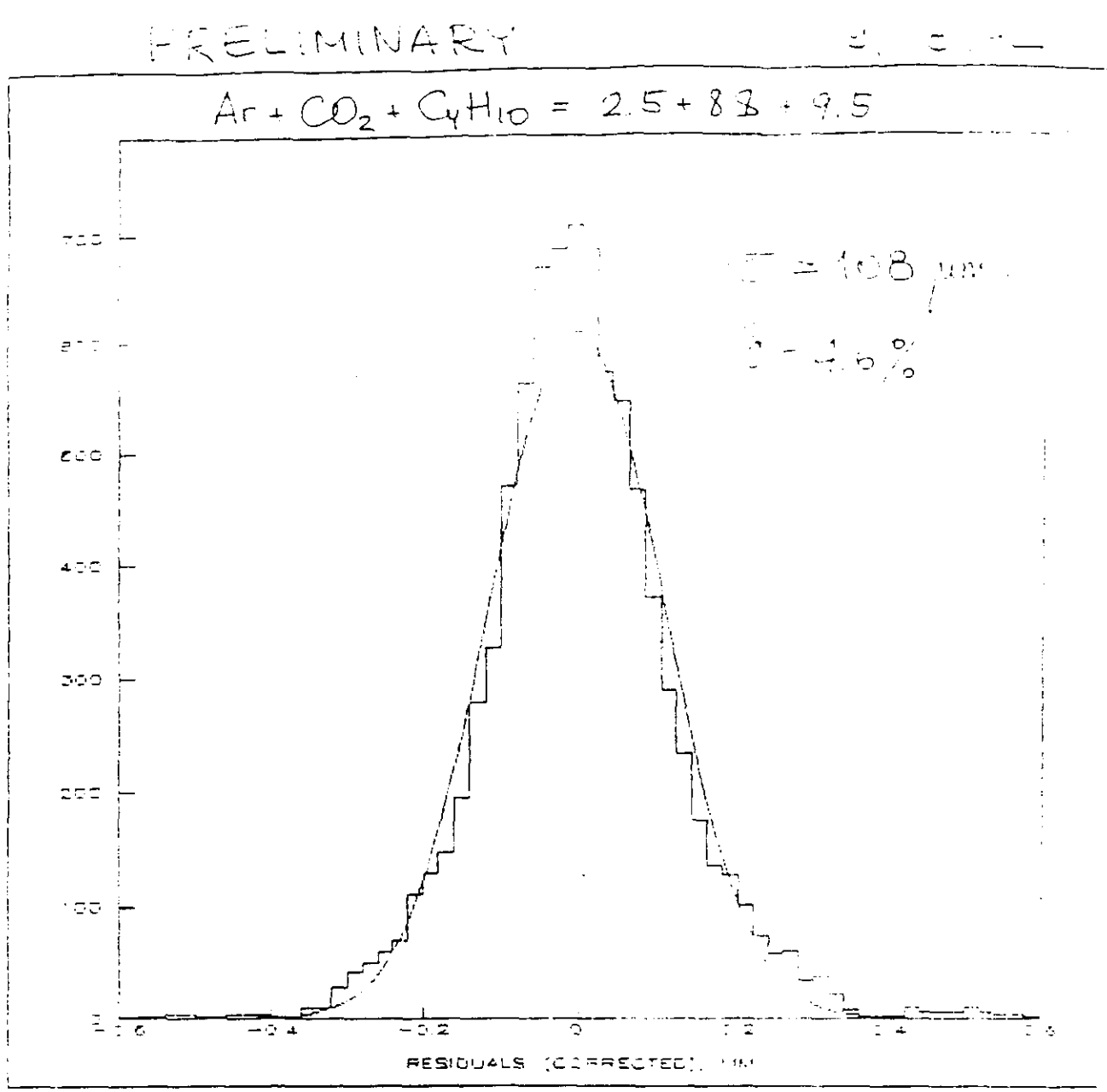


Fig. 4 The distribution in effective single wire residuals from fits to cosmic ray tracks in the 1x4 meter chamber using a $CO_2$ based gas in the chamber. The spread includes errors in wire alignment and thus is an overall $\sigma$ for the chamber.

$\pm 3$ $|\alpha| \leq 5^\circ$ $\sigma = 108\ \mu m$

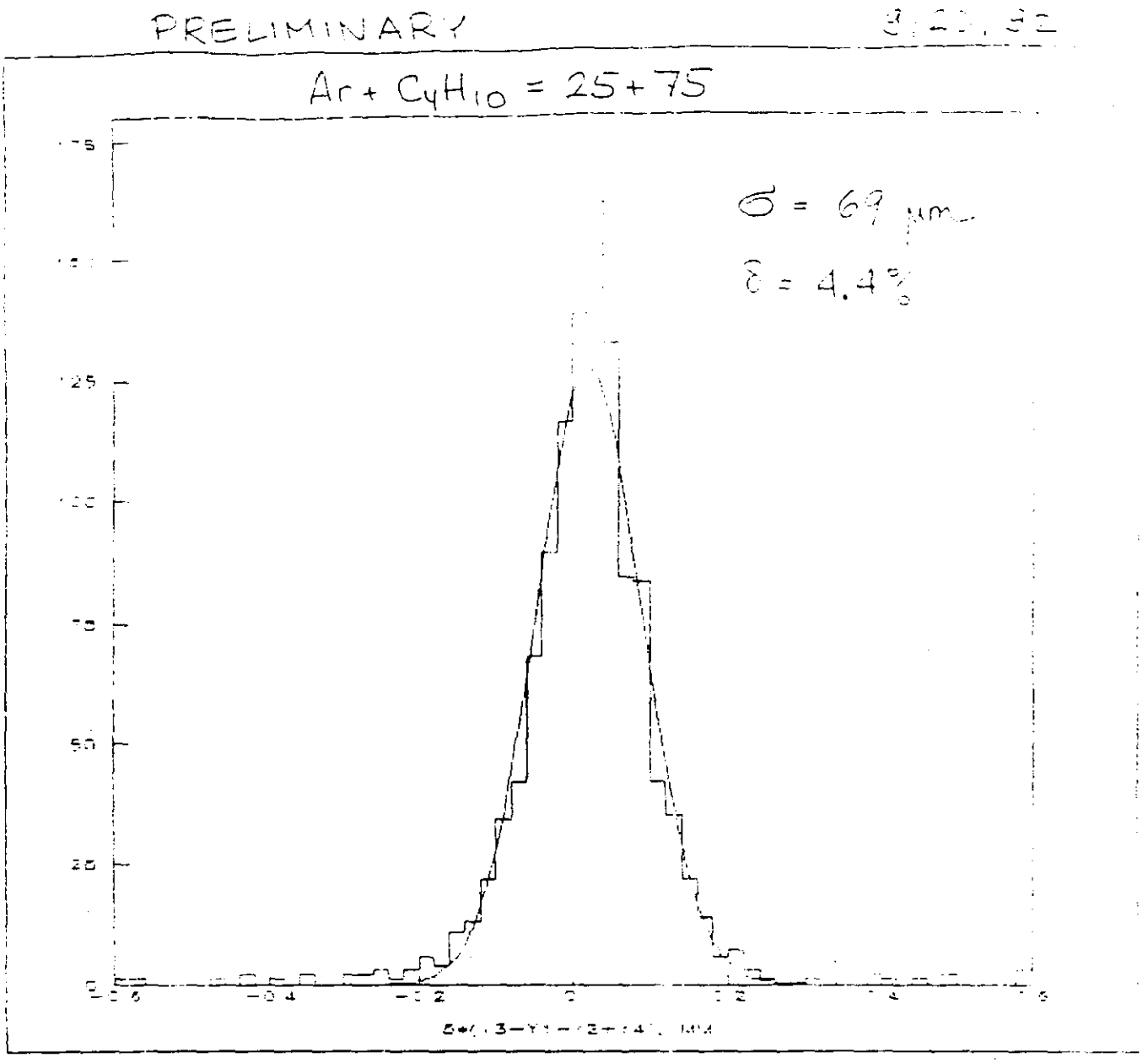


Fig. 5 The same as Fig. 4 but with a 1 to 3 mixture of Argon-Isobutane gas in the chamber.

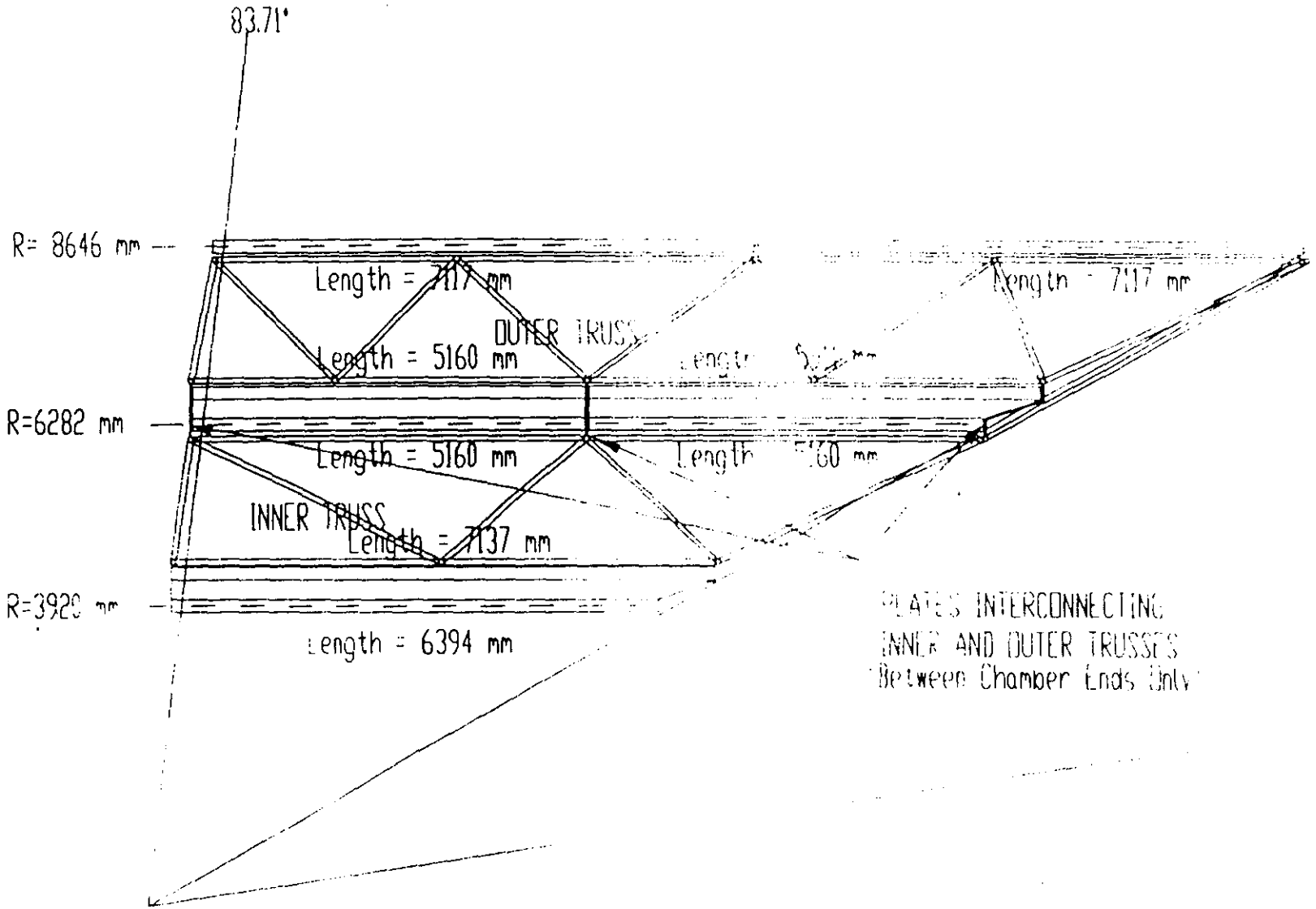


Fig. 6 Chamber layout in the GEM detector;side view

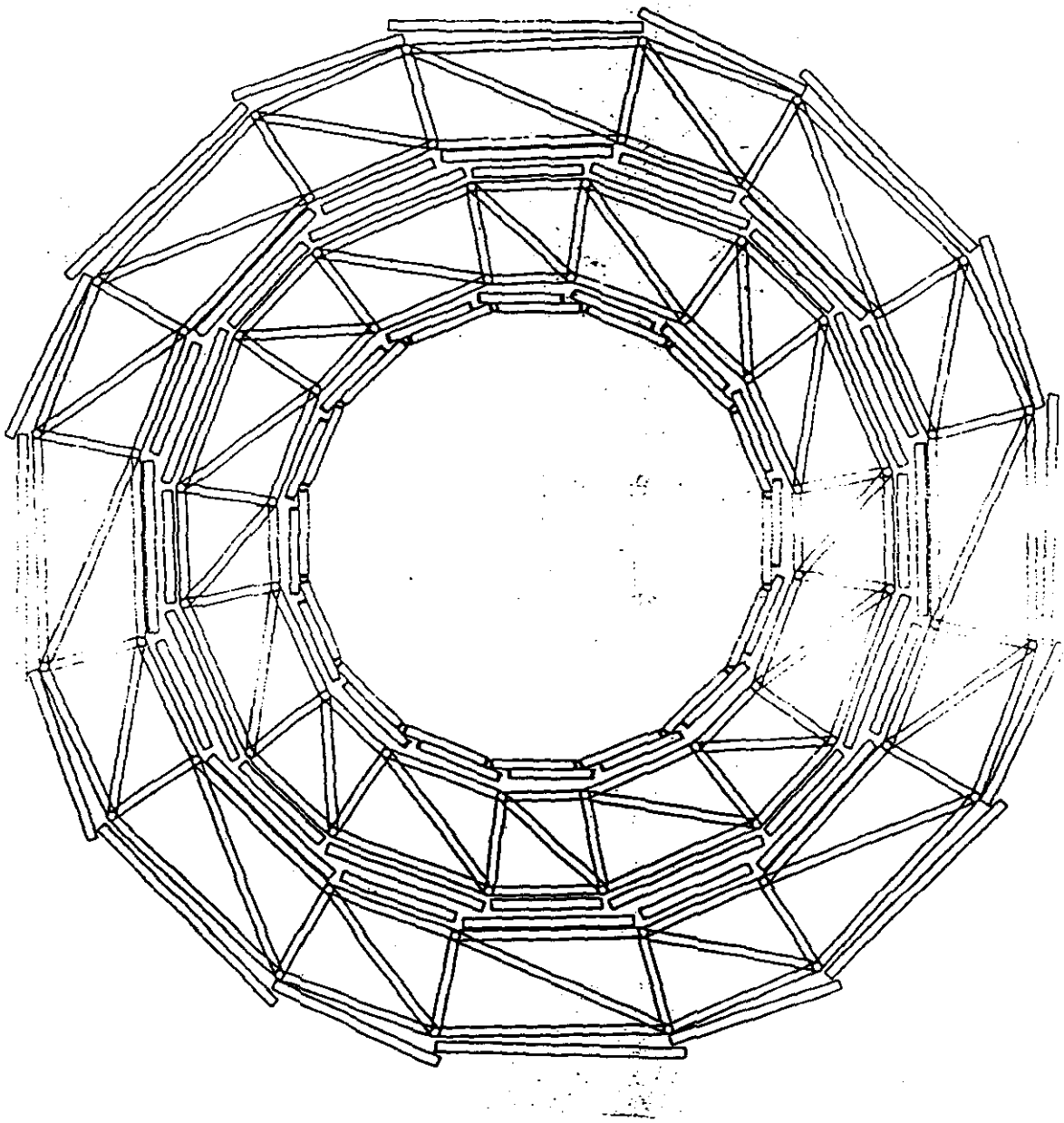

Fig. 7 Chamber layout in the GEM detector ;end view

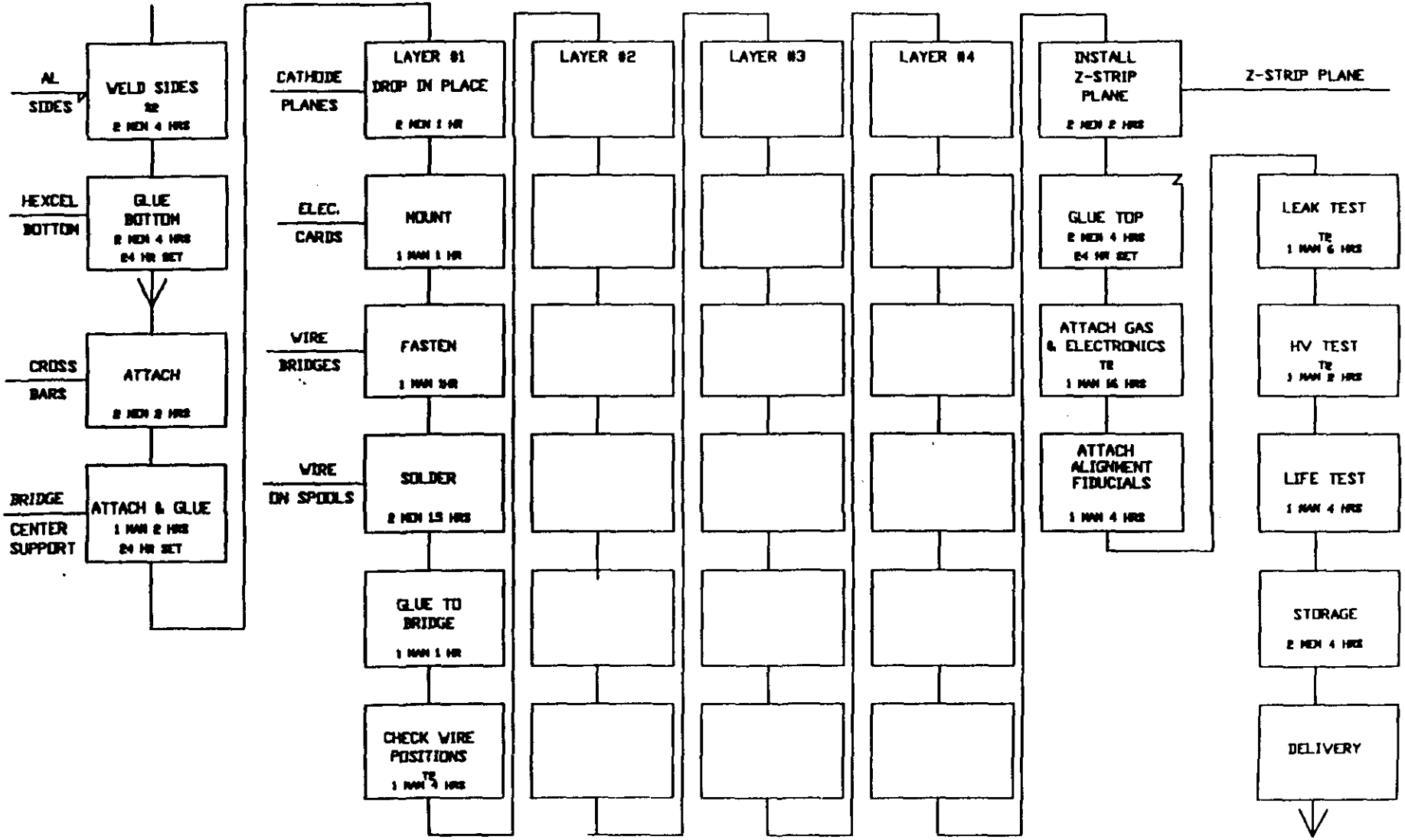


Fig: 8 Block diagram of the assembly procedure in the chamber factory

Sept. 20, 1992

## APPENDIX I-Engineering Considerations

*This Appendix was submitted as written material for the engineering review. It is appended to this report since it includes mechanical details even though it duplicates material in the main body of the report*

### I. Chamber Design

A. Philosophy

The use of a limited streamer drift tube(LSDT) technology has the following merits:

1. A well known technology: This mode of operation has been used widely in many contemporary detectors, SLD, Aleph, Delphi, etc.[1-4]. The history of behaviour in reliability, ageing, and manufacture is well documented.
2. Accuracy: It has the merit of giving pulses of large amplitude (~100mV) and fast rise time (~5 nsecs); both properties result in a small time jitter in measuring drift times. A further merit is obtained by streamer initiation on first electron arrival; this results in a better time measurement over proportional mode operation[5].
3. Well specified mechanical design: The chambers can be and have been designed with complete mechanical drawings and their specifications. This has the merit that they can be built at many places, abroad (e.g. Russia or China) or even comercially; they require standard technologies.
4. Allow correlated z-measurement: As in the applications mentioned above, the open cathode tubes allow the placement of pick-up strips facing the wires thereby allowing a measurement of streamer longitudinal position along the wire. We make use of this feature by having pick-up strips perpendicular to the wire. The time correlation with the wire pulse allows an unambiguous x-y measurement of each streamer and can accomodate several tracks in one tube.
5. Generates level 1 triggers with bunch assignment.

6. Gas options: Several gas mixtures, including non-flammable ones, are available to operate in this limited streamer drift tube mode (LSDT).
7. Achieve baseline accuracy: See below.

B. Detailed Design

A cross sectional view of a full sized chamber is shown in Figure A.I.1. The chambers are supported and their positions monitored at the points along their length where the bridges holding the wires in place are located. An L-shaped strong back will fasten to the scaffolding; the position monitor (presumed, at this time to be an optical alignment method) is located in the holes provided on the upright of the strong back; a second hole is provided on the other end of the horizontal bar for vertical monitoring of the other side. The slot against which the ends of the wire bridges are mounted are precision machined with respect to the optical hole; the upright part of the L which bears the optical hole has been welded to the side wall before the machining. The grooves in the bridge which hold the wires are precision machined with respect to the reference edge of the bridge. We have tested the machining capabilities of a CNC on a Mycalex bridge and find that it can locate the grooves in absolute position to less than 10 $\mu$m's.

The other side of the bridge is held by a slip pin which controls the height of the bridge (less tolerance required ($\pm 150\mu$m's) but is not perturbed by any "breathing" of the Al box. The bridges are not in contact with the cathodes, and suffer bending only under their own weight. This would be excessive in a 1 meter span; a central post is provided to eliminate this sag.

The cathodes are stacked in four layers resting ultimately on the Hexcel bottom. The cathode placement is not critical. The present method for making the cathode planes involves attaching L-shaped beams of 10 mil Al to a substrate of 10 mil Al with thermosetting films. The result is a layer of U-shaped tubes, which, when coverd with the

next layer on top, or with the z-strip plane give our required layer of square cross section cathodes with minimal material.

The space over the fourth layer contains the pick-up strip plane for accurate measurements in the longitudinal direction and additional drift time information.

With our design the seperation distance between bridges may be selected. We have chosen to place them at such a seperation that the droop under gravity is always below the desired measuring error rather than trust in making a correction for this, which requires assuming the tension is as planned. This better centering of the wire provides more insurance against electrostatic instability. This does require more bridges and more optical alignment points and thereby more cost. If one wishes to relax this requirement one can, of course.

Summing all the material in the chamber, excluding the sides, a particle traverses 6.4% of a radiation length.

C. Electronics and Gas System

These systems have only indirect influence on the mechanical design of the system. The most important is that their accomodation requires some dead space on the ends of the chambers. We use only one end for the electronics. Each wire is tied to a mate 2 wires away through a delay line; the time measurements made on this wire pair give a coarse ($\pm$ 15 cm) logitudinal position measurement. We use one skipped wire pair instead of adjacent pairs to avoid confusion with a track that crosses from one tube to its neighbor. To minimize dead space we plan to place the electronics package on the top of the chamber; the dead space is taken by the solder card and its support and the turning cables. See Fig. A.I.2.

D. Achievements on a Prototype Chamber.

The wire placement with respect to this optical reference point is done through several surfaces;optics to hole in strong back, strongback to chamber wall, chamber wall thickness,

bridge edge to wire groove, groove to wire seat. Each of these is called with an accuracy of 5/10,000 of an inch (12.5 $\mu$m). In the prototype the accuracy called for in wall thickness was mistakenly poorer but, fortunately the accuracy actually obtained was better; we show some examples:

1. Fig. A.I.4: Scatter in absolute position of bridge grooves i.e. from x=nx25 mm where n is the number of the groove on a 50 cm bridge.
2. Fig. A.I.5: Scatter in groove position for a 1 meter bridge.
3. Fig. A.I.6: Scatter in measurements from an outside target (equivalent to the optical hole) to the 9th wire of the prototype chamber for 3 of 4 layers each with 3 bridges. The 4th layer, the bottom one, did not have its bridge seating point cleaned. This gives the overall accuracy from the accumulation of all errors.

Finally, we can obtain the relative deviation of a bridge from its companions by looking at cosmic ray events and measuring the average deviation of the residuals for that layer. This is shown in Fig. A.I.7; also shown is the deviation as measured with our measuring device.

Of interest as a measure of chamber performance, though of only indirect relevance to mechanical design, is data taken with our prototype chamber on cosmic rays. Fig. A.I.8 shows the scatter in individual wire measurements from fits to the tracks. The scatter includes any scatter in the wire positions, though we have measured this to be insignificant compared to the scatter from the measuring process itself. One measurement was done with a filling of 10% Isobutane, 90% $CO_2$ gas, which is not the most favorable mixture for accuracy. Another measurement was done with 25% Argon, 75% Isobutane and is shown in Fig. A.I.9. The scatter is lower; this gas is faster, has lower diffusion but is, unfortunately, flammable. We have deferred measurements with a $CF_4$ based gas, which is fast and non-flammable, to tests at the TTR.

## II. Layout in the GEM Magnet.

A. Hermiticity.

1. Within a superlayer.

We take advantage of the lack of restriction in length for our chamber design to minimize the segmentation along z. This noble aim is modified in two places. A chamber 14.3 m long and 3 m wide, though possible in principal, seems rather unwieldly; we have arbitrarily limited the length to half of this (7 meters). (see Fig. A.I.10) Secondly, in order to get inter-sector overlap(see item 3), we require a strengthening plate in the middle of superlayer 2. Within superlayers 1 and 2, which are made of two four layer chambers, we achieve overlap in the r$\phi$ direction by making the widths of the two chambers unequal in each sub-layer (see Fig. A.I.11). This solution is not available in superlayer 3. Here we plan to make a chamber which is full width; it will follow the technology of the prototype but will require multiple supporting through its width as opposed to the single one in our prototype. This chamber will be tipped, as in the PDT or CSC layout to achieve overlap.

2.) Within a sector.

This is solved by the hermiticity within superlayers. The break in z within superlayers need not be along a the same radial line from superlayer to superlayer. In this case one detects the muon but does not make a three point measurement for momentum determination.

3.) Between sectors.

The solution to overlap between sectors has been addressed seriously only recently. Superlayers 1 and 3 can be arranged in that fashion since the chambers can be mounted beyond the sector radial supports. The problem comes with the middle (no.2) superlayer. We propose a solution analogous to that studied for the PDT technology at Draper. In our case we take advantage of the natural division of this superlayer in two chamber layers. Rather than tilting the chambers we propose to make the sublayers of different widths and seperate them in r. Alternate sectors will expand or contract in angular width to accomodate the differing size chambers (see Fig. A.I.11). The strength of the support structure, however, must be borne through this layer. In the case of the PDT's this has been done by having plates at the ends of the chambers fastened to the struts which carry the moments

and shears through the layer; it is natural for this to have two penetrations and two end plates for the PDT's. We would like not to compromise the length of our chambers and propose one penetration and two end plates; we appreciate that this has not been studied for rigidity. Were it to fail we would return to a segmentation into 3 lengths.

B. Layer formation.

Our natural chamber unit has been designed to be approximately 1 meter in width. In the case of superlayer 3 where we do not have two chamber layers we have proposed a wide single chamber. For manufacturing ease we would still like to retain this smaller comfortable dimension; since we overlap chamber layers in superlayers 1 and 2 we do not lose coverage in the $r\phi$ direction. However, we wish to have a rigid layer structure. This is also a requirement to take advantage of the alignment analysis done by G. Mitselmakher[A5]; this requires an alignment point at the sides of the chambers and one in the center. We do this by taking 2 chambers whose profile is shown in Fig. A.I.1 except that one is the mirror image of this so that its reference strong back is on the left. The horizontal members of the two strong backs are fastened by a sliding rod which then allows relative expansion in width but gives rigidity perpendicular to the chamber face. A hole is provided in the center of this cross rod for optical or wire alignment. It might be argued that a simple fastening between the two would be sufficient since any expansion of the support frame (e.g. for thermal reasons) would be matched by this rod, they both being of aluminum; we do this simply so that the chamber itself does not act as a constraint on the support structure. The resulting marriage is shown in Fig. A.I.12.

## III. Alignment

In order to arrive at the desired measurement accuracies for muons, GEM has set an overall placement accuracy for a trajectory measurement of 25 $\mu$m systematic and 100 $\mu$m for random measurements.It is assumed that the later, due mostly to the random nature

of single measurements on a chamber wire, will be made in sufficient number to reduce the overall error. This specifies, in the LSDT case, 8-8-4 measurements in the 3 succesive super layers. We may not be able to place the chambers to the 25 $\mu$m accuracy and keep them there as the surround changes (temperature, magnet on-off, etc.) but we expect to monitor positons to the desired accuracy so that corrections to the data can be made.

The important measurement is the deviation of a muon track from a $\phi$ = constant plane i.e. made in the r$\phi$ direction. The succesive references are as follows:

1.) An optical line is defined by an LED-Lens- Quad cell triplet[A6], the three elements of which are mounted on the end plates (see Fig. A.I.10) occuring at the ends of the chambers and along the $\theta$=30 and 90 degrees lines. The optical method of alignment is an outgrowth of the technique used in L3[A2]. We have made measurements with the elements of ref A1 and find a deviation of 5 $\mu$m is easily detectable (Fig. A.I.2).

2. From the plates (item 1.) we would form reference lines along the z-direction through the fiducial holes on the strong backs of the chambers themselves. Since our chambers have bridge supports every 2 meters or so this is a natural use of the stretched wire technique where multiple refernce points can be taken off a line. The optical method can still be used requiring "piggy-backing" off sets of optical triplets.

## IV. Manufacture

A. Parts

The merit of our design is that a major part of the manufacture can be done by standard shops with standard supplies. We list the main components:

1. Chamber boxes: The side walls are made from Al extrusions; the standard straightness achieved in a normal extrusion is sufficient. The precision machining has only to be done at the areas where the bridges are to be attached; a wall thickness specified to 5/10000 inch (12.5 $\mu$m) is both standard and sufficient. The ends of the boxes are

non-critical. We called for welding the sides; it may be that glueing is acceptable and easier.

2. Hexcel tops and bottoms-standard, though patching must be done on the large sizes.
3. Mycalex (or equivalent) bridges. These may be made in long lengths (> 0.5 m)but would require tooling costs. We have found gluing two 0.5 m pieces together satisfactory. Machining the grooves to 0.5 mils absolute is standard.
4. The present cathodes of 10 mil material were made by the M.I.T. Lincoln Laboratory. They fastened multiple L-shaped pieces to a 10 mil plate with oven setting film adhesive. This may not be the cheapest or best technique but was straightforward.
5. Gold plated tungsten wire-standard.

B. Assembly (the factory)

The steps in putting a chamber together follow closely the procedures used customarily in the many Iarocci tube factories. The main difference is the checks on wire position that we would expect to do after the laying down of each layer; in time, this may become somewhat perfunctory, since we found no wire misplacement in simply laying the wire in grooves in our prototype. The outline of the various steps in the process are shown diagramatically in Fig. A.I.13. The times estimated for each step are included. These times are padded estimates from our experience with the SLD-WIC system and from the SCARF factory at the U. of Houston (R. Weinstein).

We had made a precision measuring device, a travelling microscope on a 48 inch arm tracked by a glass scale for wire placement checking (coming from the low bidder it required considerable calibration). This was readable by a PC and could certainly be made semi-automatic with a CCD at the focal point. Outside of this step the others are familiar.

(Parenthetical note) In GEM IN-92-19 "Detector Cost Review Report" Pg 4, item III.8. A skeptical remark is made as to laying down wires at 141 secs. each. Actually this is quite conservative, SCARF lays down 800 wires a day with hand soldering. We would

be laying down, say, 10 wires at a time with multiple soldering. The precision does not enter in this step, the groove lays the wire automatically.

C. Exportability

An important aspect of the LSDT technique is that it is usable by other laboratories, not only in this country, but in other nations. We have some information on this though we hope to have a more complete report later.

1. China: The Univ. of Tsinghua has a German CNC with glass scale control. Prof. Ni Weidou while visiting here expressed the belief that the machining we require could be adequately done on their machine.
2. Russia: Dr. Igor Golutvin of Dubna felt that the machines at that laboratory might not be quite adequate. However, the loan or gift of an adequate machine seems like a good investment. Example: The bridge grooving machine which obtained 10 $\mu$m or better was a Hitachi Seiki Mod. 55 with glass scale installed; its modern replacement cost would be 100k$ to 150k$.

## V. Costs

The costs of all materials and processing for our proposal have been assembled together with backup material in "The GEM Cost Book". This is rather voluminous but has been generally distributed and I assume any reader has access to it.

(Note 1) The cost estimate on the Aluminum boxes was made by the firm which made the prototype chamber box. They started with an Al plate and had to hog out the indentations in the profile resting from time-to-time to allow the plate to rest from the heat. They based their estimate on this work. The ultimate chambers will have extruded sides; the machining will just be done at the bridge support points. We will have a revised estimate shortly and expect it to be 2 times less or better.

(Note 2) The large cost spread by outside firms on the cathodes was done under the direction of Lincoln Laboratory. They advise ignoring the two very high estimates which in their opinion come from igorance and/or lack of interest.

## VI. Schedule

A. Special lead times

We see no item or process that requires special R & D or lead time. One exception might be the manufacture of long continuous Mycalex bridges were we to choose that route as opposed to fastening or glueing sub-lengths together.

B. Manufacturing schedule.

There does not appear anything unusual in the manufacturing that is unconventional or questionable. We estimate the operation of the factory to take place over 3 or 4 years.

## References


1.) A. C. Benvenuti et al. "The Iron Calorimeter and Muon Identifier for SLD", SLAC-PUB-4677, July 1988; NIM **A276**, 94 (1989); NIM **A290**, 353 (1990); NIM **A289**, 463 (1990).

2.) Aleph Technical Report 1983, CERN/LEPC/83-2; LEPC/PI 15 May, 1983.

3.) Delphi Technical Proposal CERN/LEPC 83-3 (1983); NIM **A273** (1988) 841.

4.) K. Lau et al, NIM **A306**, 397 (1991); D. Hungerford et al, NIM **A286**, 155 (1990).

5.) G. Mitselmakher, talk at the August GEM Muon meeting.

## Figures

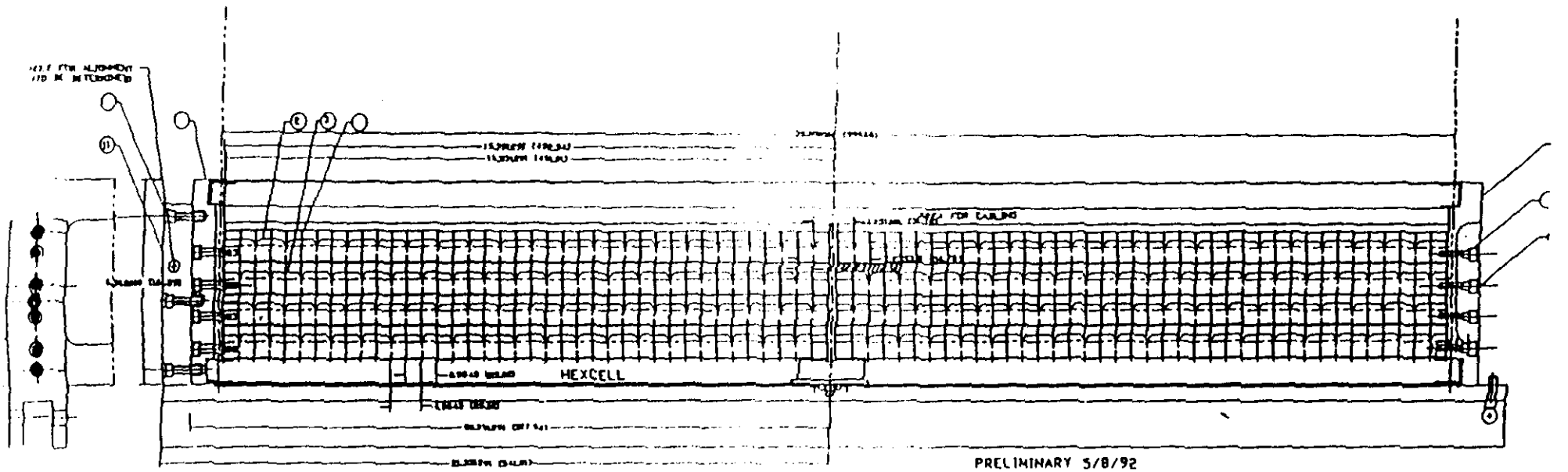


A.I.1. Cross-section of the chamber.

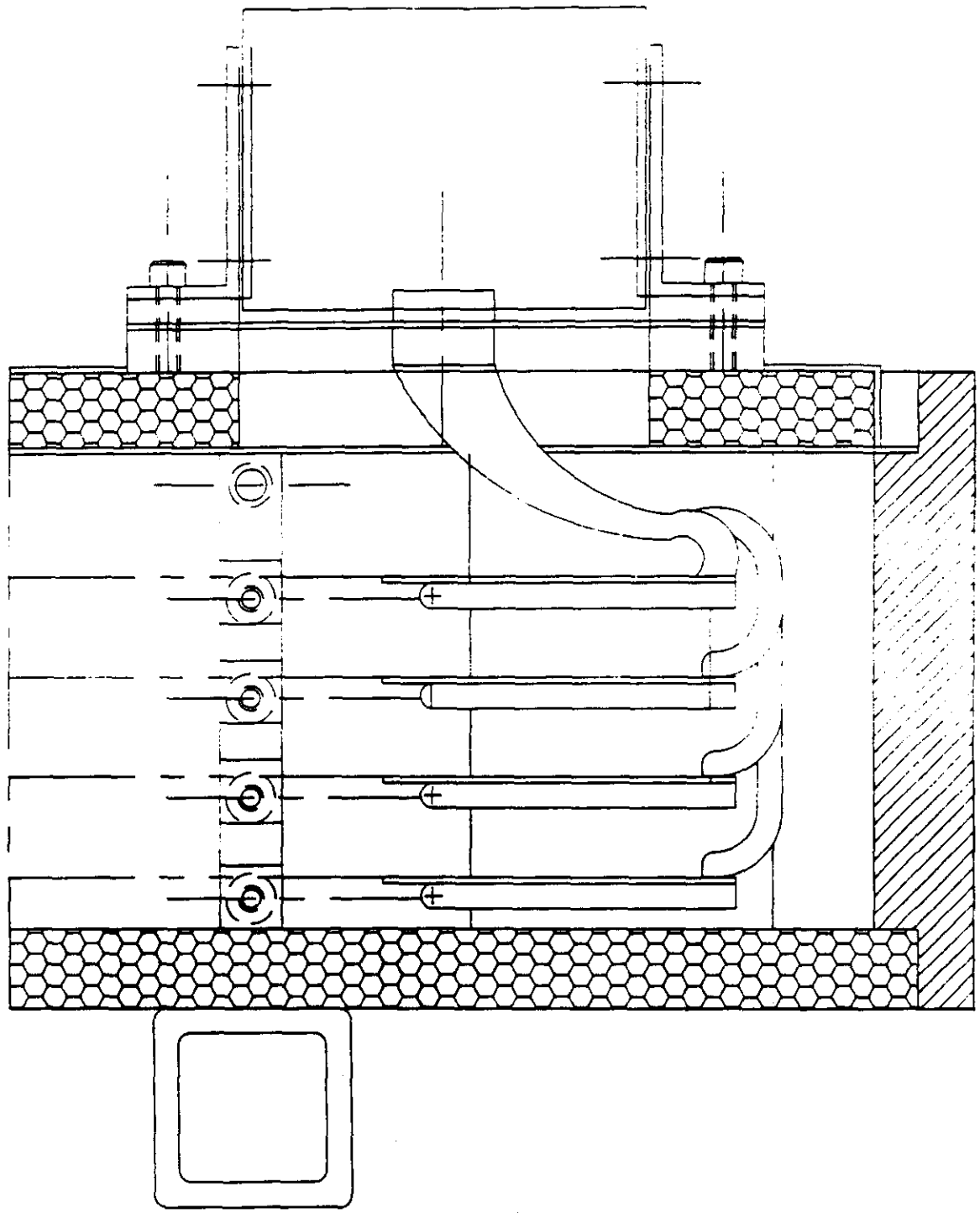

A.I.2. End view of the chamber.

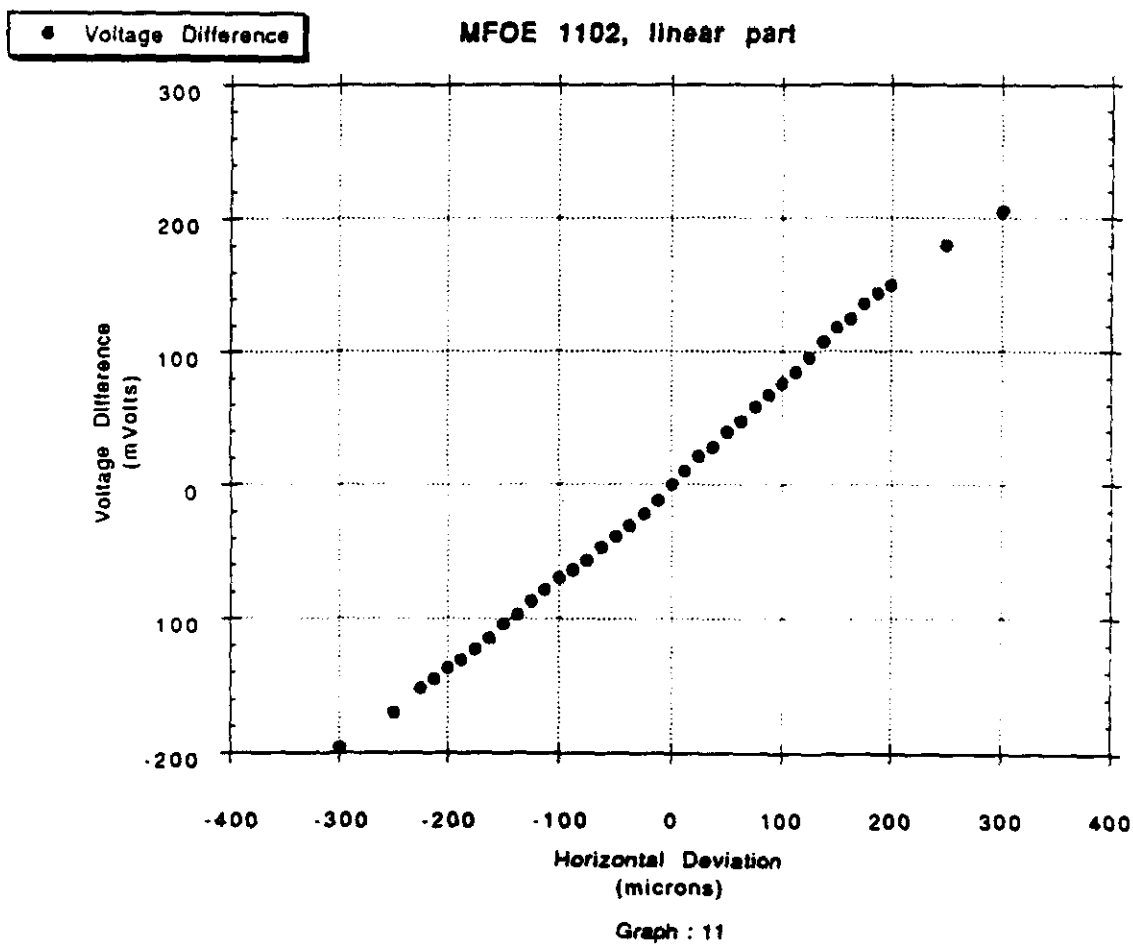


A.I.3. Sensitivity of the optical alignment to a deviation in the central element (the lens).

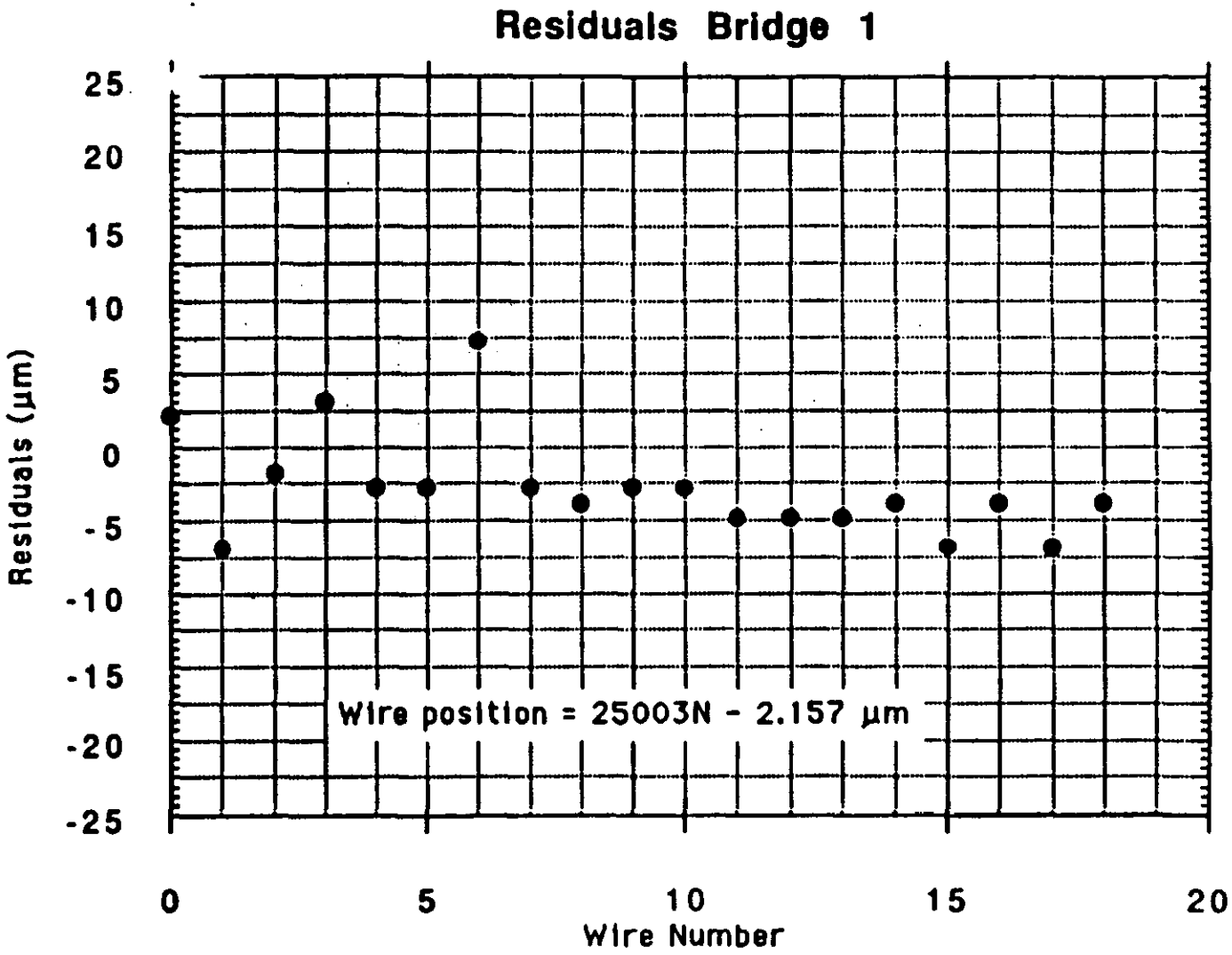


A.1.4. Scatter in deviation of bridge groove position.(0.5 in bridge)

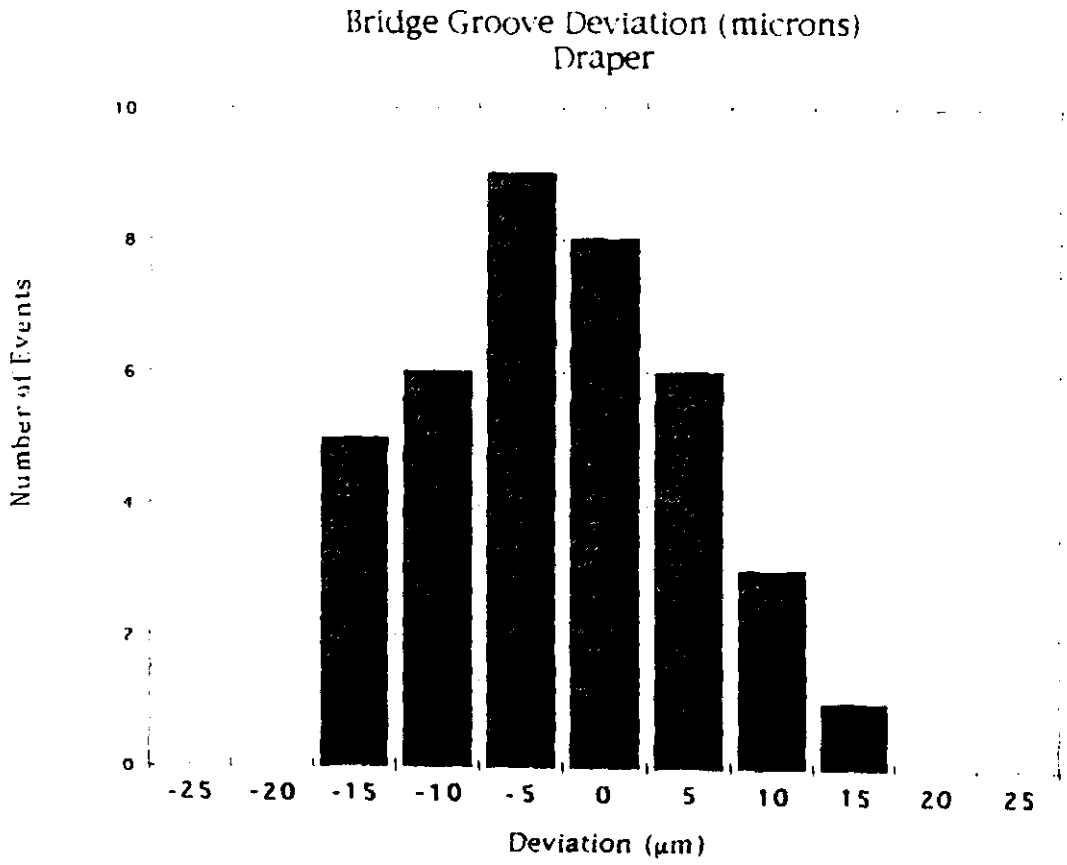


A.I.5. Scatter in deviation of bridge groove position (1.0 m bridge).

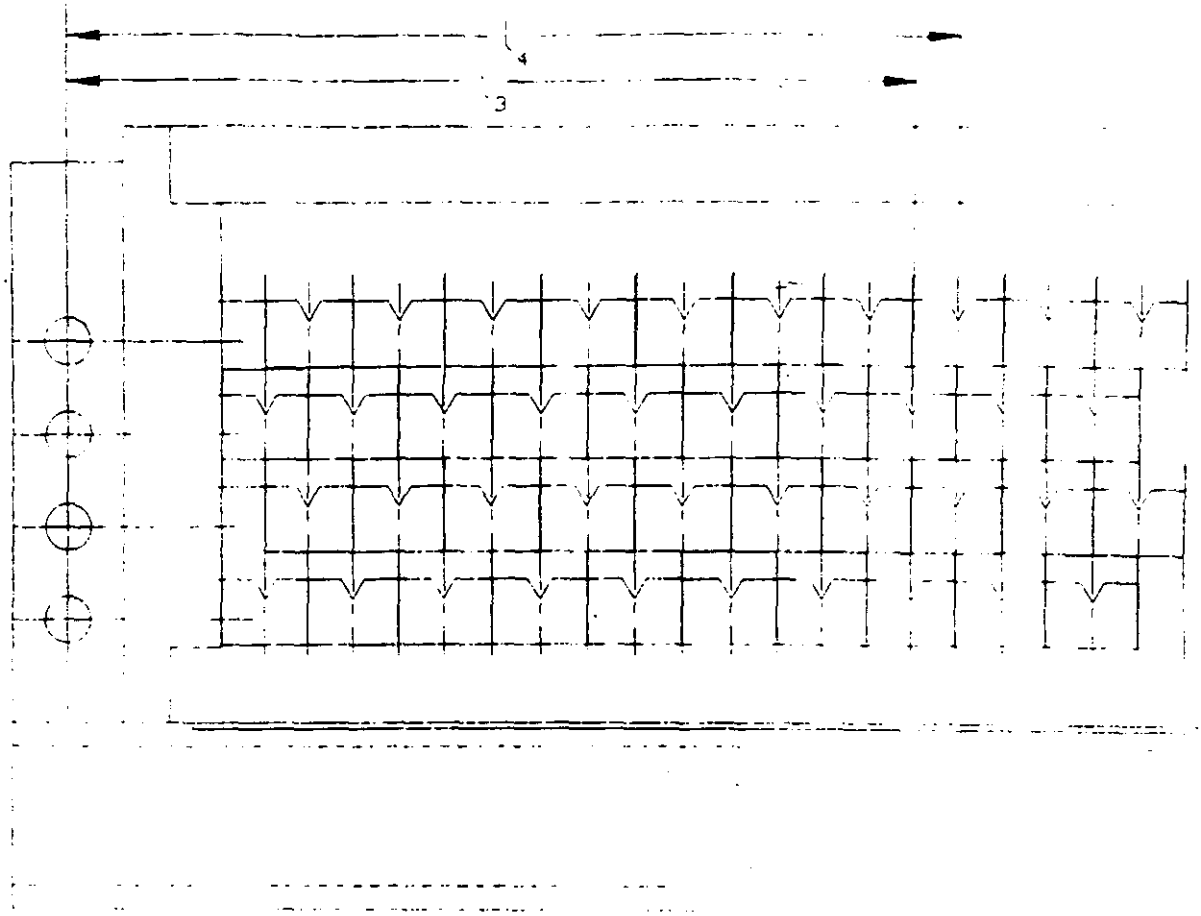


$L_3+(L_4-12.63)$ FOR 3 LAYERS

254.619
254.629
254.619
254.627
254.647
254.607
254.631
254.621
254.625

A.I.6. Spread in distance (mm) from outside target to wire no. 9.

PRELIMINARY 4/20/92

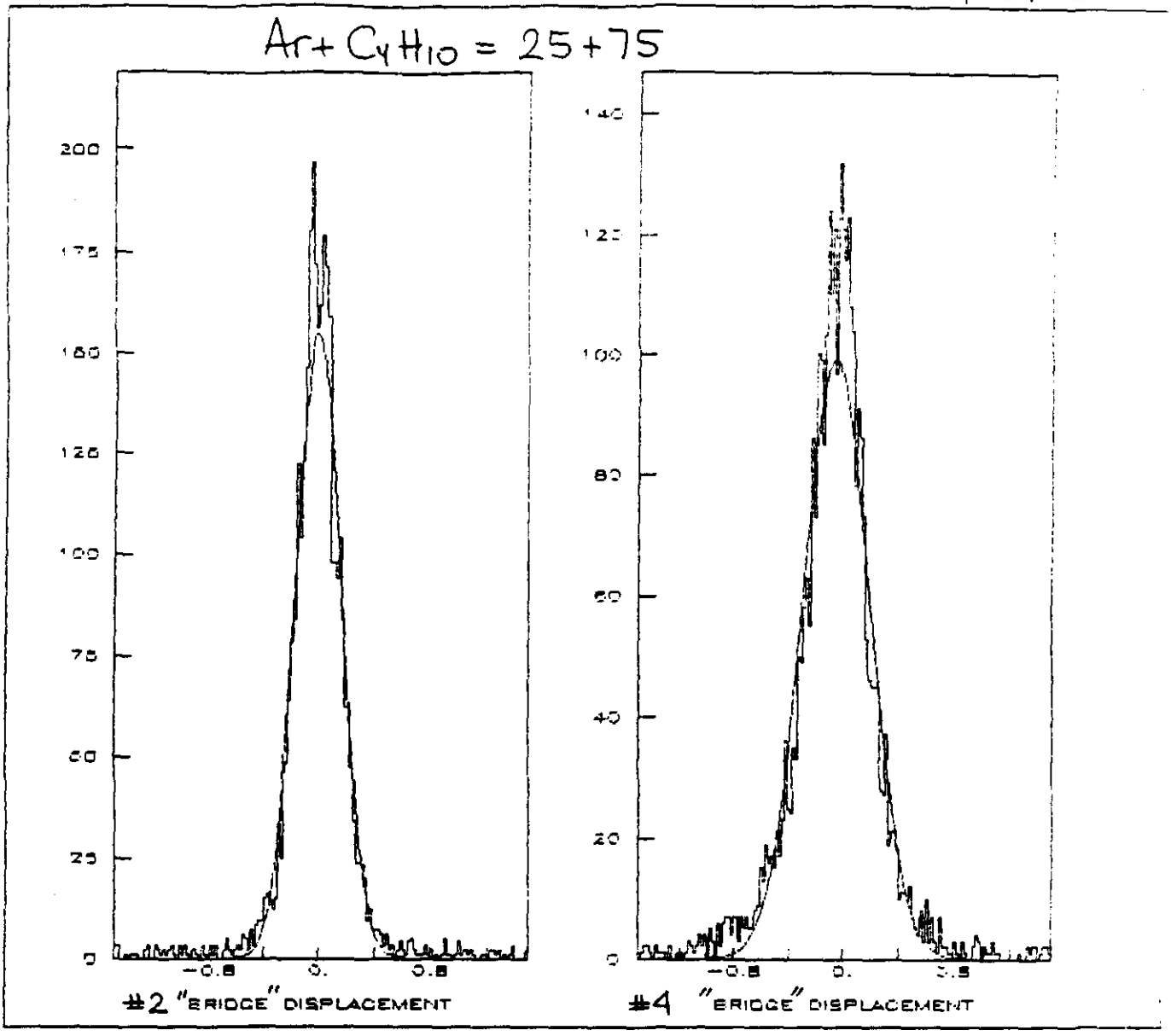


| | DIRECT MEASUREMENT | DATA FIT |
|---|---|---|
| LAYER # 2 SHIFT | +25 ± 20 μm | -7 μm |
| LAYER #4 SHIFT | +75 ± 20 μm | +56 μm |

A.I.7. Deviation in bridge position as measured by fits to cosmic rays and with our measuring device.

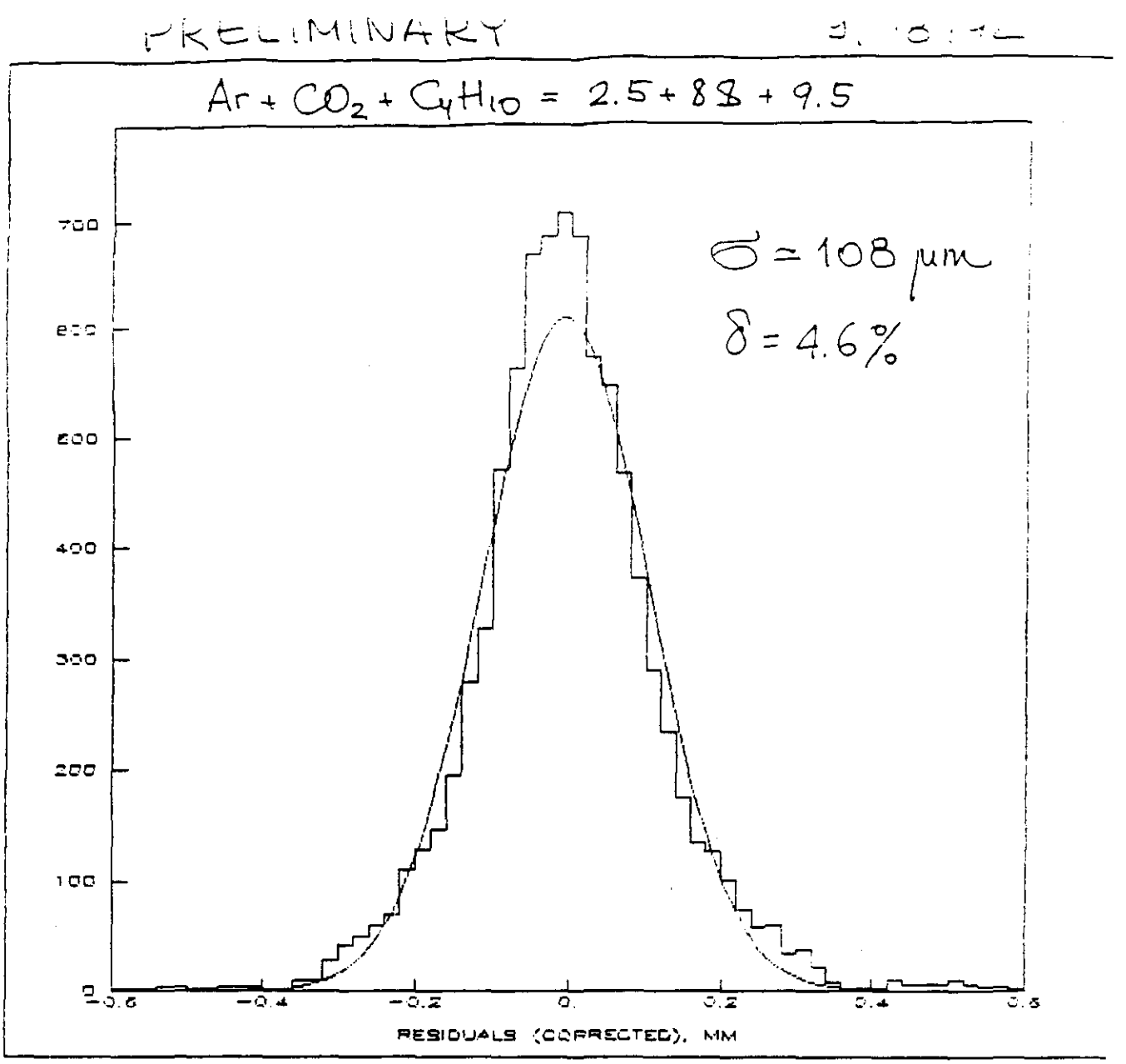


A.I.8. Residuals from fit to cosmic ray tracks with $CO_2$ based gas.

$\pm 3$ $|\alpha| \leq 5°$ $\sigma = 108$ μm

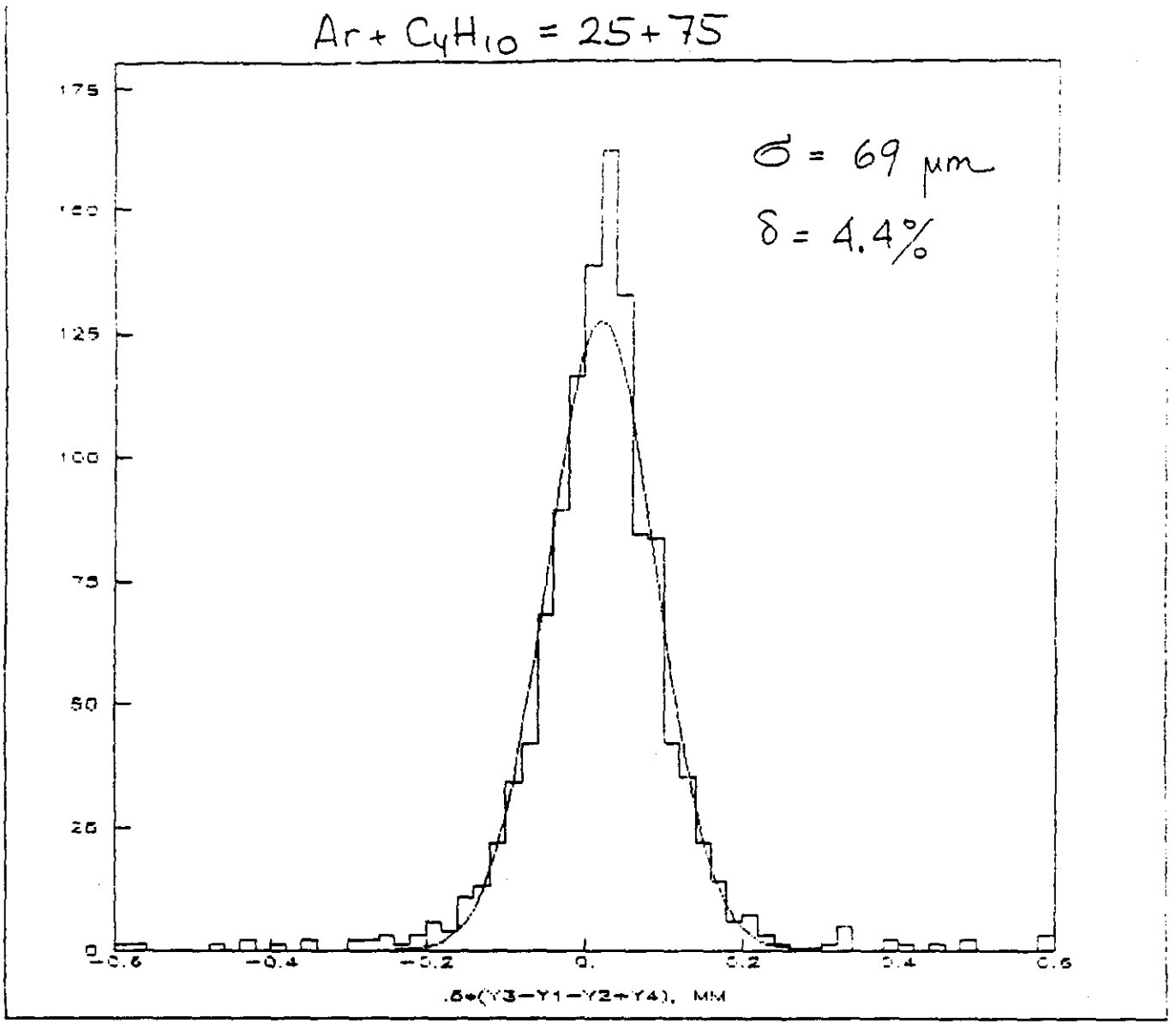


A.I.9. Residuals from fit to cosmic ray tracks with Argon-Isobutane filling.

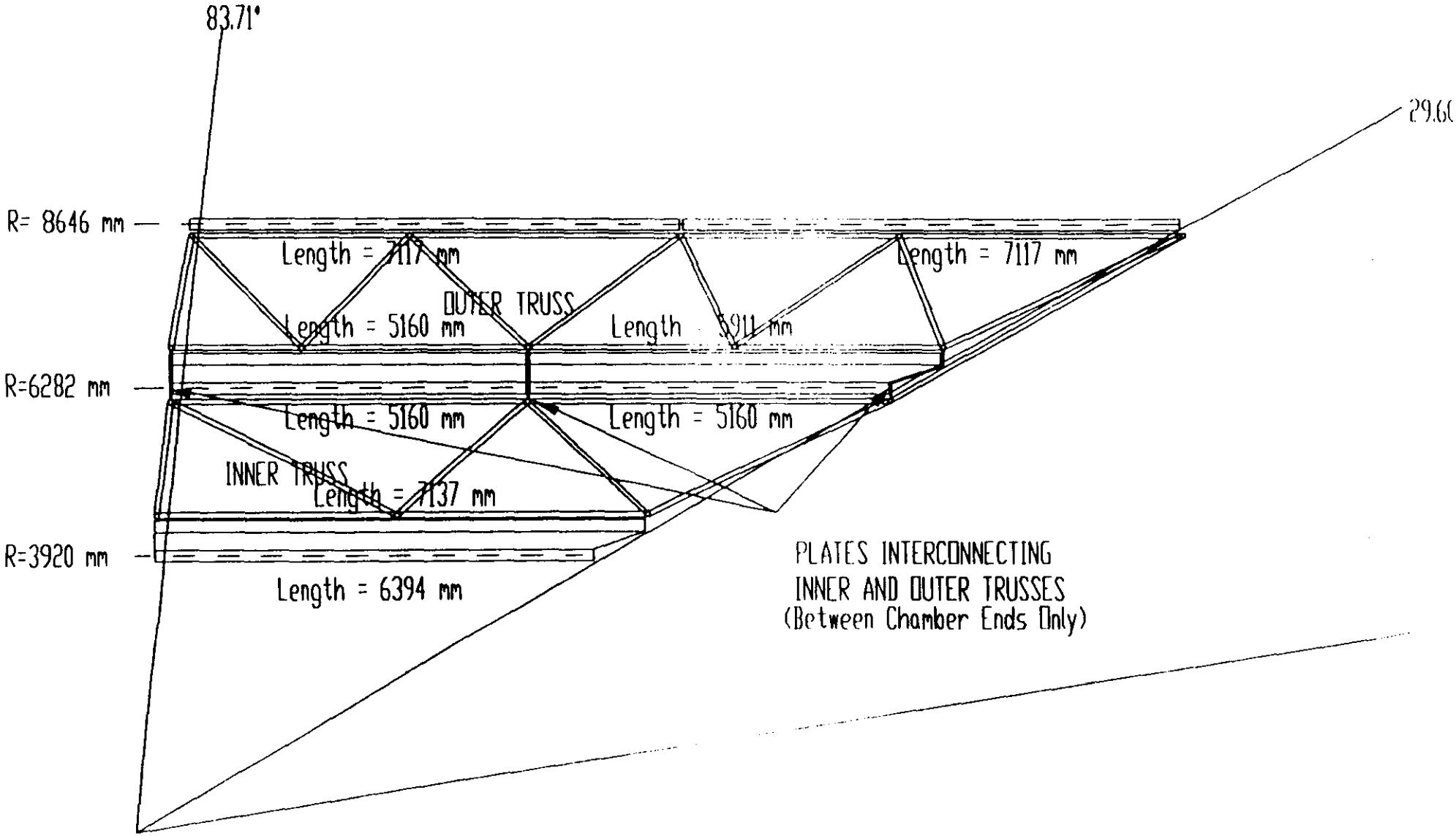


A.1.10. Side view of LSDT chamber layout.

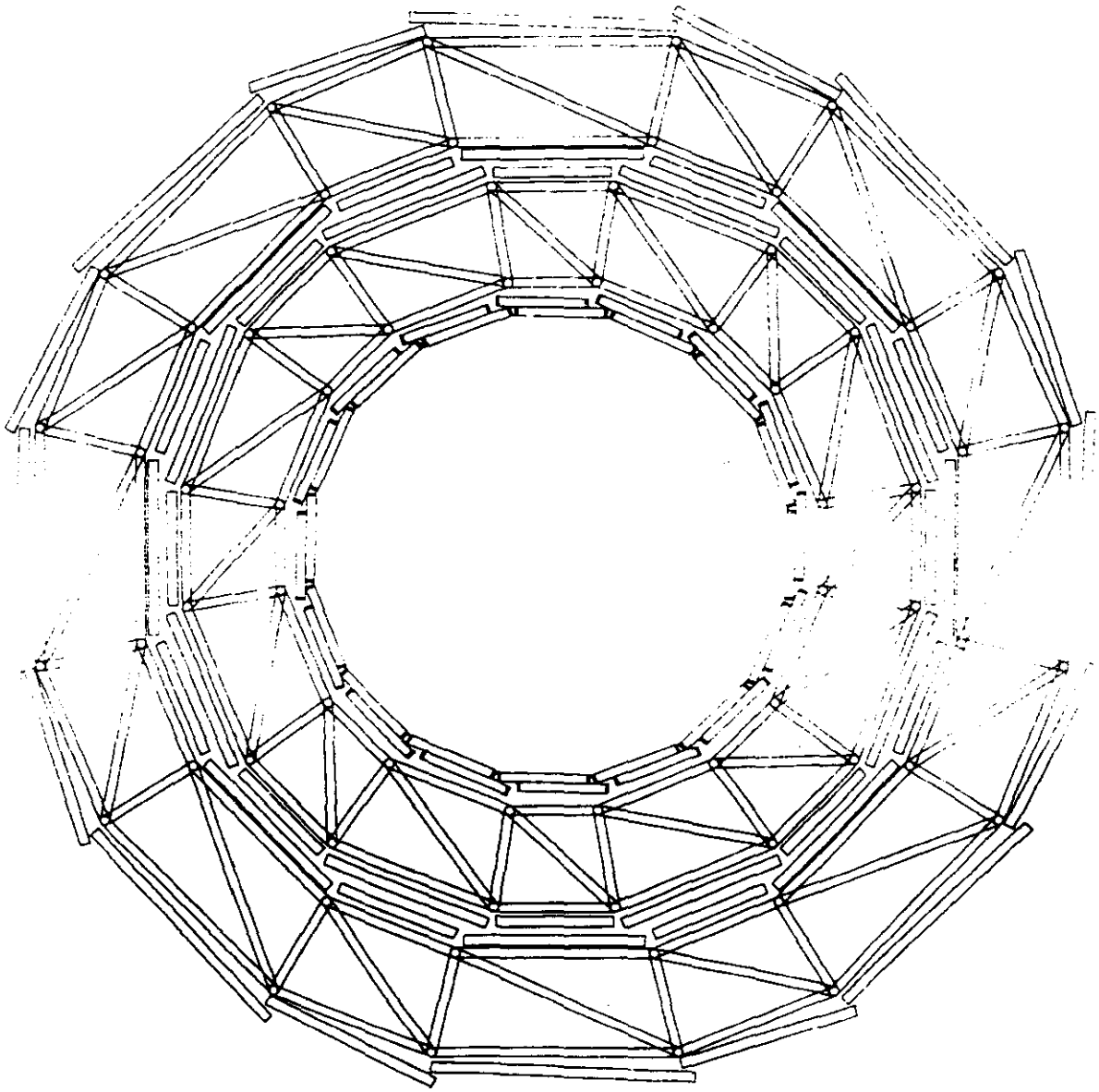

A.I.11. End view of LSDT chamber layout.

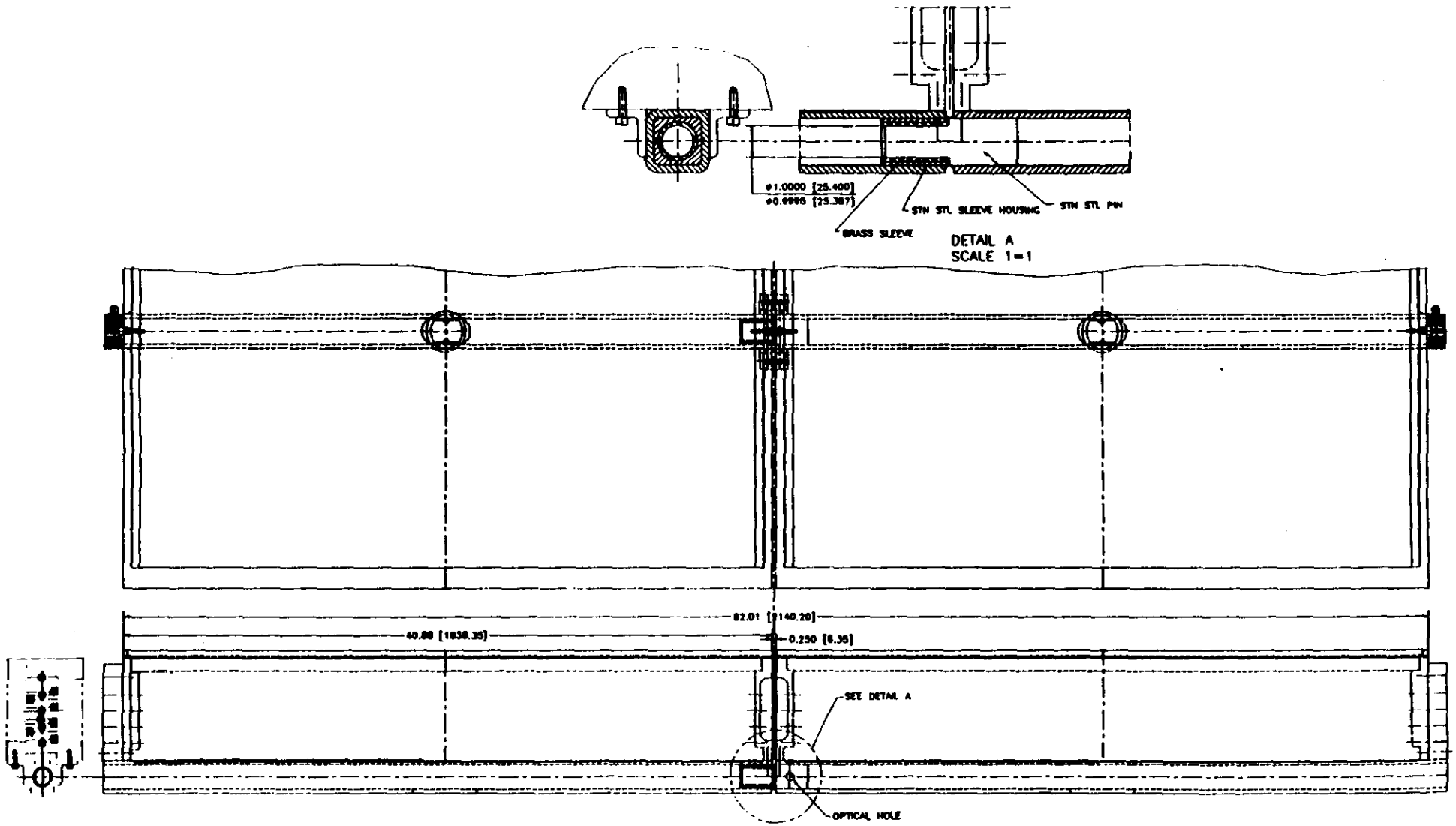


A.1.12. Fastening of two chambers to form a layer.

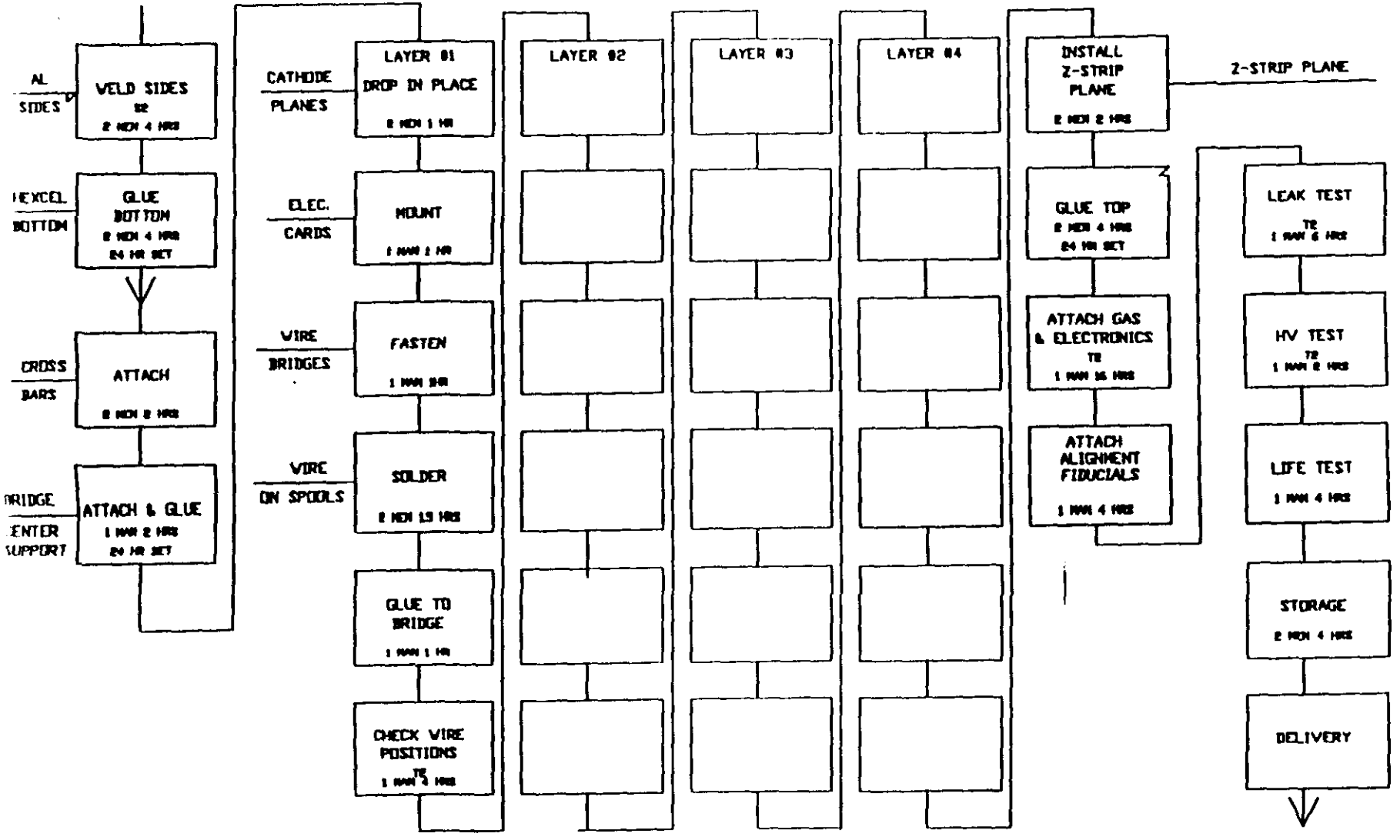


A.1.13. Diagrammatic flow of a chamber assembly procedure.

F

## Appendix II: Noise Sensitivity Comparison

It is of interest to calculate the noise sensitivity of various technologies to noise. In the case of the LSDT's the noise would shift the timing of the pulses by adding to the rise time of the pulse. For a cathode strip system the noise adds to the amplitudes of the pulses to be analyzed and will contribute directly to a mismeasurement of the center of gravity of the spark. One must also consider whether the noise is coherent (i.e. contributes equally to all surrounding strips) or incoherent; we consider both. This computation is most easily done by assuming a noise of a given frequency and finding the contribution as a function of frequency. We have computed the amplitude of noise that would spoil the space measurement by a factor of 2. Our results are presented as a comparison between a timing system (LSDT) and a strip system.

The result is shown in the plot below. It can be seen that the strip system is a factor of $10^5$ to $10^3$ more sensitive to noise than the LSDT's. At frequencies corresponding to the inverse integrating time of the strips the relative sensitivity falls to the lower figure, $10^3$.

An ameliorating condition with strips, however, is that the low frequency noise would probably be coherent; in this case one may think of schemes whereby use is made of untouched neighbouring strips to, essentially, "measure" the noise. Such schemes are conceivable but require further consideration.

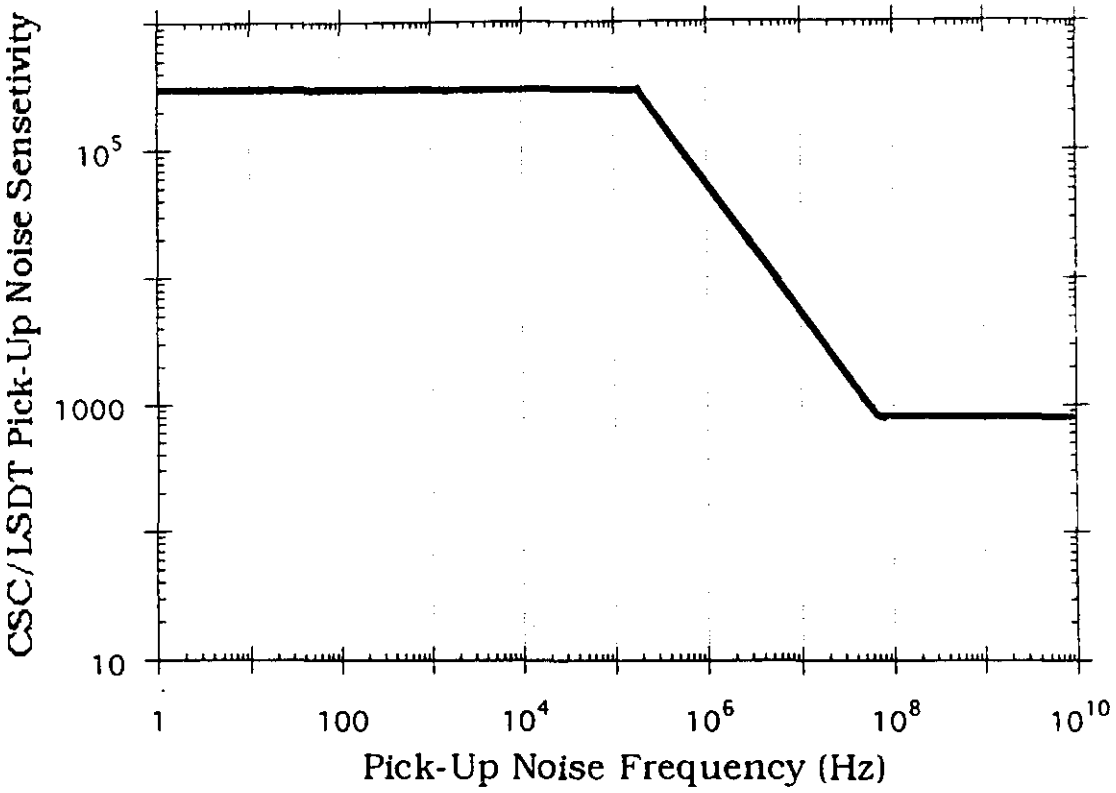
CSC/LSDT Pick-Up Noise Sensetivity
$10^5$
1000
10
1
100
$10^4$
$10^6$
$10^8$
$10^{10}$
Pick-Up Noise Frequency (Hz)

Fig.A.II.1

# Appendix III: LSNT Timing Electronics

The chamber mounted electronics will mainly consist of a high speed discriminator. The wires are operated in limited streamer mode, and the signals from the wires are about 50 mv. No conventional preamplifier is required, and the discriminator is connected directly to the wire. The output is differential ECL (possible positive ECL) which is capable of transmitting the timing signals over 20 meters of twisted pair cable without substantial degradation. Suitable commercial integrated circuits exist for this application. If a new IC were to be developed, the power required could be substantially reduced from existing chips. A simple serial (slow) communications link will allow setting the discriminator threshold and enabling or disabling individual channels. This slow communications link could be shared with the alignment system.

The remainder of the muon readout will be on cards, located on the magnet coil or pole structure. The Muon chamber readout requires a deadtimeless, pipelined TDC. This will be a custom integrated circuit. A block diagram is shown in the figure.

A differential receiver accepts the signal from the chamber, and drives both the trigger system and the TDC, which measures the time until the next (or since the last) 60Mhz clock (the beam crossing clock). This limited range (16 Nsec) high resolution (0.5 ns) TDC can be implemented as a digital interpolator or as a time to amplitude converter follower by a pipelined ADC. This TDC produces a 6 bit word (including overflow) at a 60 MHz rate. The double hit resolution is less than 26 nsec. It will be capable of accepting only one input signal during each beam crossing interval, but can accept one during every beam crossing interval.

A 6 bit wide, 256 step digital pipeline stores this digital data until the first level trigger. The trigger delay is 4.2 microseconds for 256 steps. This is easily adjusted to match the final requirement. Since this is a digital delay, there are no intrinsic restrictions on the length. When the first level trigger arrives, the first relevant time slot is at the end of the pipeline. For the next 15 time slots (for a 250 nsec drift time) all TDC hit data is collected and extended by adding the time slot number (by counting steps since the trigger arrival) and becomes 10 bits. This sparse data is stored in a multi-event buffer on the chip (one buffer for each channel), and is either read out immediately or stored until a second level trigger decision (asynchronous, but monotonic).

The readout can be organized in many ways, but a simple unidirectional multiplexed output is certainly adequate. All channel multi-event buffers on the chip are multiplexed to one output port. A channel number is added to the data. This is an 8 channel TDC chip, so the data word becomes 13 bits. Eight TDC chips can be multiplexed together on the board, resulting in a 16 bit data word (adding 3 more address bits). This logical block of 64 TDC channels can now be multiplexed in a similar way with seven other logical blocks to produce a relatively small number (200) of data streams into the data acquisition system, which is located far from the experiments. A simple FDDI type optical link will be sufficient for the data stream. Assuming 10% hits, and 10 khz level 2 accept rate, the data rate is only 1 Mbyte/sec (plus a little overhead).

This custom integrated circuit can be implemented entirely in CMOS, and is a practical object even with currently available CMOS processes.

There will, of course, be some control communication required to and from these TDC boards. This will be a relatively slow and low cost serial network. This link will set up the running conditions, test, calibrate, and so on.

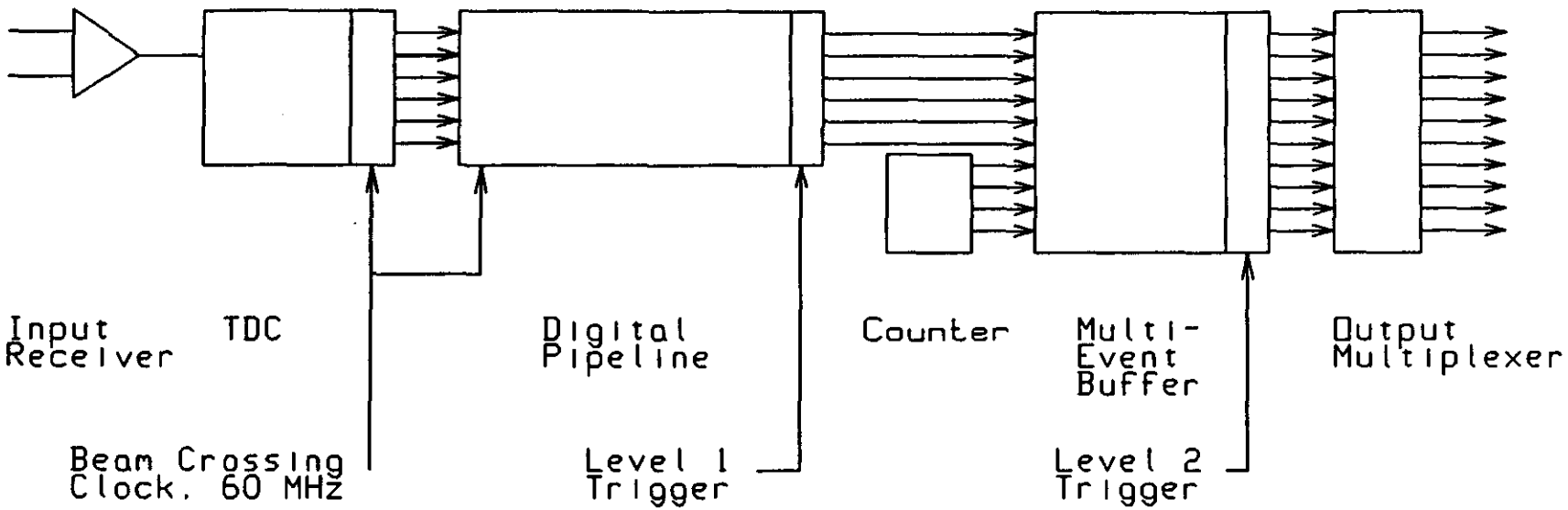


# Muon System Pipeline TDC

Fig.A.III.1

## Appendix IV: LSDT's as a Level 1 Trigger

### BRIEF SUMMARY.

We calculate a muon momentum and angle of a track with respect to the SuperLayer 2 using only Yes-No information from chambers in SL2 and SL3. Then, given information about that angle, we get bunch crossing time using information from SL2 only. The time necessary to complete the calculations does not exceed 1 μs (including about 300 ns max drift time). Monter Carlo shows that inefficiency of the time trigger is less than 2%. Also, it should be mentioned that the analysis we have done indicates that the angle with an accuracy enough for bunch crossing determination, (about $1\text{-}2^0$) could be probably extracted from SL2 alone. Further studies will be done to confirm this.

Thus, this particular scheme should be considered as an example showing the feasibility of a trigger based on LSDT's only.

### ASSUMPTIONS

1. We do not assume that a LSDT gas, still to be chosen, will be flat, i.e. the function of drift time vs. distance T(r) is not necessary linear. We looked at several gases we use now in our studies:

a) $Ar+C_4H_{10}=25+75$,

b) $CF_4+CO_2+C_4H_{10}=69+20+11$,

c) $Ar+CO_2+C_4H_{10}=2.5+88.+9.5$

and found that all these gases could be very well fitted by just two terms, linear and parabolic, data deviating from the fits no more than by several nanoseconds in the worst points (Figs 1-3). This accuracy is quite enough for trigger purposes.

2. To proceed with analysis of time budget, we will use the fact that it takes about 50 ns to make one arithmetic operation with two 6 bit numbers. This assumes rather simple and already developed electronics. There are other ways to speed up these calculations (e.g. by means of look-up tables).

## MOMENTUM TRIGGER

Fig.A.IV.4 gives an idea how the momentum trigger can be arranged on the basis of measurements in the middle and outer SuperLayers (SL2 and SL3).

Given only Yes-No information from a 4-layer chamber, one can the trivially localize a track within one cell. This provides an error in angle $\alpha_2$ of about .005 rad, or better than $0.3^o$. For 10 GeV/c muons the angle $\alpha_2$ is equal to $4.3^o$, so that $0.3^o$ accuracy allows one to tune a $p_T$ cut up to about 50 GeV/c. [One can estimate that measurement error and multiple scattering (see Sub-appendix-I) contributions will be $\delta p/p=.005*p+.066$.]

The number of calculations necessary to get a momentum trigger is obviously very small (2 arithmetic operations p=Const/(X3-X2) and one comparison with a $p_T$ cut set for the trigger). Thus, the information about momentum ($p_T$) is available in 150 ns (+ Drift Time).

## TIME TRIGGER

**IDEA:**

If a track goes between wires (Fig.A.IV.5), and given that drift time vs. distance is $T=a*R+b*R^2$, one can easily extract zero time. A priori the track can go either between wires or pass by the same side of two wires.

The point is that in the first case the formulae will give a right answer, while the second case will give some "crazy" result. Thus, the idea is to look at all possible pairs of cells along a track in Chamber#1 and Chamber#2 of the SuperLayer 2 (6 pairs per chamber) and to find which answer out of 12 occurs most frequently. The right answers should obviously coincide, while wrong answers will not, as a consequence of their rather random spread.

Also, it should be noted here that by means of look-up tables at this stage one can identify a good fraction of bad pairs and eliminate them from further analysis.

**MONTE CARLO:**

1. First, we ran a MC without introducing any measurement errors and δ-electron production, to check how many pairs have a track between wires. Fig.A.IV.6 shows that in average each event has about 7.4 pairs (out of 12) with a track going between wires (right answers). Also, one can see that wrong answers are spread far away around so that a probability for coincidence of two wrong answers should be very low.

Table 1 shows that in case of measurements without errors, each event has at least 6 right answers.

2. To figure out the sensitivity of such kind of trigger to measurement errors, we put in the MC the following error sources:

a) $\delta$-electron production ($\varepsilon$ - probability to get a $\delta$-electron per cell, $\delta$-electrons had a random distribution between 0 and actual distance from a track to a wire). Typical probability is 3-5% as was measured in our Fermilab tests.

b) $\delta T$, drift time error due to diffusion, misalignment, electronics, etc. (2 ns error is considered to be typical which corresponds to about 100 $\mu$m space resolution.)

c) $\delta\alpha$, angle error (as was mentioned above, a typical angle error does not exceed about .005 rad).

We ran the MC with uniform angular spread of tracks within $-11^0<\varphi<+11^0$. A beam crossing number was assigned to each of 12 answers obtained for a track depending on the bucket (16 ns wide) the answer had dropped in.

Tracks had no spread in $\theta$ so that no time of flight corrections were necessary. Later we will show that LSDT's have a very important advantage in terms of time of flight corrections since the z-coordinate is available from the same wires (by means of time difference from connected wire pairs) so that there is no need to correlate $r_\varphi$-measurements with independent z-measurements as needed, for example, in CSC's.

At this first stage we also did not put multiple scattering in the MC. Nevertheless, it will be shown (see Sub-appendix I) that the multiple scattering do not lead to errors exceeding our typical measurement errors.

Applied separately, the measurement errors mentioned above result in trigger inefficiencies as presented in Fig.A.IV.7(a,b,c). One can see that the typical errors (marked by arrows) are far away from dangerous boundaries where inefficiency drastically increases.

Fig.A.IV.8 shows inefficiency vs. muon momentum when all three errors are turned on. Also, it is shown that inefficiency remains very small even when all errors have been arbitrary doubled(!).

It is worthwhile mentioning that neutrons with a rate estimated to be $10^3$ $cm^{-2}s^{-1}$ after 20 cm of polyethylene shielding, are equivalent to $\delta$-electrons giving a small addition of about .5% to $\varepsilon$. Also, should it be necessary, the neutrons can be easily sorted out on the basis of z-coordinate correlation

between planes in the chamber (this information is immediately available in LSDT's from time differences on the connected wires).

3. Fig.A.IV.9 was obtained assuming that times were measured with a clock ticking each 16 ns (the natural SSC clock each subdetector system should have implemented). Even this poor accuracy turns out to be quite adequate to the task.

4. Fig.A.IV.10 shows that even rather big angle error ($1^0$ or so) is still tolerable. The angle with an error of this order can be probably extracted from SL2 signals only.

4. Although the inefficiency seems to be small enough already, there is a simple possibility to improve it by using similar information from SuperLayer #3 (this gives rise an increase in trigger electronics). Instead of 12 answers (6+6) to choose from, the trigger system will use 18 answers (6+6+6). Fig.A.IV.11 shows that this makes the trigger much more robust.

**CHAIN OF CALCULATIONS:**

Table 2 gives the chain of arithmetic operations to be done to get the timing trigger. There are three input parameters: T1, T2 - times from a pair of cells and $\alpha$ - estimated track inclination. The chip having three parallel ways of calculations will generate an answer for each pair of cells in 8 steps, or in 400 ns.

Then, a time of about 200 ns is needed to select the most frequent answer.

**TIME BUDGET:**

| | |
|---|---|
| Full Drift Time | - 300 ns |
| Angle Calculations (2 steps) | - 100 ns |
| 12 $T_0$'s (8 steps) | - 400 ns |
| Final $T_0$ | - 200 ns |
| Total | - 1 μs |

## EXPERIMENTAL DATA

Preliminary analysis of the first data we obtained with a Large Scale Prototype at MIT (the chamber has obviously only 4 layers) confirms the

scheme presented above. The single track events have been fitted, then, inclination angle obtained from the fit has been smeared with an error we used in MC (.005 rad). Then after that, using two-term fit of laser data, we tried to find a zero-time. The distribution of answers (6 answers per track) is plotted in Fig.A.IV.12(a) which is very similar to the MC distribution (Fig.A.IV.12(a)). The efficiency turns out to be about 95% in agreement with the MC. The following table gives a more detailed comparison:

| | MC | DATA |
|---|---|---|
| RIGHT $T_0$ | 93.6% | 94.9% |
| WRONG $T_0$ | 6.1% | 4.8% |
| NO $T_0$ | .3 % | .4% |

More information will be available after tests at TTR at the SSC Lab.

## Sub-appendix I - Contribution of Multiple Scattering in the Calorimeter.

**1.** To calculate $T_0$, the scheme requires the determination of $\alpha_2^T$ - inclination angle of a track in the SuperLayer#2 (superscript T stands for "Total"). This angle is $\alpha_2^T = \alpha_0 + \alpha_2$, where $\alpha_2$ is an angle due to track bending in the magnetic field, $\alpha_0$ is a geometrical angle (angle of a straight line coming out of the vertex). Angle $\alpha_2$ is momentum dependent and determined as follows (fig.A.IV.4):

$$\alpha_2 = \frac{d}{\Delta L} \text{ , where } \Delta L = L_3 - L_2 \text{ .}$$

**2.** If there is no multiple scattering, the track line is described by the following expression (fig.A.IV.1):

$$y = \frac{x^2}{2R} \text{ , where R = p / (eB) is a radius of cuvature .}$$

A muon coming out of the calorimeter has a y-coordinate $y_1$ and an inclination angle $\alpha_1^T$ ($\alpha_1^T = \frac{\partial y_1}{\partial x}$). (In the following calculations we will assume that axis X is perpendicular to the chamber. We are looking for the error in determination of angle $\alpha_2$ and this does not depend on a sector rotation with respect to a muon.)

**3.** The consequence of multiple scattering is that a muon has some displacement $\delta y_1$ and a slight change of an angle $\delta\alpha_1$ in the outcoming point. Let's call for simplicity sake $\delta y_1 = \Delta$ and $\delta\alpha_1 = \theta$. The RMS's and correlation of this parameters depend on the calorimeter thickness and are as follows:

$$\theta_0 = \frac{14.1 MeV}{\mathrm{p}} \sqrt{\frac{X_{cal}}{X_0}} ; \qquad \Delta_0 = \frac{1}{\sqrt{3}} X_{cal} \theta_0 ; \qquad \rho_{\theta\Delta} = \frac{\sqrt{3}}{2}$$

**4.** This results in a change of a trajectory; now it will be:

$$y = \frac{x^2}{2R} + bx + c$$

where b=θ and c=Δ-θ$L_1$ to satisfy new boundary conditions on the calorimeter surface.

5. Actual angle $\alpha_2$ will be:

$$\alpha_2 = \alpha_1^T - \alpha_0 = \frac{\partial y_2}{\partial x} - \frac{y_2}{L_2} = \frac{L_2}{2R} - \frac{c}{L_2} .$$

(Notice that this does not depend on the sector rotation.)

6. Angle $\alpha_2$ as measured ($\alpha_2 = \frac{d}{\Delta L}$):

$$\alpha_2^{meas} = \frac{\frac{L_2}{L_3} y_3 - y_2}{\Delta L} = \frac{1}{\Delta L}\left(\frac{L_2}{L_3}\left(\frac{L_3^2}{2R} + bL_3 + c\right) - \left(\frac{L_2^2}{2R} + bL_2 + c\right)\right) = \frac{L_2}{2R} - \frac{c}{L_3}$$

7. Error in Angle Measurement:

$$\delta\alpha_2 = \alpha_2^{meas} - \alpha_2 = \frac{c}{L_2} - \frac{c}{L_3} = (\Delta - \theta L_1)\frac{\Delta L}{L_3 L_2}$$

Taking into account RMS's and the correlation function one gets:

$$\overline{\delta\alpha_2^2} = \theta_0^2 (L_1^2 - L_1 X_{cal} + \frac{1}{3} X_{cal}^2) \frac{\Delta L^2}{L_3^{\,2} L_2^{\,2}} .$$

Using the LOI numbers ($L_1$=3.9m, $L_2$=6.3m, $L_3$=8.7m, X=2.5m, Cu calorimeter of effective 12λ thickness) for p=10 GeV/c one gets **an angle error of about δα~.002, which is smaller than the assumed measurement error (and, of course, it is far away from the biggest tolerable error)**.

8. Momentum Error Due to Multiple Scattering.

The angle $\alpha_2$ gives a measure of $p_T$.

Without multiple scattering:

$$\alpha_2(no\ \text{m.s.}) = \frac{L_2}{2R} = \frac{eBL_2}{2p} .$$

Due to multiple scattering, the measured angle will have an error:

$$\delta\alpha_2 = \alpha_2^{meas} - \alpha_2(no\ \text{m.s.}) = -\frac{c}{L_3},$$

which corresponds to a momentum error of **δp/p~.066**.

| y = m1*M0 + m2*M0*M0 | | |
|---|---|---|
| | Value | Error |
| m1 | 17.357073062 | 0.094725 |
| m2 | 0.28546071821 | 0.0104131 |
| Chisq | 13.306709135 | NA |
| R | 0.99994534341 | NA |

T=a*X + b*X^2
(Points are calculated
from accurate fit of LASER DATA).
Ar+IB =25+75

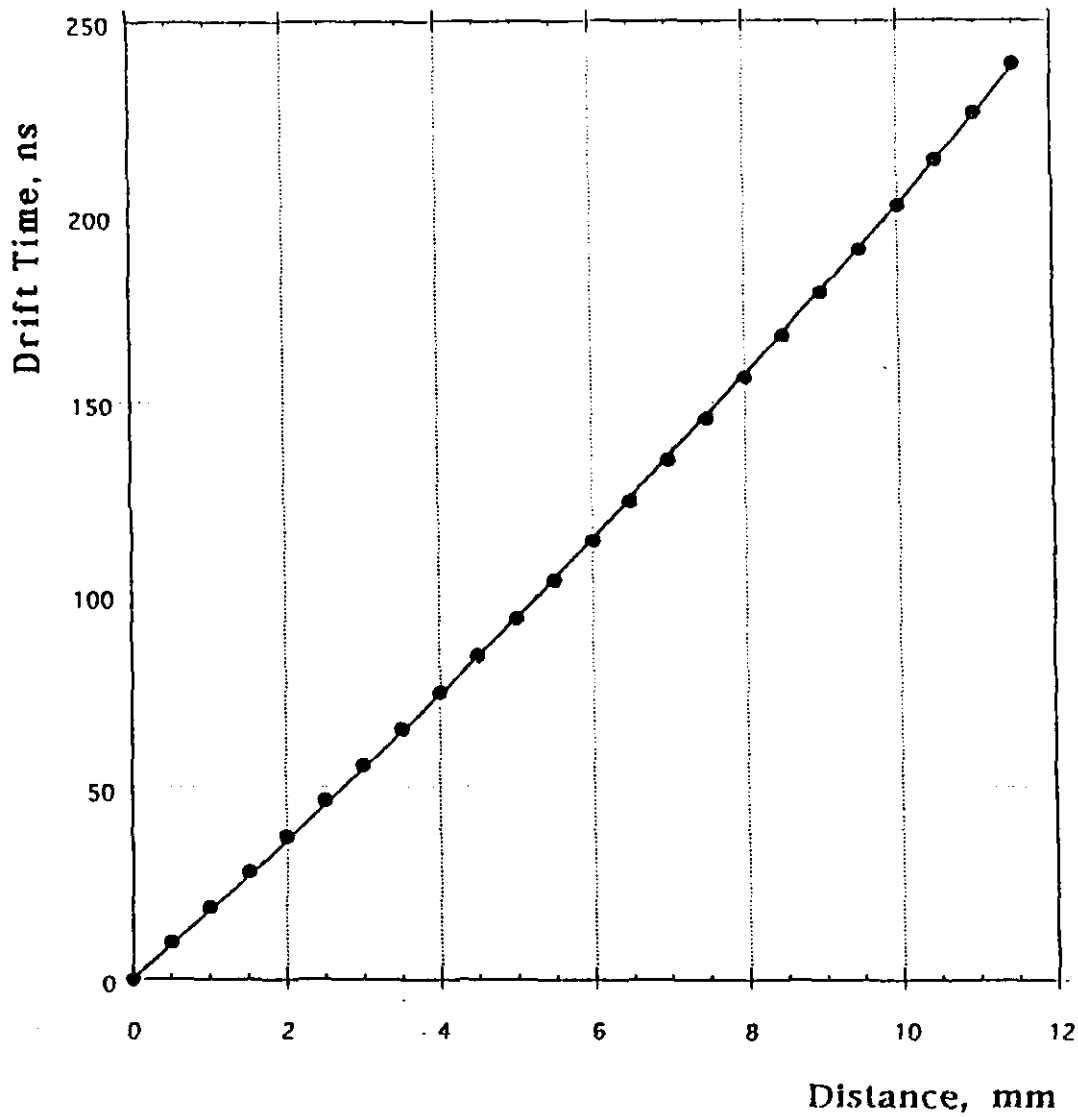


Fig.A.IV.1

| y = m1+m2*M0 + m3*M0*M0 | | |
|---|---|---|
| | Value | Error |
| m1 | 3.3417585497 | 0.484641 |
| m2 | 5.031063318 | 0.23408 |
| m3 | 1.4116950994 | 0.0239047 |
| Chisq | 2.9760939244 | NA |
| R | 0.99995388072 | NA |

$CF_4 + CO_2 + C_4H_{10} = 69 + 20 + 11$

U = 5.4 kV

Laser Data

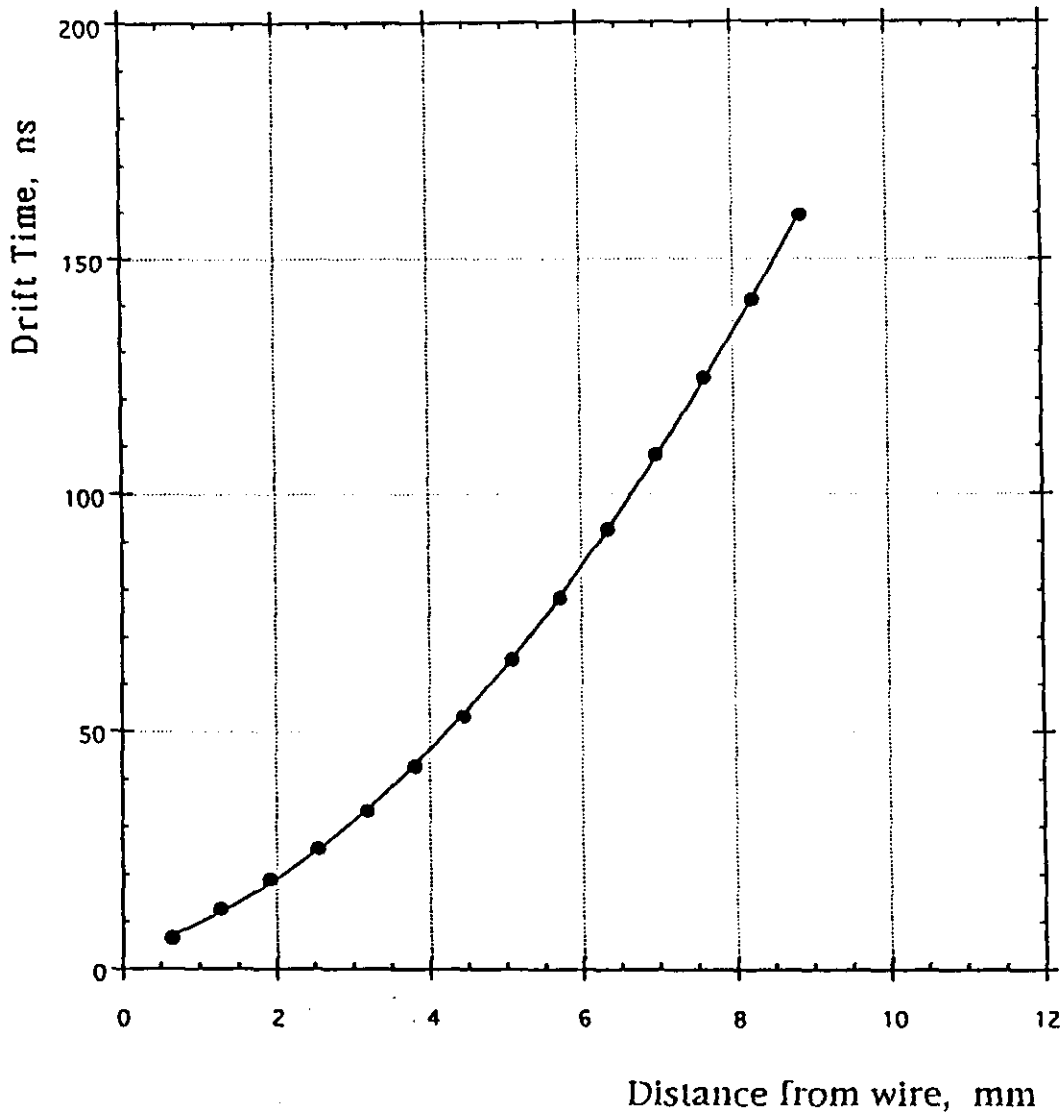


Fig.A.IV.2

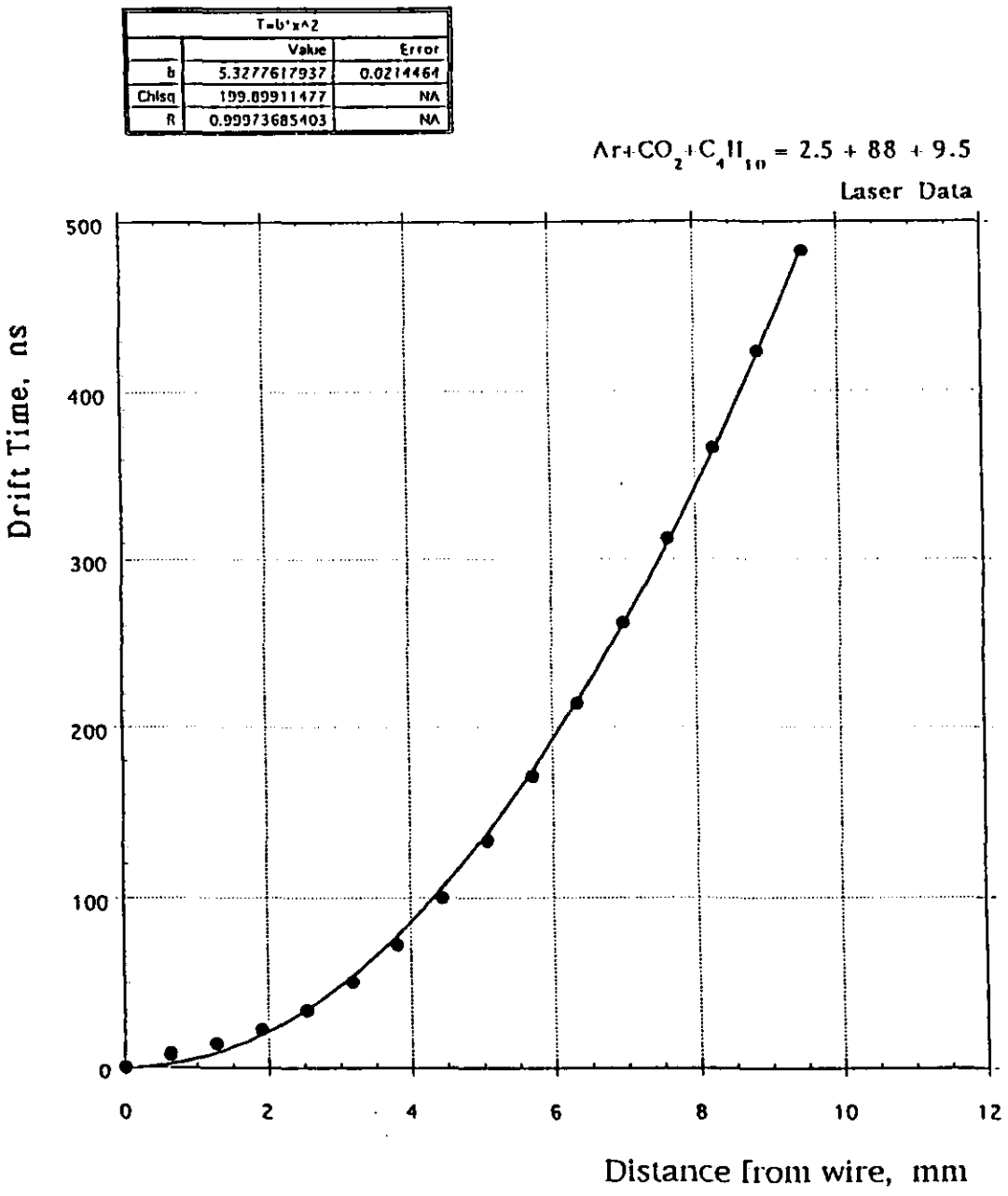
T=b*x^2
Value
Error
b
5.3277617937
0.0214464
Chisq
199.89911477
NA
R
0.99973685403
NA
Ar+CO2+C4H10 = 2.5 + 88 + 9.5
Laser Data
Drift Time, ns
500
400
300
200
100
0
0
2
4
6
8
10
12
Distance from wire, mm

Fig.A.IV.3

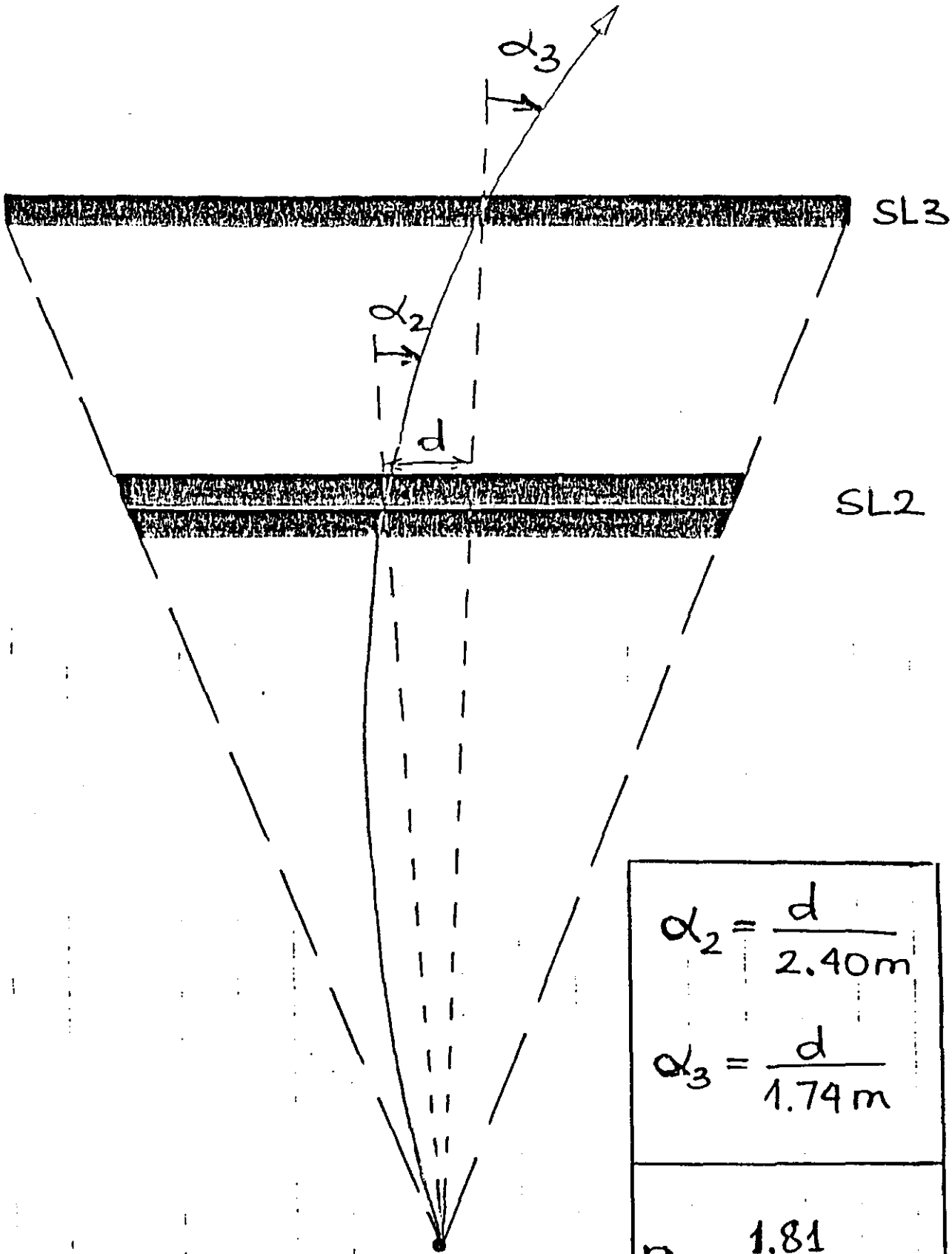


$$\alpha_2 = \frac{d}{2.40\,m}$$

$$\alpha_3 = \frac{d}{1.74\,m}$$

$$p = \frac{1.81}{d\,(m)}$$

$\alpha_2 = 4.4°$ for $p = 10$ GeV/c

Fig.A.IV.4

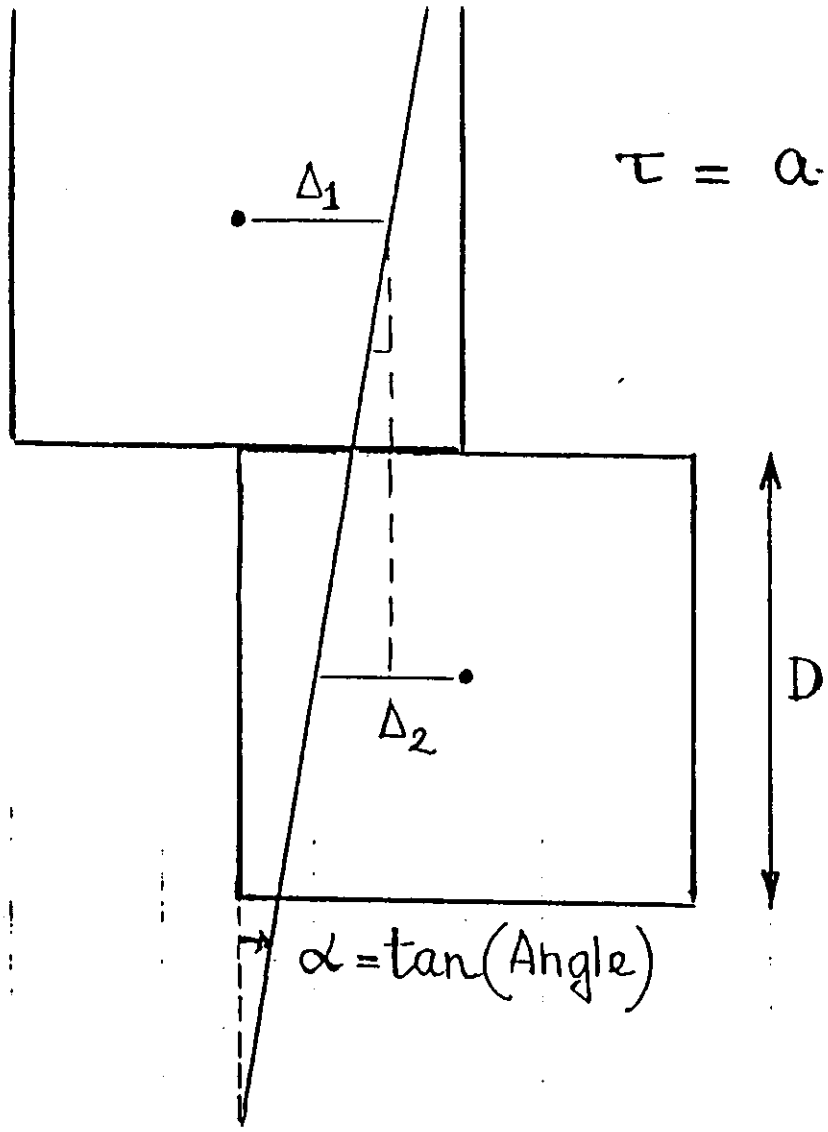


$$\tau = a \cdot \Delta + b \cdot \Delta^2$$

$$T_0 = \frac{T_1 + T_2}{2} - \frac{a \cdot C_0}{2} - \frac{b}{4}\left(C_0^2 + \frac{(\Delta T)^2}{(a + bC_0)^2}\right)$$

$$C_0 = \frac{D}{2} + \alpha \cdot D$$

Fig.A.IV.5

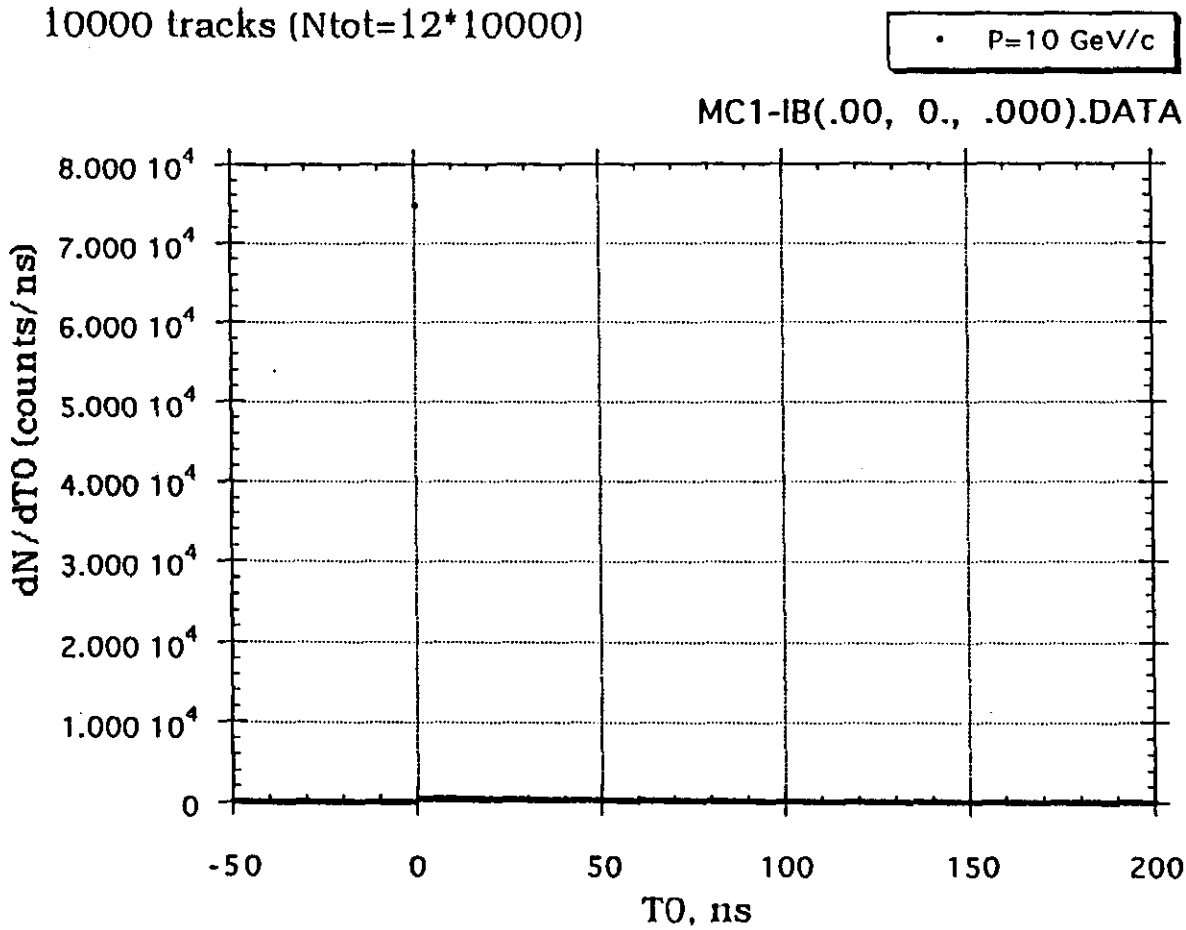
10000 tracks (Ntot=12*10000)
P=10 GeV/c
MC1-IB(.00, 0., .000).DATA
8.000 10^4
7.000 10^4
6.000 10^4
5.000 10^4
4.000 10^4
3.000 10^4
2.000 10^4
1.000 10^4
0
dN/dT0 (counts/ns)
-50
0
50
100
150
200
T0, ns

Fig.A.IV.6

-ps=.000 Terror(ns)=0.0 Aerror(rad)=.000

| | | | | |
|---|---|---|---|---|
| 10. GeV: | Nyes-Nno-Nwrong= | 9998 | 0 | 2 |
| 20. GeV: | Nyes-Nno-Nwrong= | 10000 | 0 | 0 |
| 40. GeV: | Nyes-Nno-Nwrong= | 10000 | 0 | 0 |
| 80. GeV: | Nyes-Nno-Nwrong= | 9998 | 0 | 2 |
| 160. GeV: | Nyes-Nno-Nwrong= | 9999 | 0 | 1 |
| 320. GeV: | Nyes-Nno-Nwrong= | 10000 | 0 | 0 |

| | | | | | | |
|---|---|---|---|---|---|---|
| 0 | 0 | 0 | 0 | 0 | 0 | 0 |
| 1 | 0 | 0 | 0 | 0 | 0 | 0 |
| 2 | 0 | 0 | 0 | 0 | 0 | 0 |
| 3 | 0 | 0 | 0 | 0 | 0 | 0 |
| 4 | 0 | 0 | 0 | 0 | 0 | 0 |
| 5 | 0 | 0 | 0 | 0 | 0 | 0 |
| 6 | 796 | 1003 | 1162 | 1199 | 1239 | 1245 |
| 7 | 2293 | 2593 | 2639 | 2642 | 2656 | 2716 |
| 8 | 5104 | 4673 | 4596 | 4510 | 4449 | 4417 |
| 9 | 1640 | 1565 | 1426 | 1468 | 1444 | 1447 |
| 10 | 165 | 162 | 171 | 176 | 208 | 166 |
| 11 | 2 | 2 | 5 | 5 | 4 | 7 |
| 12 | 0 | 2 | 1 | 0 | 0 | 2 |

COINCIDENCE LEVEL

| | | | | | |
|---|---|---|---|---|---|
| P=10 GeV/c | =20 | =40 | =80 | =160 | =320 |

Table 1

$CF_4+CO_2+C_4H_{10}$ = 69+20+11

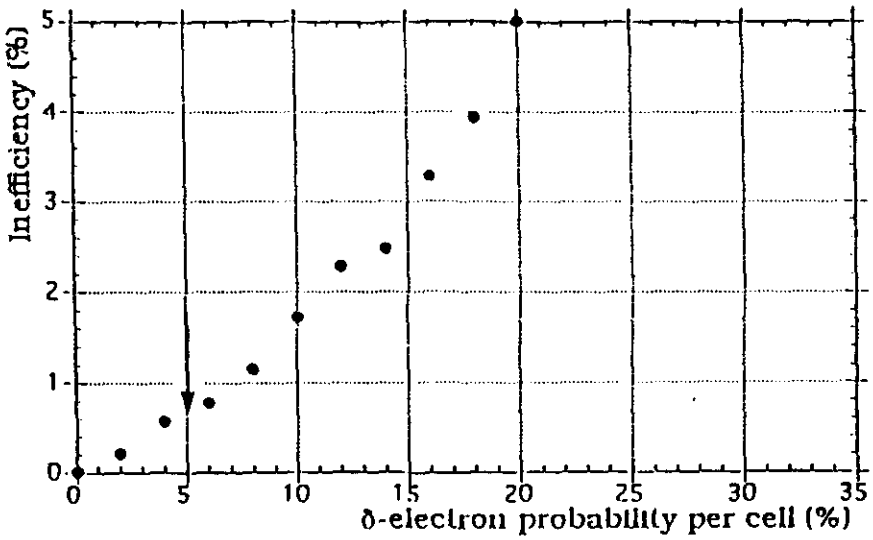


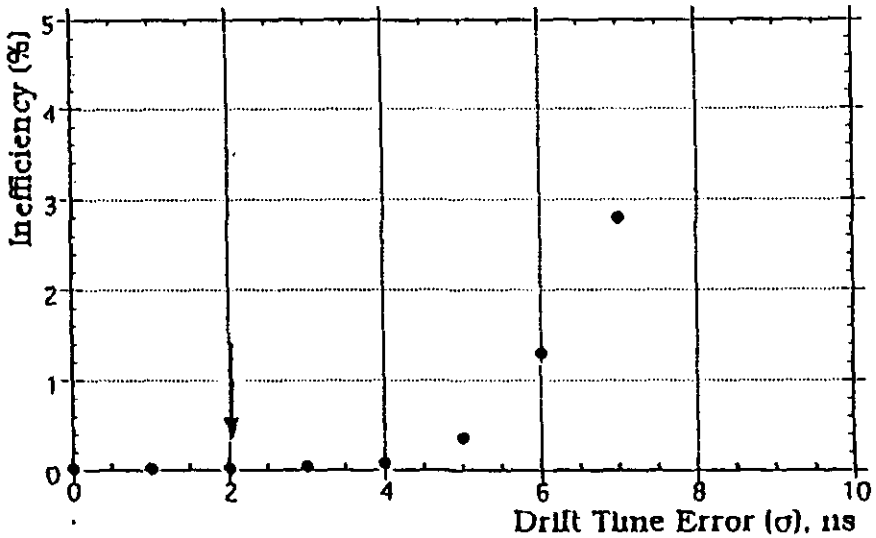


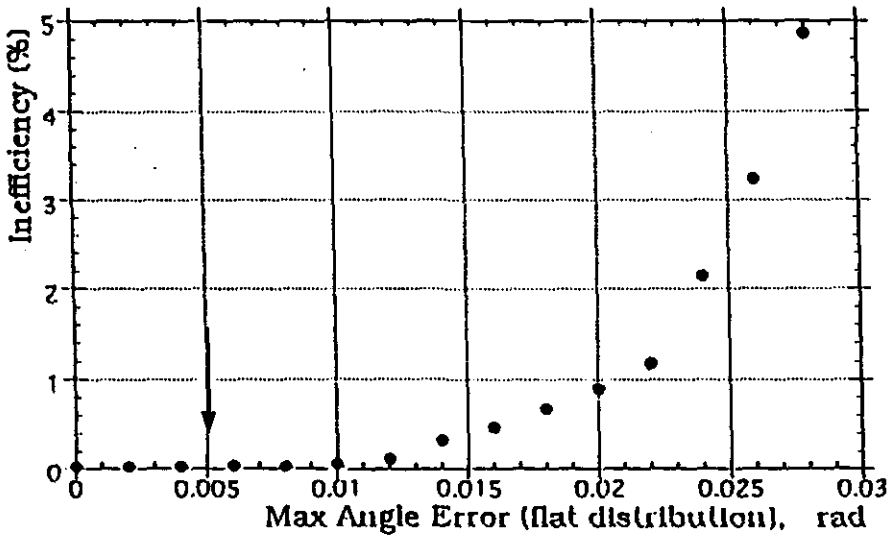


Fig.A.IV.7

SL2

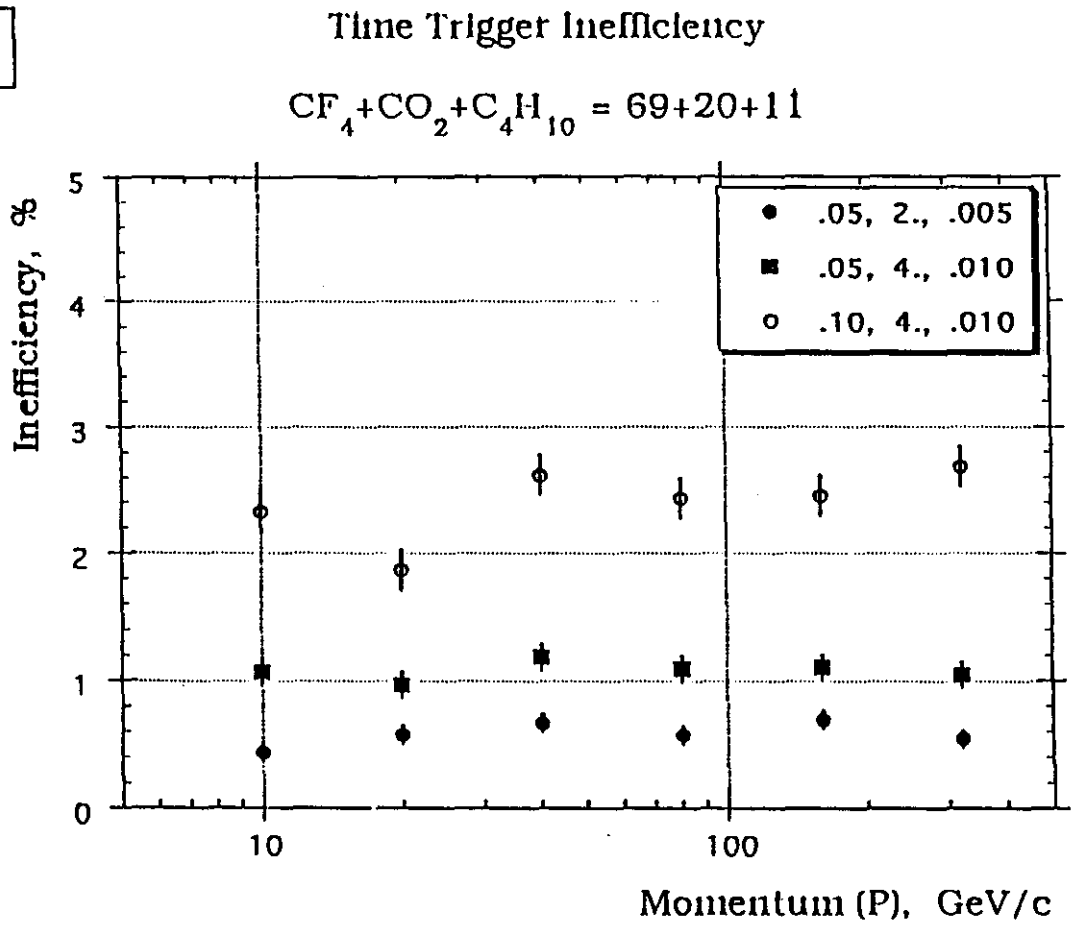
Time Trigger Inefficiency
$CF_4+CO_2+C_4H_{10}$ = 69+20+11
Inefficiency, %
0
1
2
3
4
5
10
100
Momentum (P), GeV/c
.05, 2., .005
.05, 4., .010
.10, 4., .010

Fig.A.IV.8

SL2

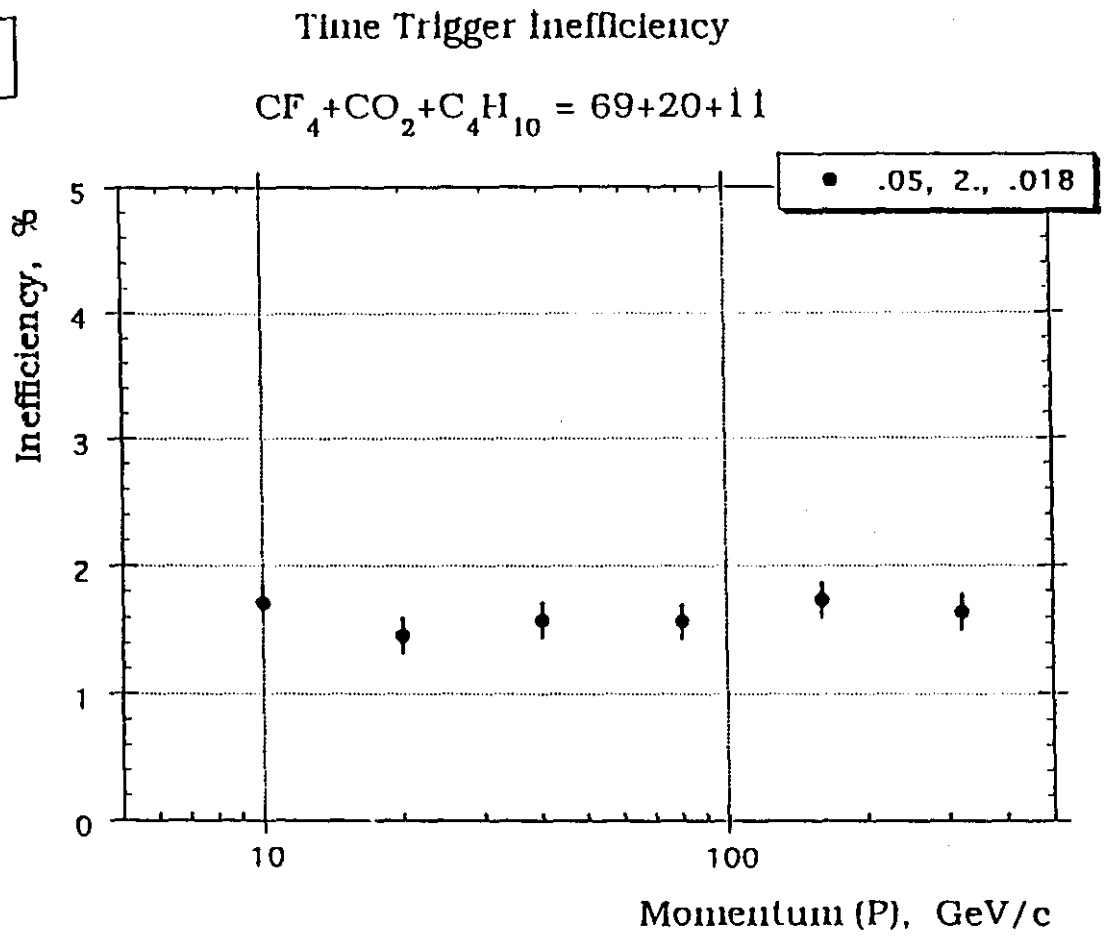
Time Trigger Inefficiency
$CF_4+CO_2+C_4H_{10}$ = 69+20+11
.05, 2., .018
Inefficiency, %
0
1
2
3
4
5
10
100
Momentum (P), GeV/c

Fig.A.IV.9

SL2

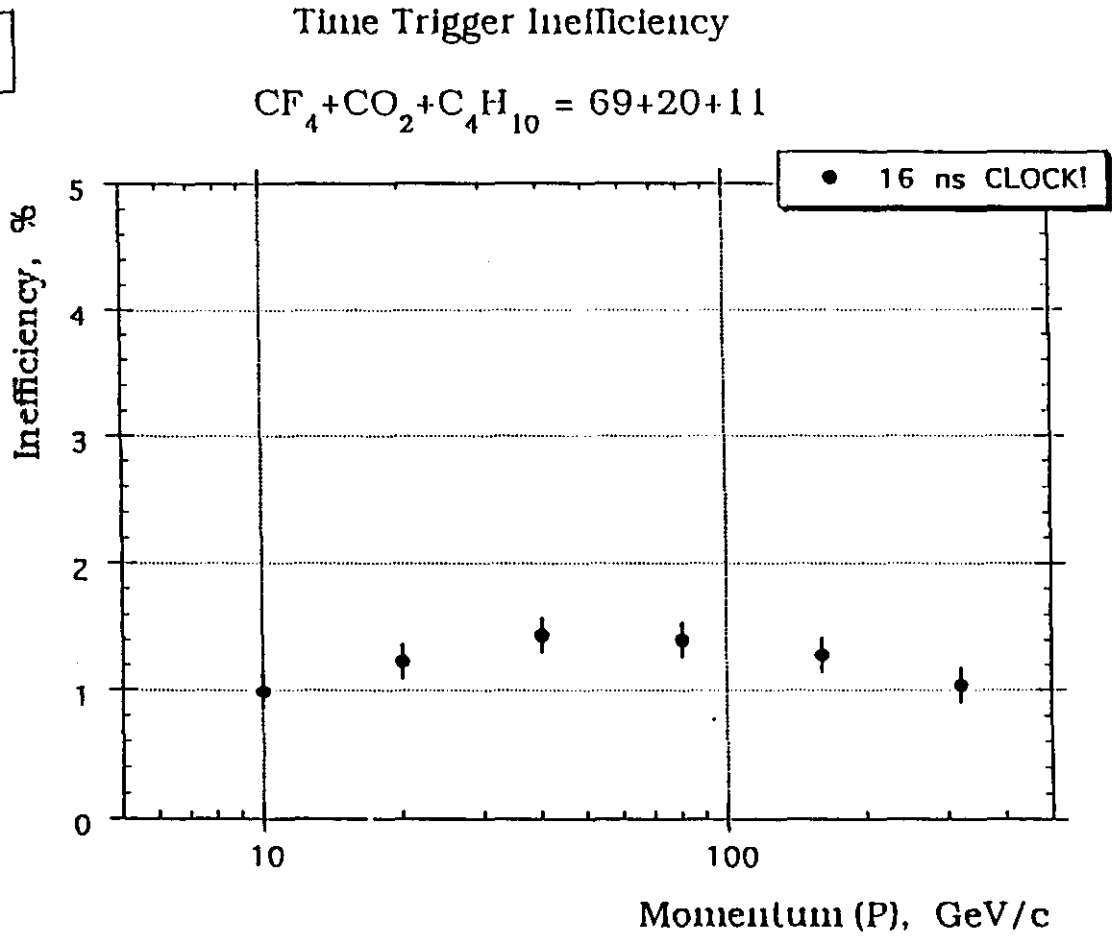


Fig.A.IV.10

$CF_4+CO_2+C_4H_{10}$ = 69+20+11

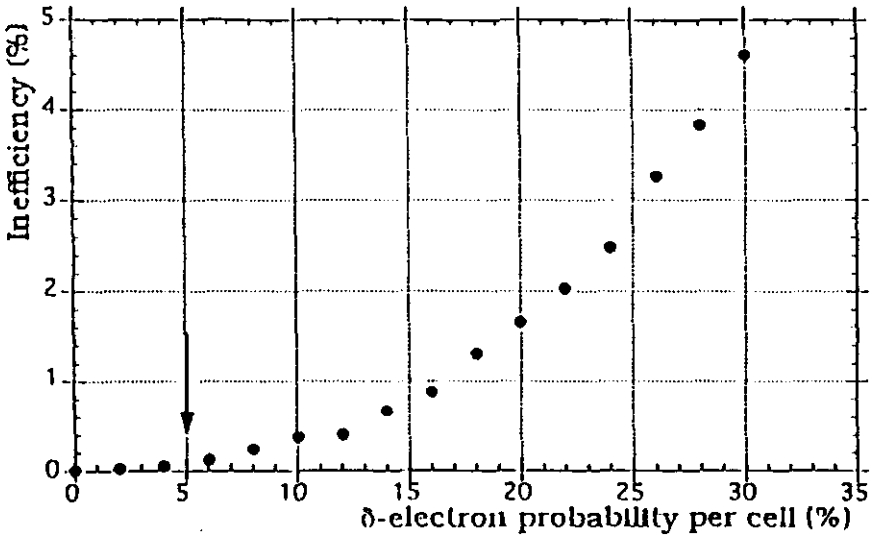


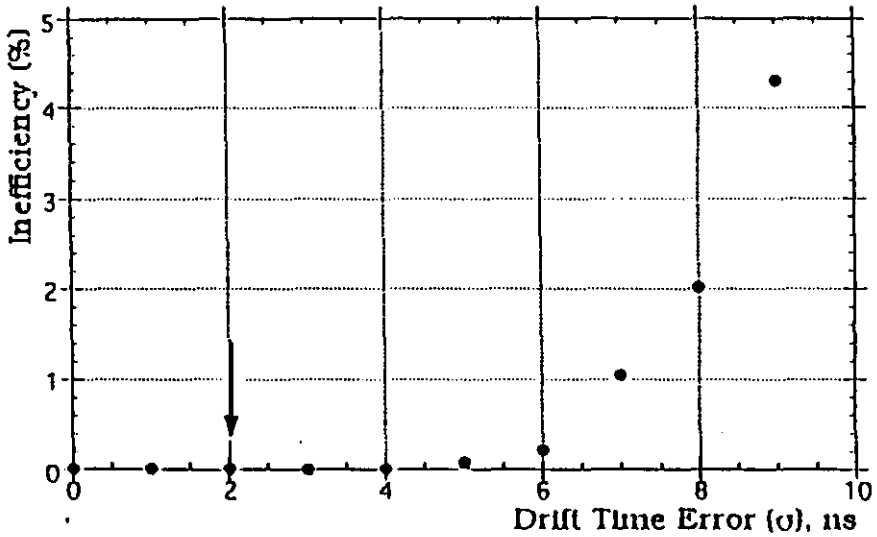


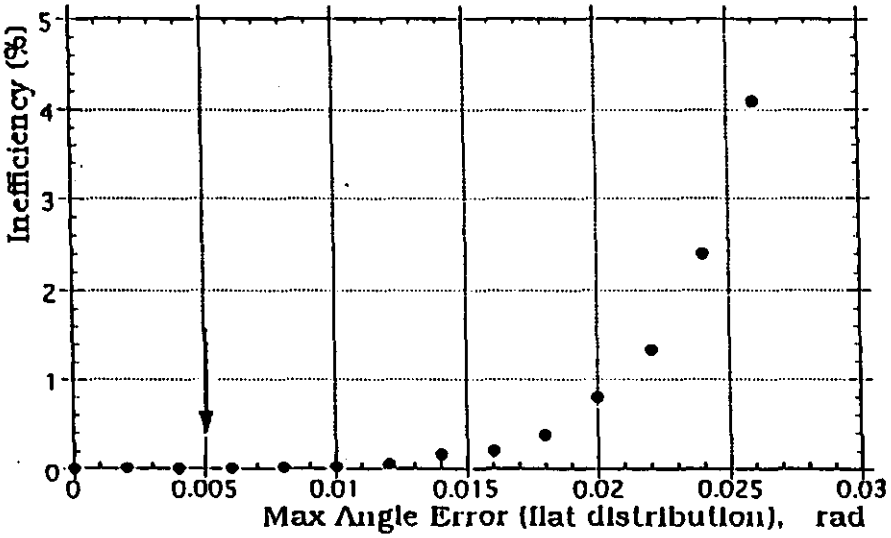


Fig.A.IV.11

$(a+bC_0)^2$

CONSTANTS

( INPUTS : T1, T2, $\alpha$, a, b, C1, C2 )

| | | | |
|---|---|---|---|
| # 0 INPUT | X1 = T1 | Y1 = T2 | Z1 = $\alpha$ |
| # 1 | X1 = X1 + Y1 ($T_1+T_2$) | Y1 = X1 − Y1 ($T_1-T_2$) | Z1 = Z1 · C2 ($\alpha C_2$) |
| # 2 | X1 = X1/2 ($\frac{T_1+T_2}{2}$) | Y1 = Y1 * Y1 $(T_1-T_2)^2$ | Z1 = Z1 + C1 ($C_0=(a+\alpha C_2)$) |
| # 3 | X2 = a · Z1 ($a\cdot C_0$) | Y2 = Z1 * Z1 $(C_0)^2$ | Z1 = b · Z1 ($b\cdot C_0$) |
| # 4 | X2 = X2/2 ($\frac{a}{2}C_0$) | Y2 = b · Y2 ($bC_0^2$) | Z1 = a + Z1 ($a+bC_0$) |
| # 5 | X1 = X1 − X2 ($\frac{T_1+T_2}{2}-\frac{a}{2}C_0$) | Y2 = Y2/4 ($\frac{b}{4}C_0^2$) | Z1 = Z1 * Z1 $(a+bC_0)^2$ |
| # 6 | X1 = X1 − Y2 ($\frac{T_1+T_2}{2}-\frac{a}{2}C_0-\frac{b}{4}C_0^2$) | Y2 = b/4 ($\frac{b}{4}$) | Z1 = Y1/Z1 $(\Delta T^2/(a+bC_0)^2$) |
| # 7 | — | — | Z1 = Z1 * Y2 $\frac{b}{4}(\Delta T^2/(a+bC_0)^2)$ |
| # 8 | X1 = X1 − Z1 ($T_0$) | — | — |

Table 2

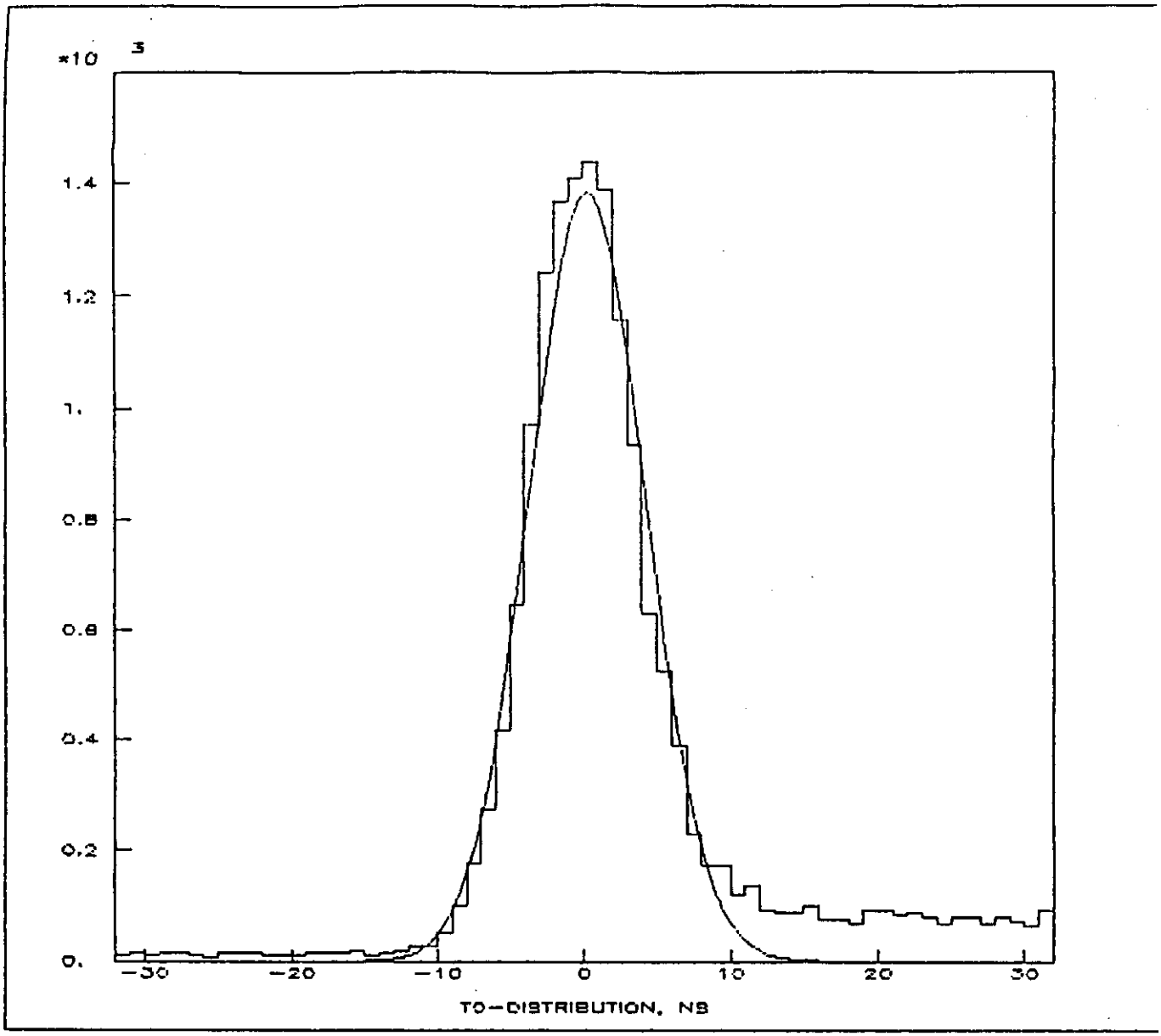


Fig.A.IV.12(a)

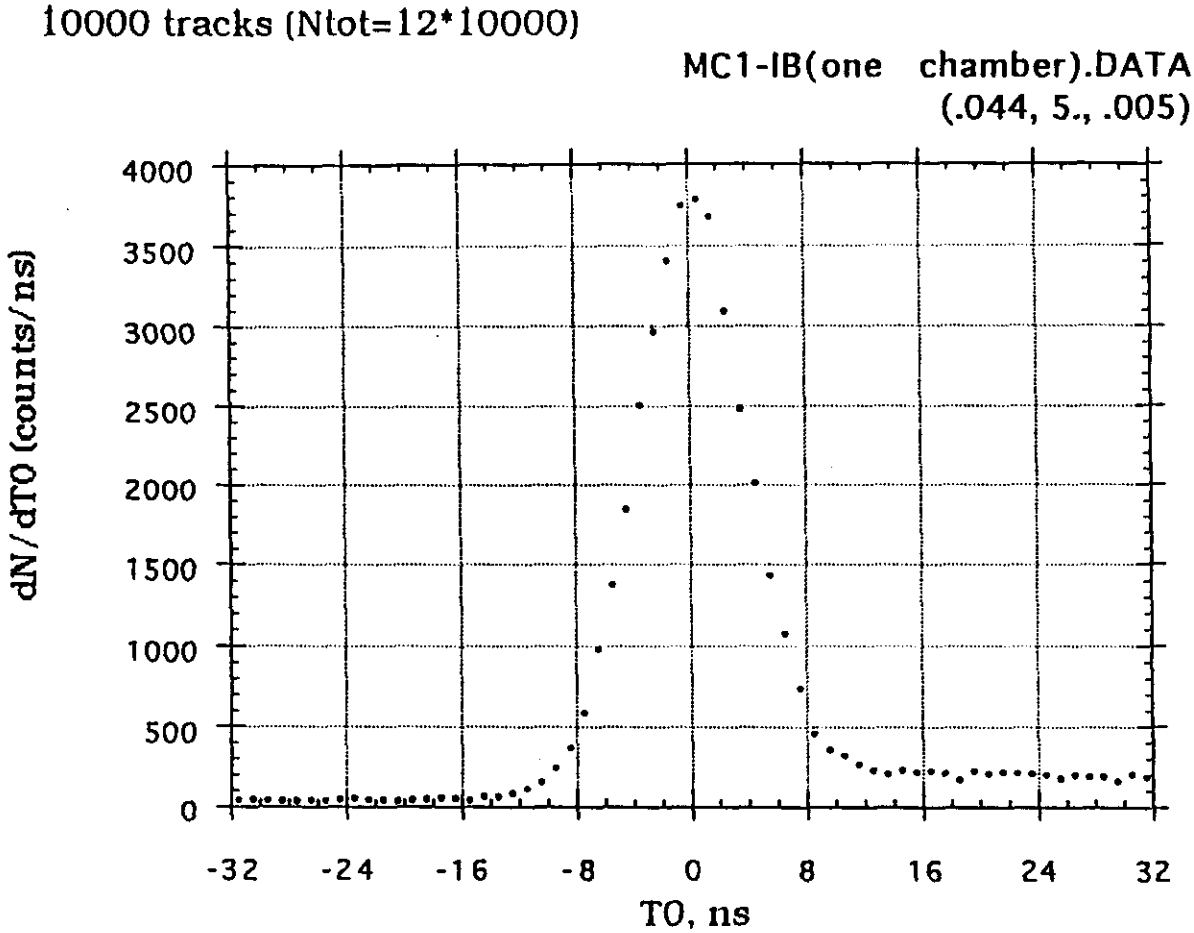
10000 tracks (Ntot=12*10000)
MC1-IB(one chamber).DATA
(.044, 5., .005)
dN/dT0 (counts/ns)
4000
3500
3000
2500
2000
1500
1000
500
0
-32
-24
-16
-8
0
8
16
24
32
T0, ns

Fig.A.IV.12(b)

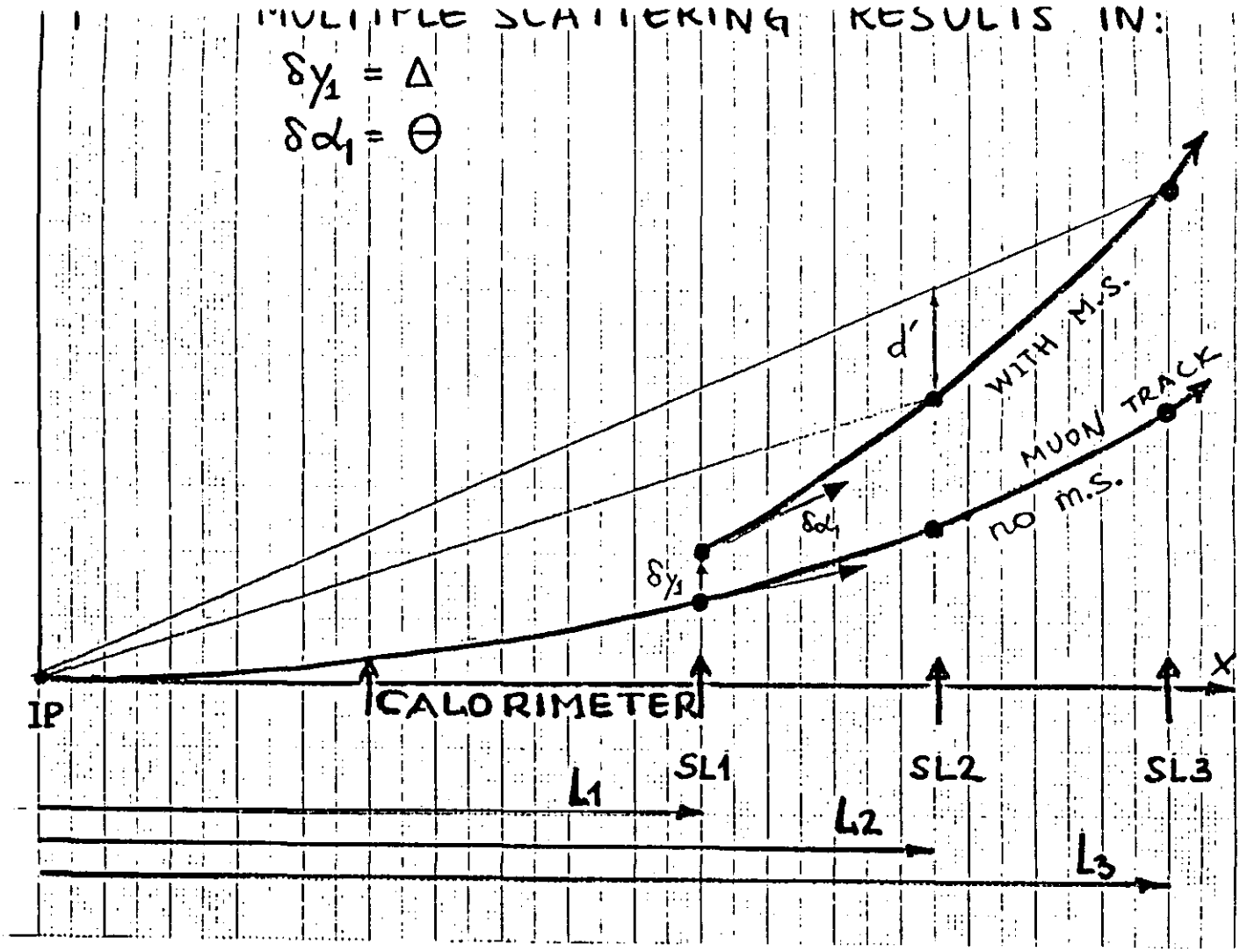
MULTIPLE SCATTERING RESULTS IN:
$\delta y_1 = \Delta$
$\delta \alpha_1 = \Theta$
d'
WITH M.S.
MUON TRACK
NO M.S.
$\delta \alpha_1$
$\delta y_1$
IP
CALORIMETER
SL1
SL2
SL3
X
$L_1$
$L_2$
$L_3$

Fig.A.IV.

## Appendix V: Answers to "Expectations for the October 1 Report"

In this appendix we include short answers to the queries proposed in the "Expectations....." and in that format to summarize our proposal. Details relevant to each topic can be found in the main text or in referenced material.

### (I) Performance-Spatial

(1) Wire resolution(but includes bridge misalignment errors)

(a) with $CO_2$ gas: 103 $\mu$m achieved

(b) with Argon-Isobutane: 70$\mu$m achieved

(c) with $CF_4$ gas: 72 $\mu$m in Fermilab tests

(2) Alignment

(a) Wire to wire: 23 $\mu$m achieved

(b) Layer to layer: $\sim$ 20 $\mu$m achieved

(c) Super to super: Optically-for each triplet we get $\sim$ 5 $\mu$m. So with 4 serial measurements we would estimate 10 $\mu$m

### (II) Lorentz angle

We measure a small shift in drift time in a 0.8 Tesla field- 10 nsec out of 300 nsec. and inappreciable change in resolution- $\sim$ 10% worse

### (III) Performance-Temporal

(1) Rate capability

(a) Dead time: 100 nsecs/wire

(b) Local wire limitation:$\sim$ several msec within 5 mm of a previous hit

(c) Global limitation:negligible; 1 $\mu$sec for triggering purposes

### (IV) Performance-Backgrounds

(1) Sensitivity to neutrons: We measured the "efficiency" for neutrons in our chamber tube to be 0.5%. With the neutron fluxes expected this amounts to a 10 kHz rate in a

typical wire (8 meters long). A life time for such a wire with no particular precautions would be $\sim$ 200 years at a luminosity of $10^{33}$ cm$^2$/sec.

(2) Sensitivity to gamma rays:We measured this with the capture gammas from a borated polyethlene moderator surrounding a $Cf^{252}$ source, the expected gammas from the GEM surround. 5 cm of lead reduced the counting rate in our tubes to the level of the neutron rate.

**(V) Pattern Recognition Capability**

Since we have z-strips with time correlation we get an x-y measurement on a track. The only limitation on resolving a bundle of tracks would be to have two tracks in the same tube within the time resolution of the electronics i.e. within 100 nsec.

**(VI) Sensitivity to Environment**

(1) Temperature (i.e. density): for a 1% change in density, there would be a spatial change of 17 $\mu$m for A-Isobutane and 50 $\mu$m for a $CO_2$ based gas. Pressure and temperature must be monitored.

(2) Gas mixture: The gas mixture must be mixed to 1% precision. Even then a velocity monitor will be used in the incoming and outgoing gas.

(3) Noise: To disturb our accuracy electrical noise would have to be in the mvolts range. The wires are totally enclosed in a metal box.

**(VII) Robustness**

(1) Wire loss: One wire break or attachment slip only loses one tube.

(2) Wire security: The wires are held in their assigned grooves with a drop of epoxy; they do not move.

(3) Mechanical rigidity:The 1x4 meter chamber flexes $< 25$ $\mu$m in the 4 m direction and 4 mm in the 17 cm direction (depth) when supported at both ends.

**(VIII) Cost**

see Sect. VI of the main text. The total for manufacture and assembly (excluding electronics) is \$ 24.7x$10^6$. We believe this number may be too high by \$ 4x$10^6$ due to a misunderstanding on the part of one of the estimators.

**(IX) Safety**

We would like not to exclude the use of an Argon-Isobutane mixture at the present time. If used, this would present a flammability problem

## Level 1 Triggering

(I) Beam crossing tagging time:

(1) Time jitter: $< 10$ nsec

(2) Complexity: Relativally complex but straight forward.

(II) Trigger formation time: 1 $\mu$sec

(III) Sensitivity to backgrounds: We estimate that the presence of backgrounds, delta rays and neutrons, would reduce the trigger efficiency to 99% at a luminosity of $10^{34}$ sec/cm$^2$.

(IV) Costs \$21.4/channel

## Appendix VI: Detail of Costs

The following pages are the work sheets from which the costs for the construction of the full LSDT system are based. We also have back-up letters on most of the items.

# MUON SYSTEM
# COST ESTIMATION WORKSHEET

**WBS Element Title:** Central Region Sector Assembly; LSDTs; Off-Site; Shipping

**WBS Element No:** 03.2.1.2.3.1.1 **Date:** 16 June 92 **Rev:** 0 **Estimator:** T. Hamilton

**Scope:** This element covers the labor and cost required for packaging and shipping the assembled LSDTs.

**Engineering/Design** **PY:** **Comp. Rate($K/PY):** **PoP:**
N/A

**M&S: Engineering/Design and Inspection/Administration** **($K):** 2
Misc. office supplies for Engineering/Design: $1K
PC/Mac/workstation charges: $1K

**Inspection/Administration** **PY:** .23 **Comp. Rate($K/PY):** 69 **PoP:** 1/95-10/96
Assumes Eng (SSCL) oversight of packag/shipp activity: 1 eng, averaging 1/8-time for 22 mos = .23 PY

**Procurement/Fabrication Material** **($K)** 50
Misc. packaging material/pallets: $50K

**Installation/Assembly** **PY:** .46 **Comp. Rate($K/PY):** 107 **PoP:** 1/95-10/96
Assumes Sr. Technician (nat'l avg) packaging activity: 2 techs, 1/8-time for 22 mos = .46 PY

**Material: Installation/Assembly** **($K)** 101
Misc. office supplies for Install/Assembly: $1K
Shipping charge estimate $100K

**Contingency** **Total:** 30

| | | | |
|---|---|---|---|
| Technical: | 16 | Basis: | new design, some R&D required |
| Cost: | 6 | Basis: | in-house estimate, minimal experience |
| Schedule: | 8 | Basis: | delays completion of critical path item |

**Comments**

# MUON SYSTEM
# COST ESTIMATION WORKSHEET

**WBS Element Title:** Central Region Sector Assembly; LSDTs; Off-Site; Test

**WBS Element No:** 03.2.1.2.3.1.2 **Date:**29 June 92 **Rev:** 0 **Estimator:** J. Kelsey

---

**Scope:** This element covers the labor and labor cost required for testing the LSDTs during and after assembly.

---

**Engineering/Design** **PY:** **Comp. Rate($K/PY):** **PoP:**
N/A

---

**M&S: Engineering/Design and Inspection/Administration** **($K):** 3
Misc. office supplies for Engineering/Design: $1K
PC/Mac/workstation charges: $2K

---

**Inspection/Administration** **PY:** .50 **Comp. Rate($K/PY):** 133 **PoP:** 8/94-7/96
Assumes Engineering (nat'l avg) oversight of test activity: 1 eng, 1/4-time for 2 yrs = .50 PY

---

**Procurement/Fabrication Material** **($K)** 354
from Weinstein/Osborne estimate:

| | |
|---|---|
| wire seating, laser checker: | $40K |
| wire clamping tester: | $4K |
| leak tester: | $8K |
| Mac IIx, Mac, scope, MCA, Amps, HV | $292K |
| Assumed misc. equip: | $10K |

---

**Installation/Assembly** **PY:** 5.66 **Comp. Rate($K/PY):** 110 **PoP:** 8/94-7/96
from Weinstein/Osborne estimate:

| | |
|---|---|
| wire seating, laser checker set-up: 1 eng (nat'l avg) full-time for 4 mos | .33 PY |
| 1 sr. tech (nat'l avg), full-time for 4 mos | .33 PY |
| wire clamping tester set-up: 1 eng (nat'l avg) full-time for 3 mos | .25 PY |
| 1 sr. tech (nat'l avg), full-time for 3 mos | .25 PY |
| leak tester set-up: 1 eng (nat'l avg) full-time for 1 mos | .08 PY |
| 1 sr. tech (nat'l avg), full-time for 5 mos | .42 PY |

-although Wein/Os estimate was for central and end cap regions, set-up is still required, therefore no 76% scaling

Assumes Sr. Technician (nat'l avg) test activity: 2 techs, full-time for 2 yrs = 4.00 PY

---

**Material: Installation/Assembly** **($K)** 7
Misc. office supplies for Install/Assembly: $7K

---

**Contingency** **Total:** 30

| | | | |
|---|---|---|---|
| Technical: | 16 | Basis: | new design, some R&D required |
| Cost: | 6 | Basis: | in-house estimate, minimal experience |
| Schedule: | 8 | Basis: | delays completion of critical path item |

---

**Comments**

# MUON SYSTEM
# COST ESTIMATION WORKSHEET

**WBS Element Title:** Central Region Sector Assembly; LSDTs; Off-Site; Assembly

**WBS Element No:** 03.2.1.2.3.1.3 **Date:**29 June 92 **Rev:** 0 **Estimator:** J. Kelsey

---

**Scope:** This element covers the labor and labor cost for the assembly of the LSDT chambers, and the cost for purchasing assembly equipment..

---

**Engineering/Design** **PY:** **Comp. Rate($K/PY):** **PoP:**
N/A

---

**M&S: Engineering/Design and Inspection/Administration** **($K):** 14

| | |
|---|---|
| Misc. office supplies for Administration | $5K |
| PC/Mac/workstation charges: | $8K |

---

**Inspection/Administration** **PY:** 2.25 **Comp. Rate($K/PY):** 133 **PoP:** 7/94-6/96

Assumes Eng (nat'l avg) oversight of assy equipment purchase activity: 1 eng, full-time for 3 mos = .25 PY
from Weinstein/Osborne estimate: ('cost of production')
- reduced to 76% (for central region only), actually reduced from 36 mos to 24 mos (67%)
Assumes Eng (nat'l avg) oversight of assembly activity: 1 eng, full-time for 2 years = 2.00 PY

---

**Procurement/Fabrication Material** **($K)** 405

| | |
|---|---|
| from Weinstein/Osborne estimate: | |
| wiring machine: | $40K |
| automatic solderer | $18K |
| automatic wire cutter: | $5K |
| Assumed misc. nuts/bolt, pins, etc: | $50K |

---

**Installation/Assembly** **PY:** 28.00 **Comp. Rate($K/PY):** 94 **PoP:** 7/94-6/96

| | |
|---|---|
| from Weinstein/Osborne estimate: | |
| wiring machine set-up: 1 eng (nat'l avg) full-time for 6 mos | .50 PY |
| 1 sr. tech (nat'l avg), full-time for 6 mos | .50 PY |
| automatic solderer set-up: 1 eng (nat'l avg) full-time for 4 mos | .33 PY |
| 1 sr. tech (nat'l avg) full-time for 4 mos | .33 PY |
| automatic wire cutter: 1 eng (nat'l avg) full-time for 2 mos | .17 PY |
| 1 sr. tech (nat'l avg) full-time for 2 mos | .17 PY |
| assembly: 5 sr. techs (nat'l avg) full-time for 24 mos | 10.00 PY |
| 8 jr. tech (nat'l avg), full-time for 24 mos | 16.00 PY |

---

**Material: Installation/Assembly** **($K)** 24

| | |
|---|---|
| Misc. office supplies for Install/Assembly | $24K |

---

**Contingency** **Total:** 30

| | | | |
|---|---|---|---|
| Technical: | 16 | Basis: | new design, some R&D required |
| Cost: | 6 | Basis: | in-house estimate, minimal experience |
| Schedule: | 8 | Basis: | delays completion of critical path item |

---

**Comments**

**MUON SYSTEM**
**COST ESTIMATION WORKSHEET**

**WBS Element Title:** Central Region Sector Assembly; LSDTs; Off-Site; Fac Prep

**WBS Element No:** 03.2.1.2.3.1.4 **Date:** 29 June 92 **Rev:**0 **Estimator:** J. Kelsey

---

**Scope:** This element covers the labor and labor costs for preparing LSDT chamber assembly off-site facility for assembly/test, etc. for the LSDT chambers.

---

**Engineering/Design** **PY:** **Comp. Rate($K/PY):** **PoP:**
N/A

---

**M&S: Engineering/Design and Inspection/Administration** **($K):** 5
Misc. office supplies for Inspection/Administration: $2K
Misc. office supplies for Installation/Assembly: $3K

---

**Inspection/Administration** **PY:** .75 **Comp. Rate($K/PY):** 133 **PoP:** 1/94-9/94
from Weistein/Osborne estimate ('factory set-up):
Engineer (nat'l avg) oversight of set-up: 1 eng, full-time for 9 mos = .75 PY

---

**Procurement/Fabrication Material** **($K)**
N/A

---

**Installation/Assembly** **PY:** 3.75 **Comp. Rate($K/PY):** 97 **PoP:** 1/94-9/94
from Weistein/Osborne estimate ('factory set-up):
Sr. Tech (nat'l avg) perform set-up: 3 sr. tech, full-time for 9 mos = 2.25 PY
Jr. Tech (nat'l avg) perform set-up: 2 jr. tech, full-time for 9 mos = 1.50 PY

---

**Material: Installation/Assembly** **($K)** 365
Misc. office supplies for Installation/Assembly: $5K
Rent/Lease 24000 sqft (from Weinstein/Osborne est) $120k/yr for 3 yrs $360K

---

**Contingency** **Total:** 23

| | | | |
|---|---|---|---|
| Technical: | 0 | Basis: | none |
| Cost: | 15 | Basis: | engineering judgement, manpower level concern |
| Schedule: | 8 | Basis: | delays completion of critical path item |

---

**Comments**

# MUON SYSTEM
# COST ESTIMATION WORKSHEET

**WBS Element Title:** Central Region Sector Assembly; LSDTs; Off-Site; Machining/Inspection

**WBS Element No:** 03.2.1.2.3.1.5 **Date:** 29 June 92 **Rev:** 1 **Estimator:** Hamilton/Weinstein/Osborne/Kelsey

**Scope:** This element covers the labor and labor costs for the machining and inspection of LSDTs and assembly fixturing. Also, costs for oversight and purchasing of stock and material for machining.

---

**Engineering/Design** **PY:** **Comp. Rate($K/PY):** **PoP:**

N/A

---

**M&S: Engineering/Design and Inspection/Administration** **($K):** 42

| | |
|---|---|
| Misc. office supplies for Inspection/Administration: | $14K |
| PC/Mac/workstation charges: | $20K |
| Travel: 1 person, 4 trips to machine shop, inspection shop @$2K/trip | $8K |

---

**Inspection/Administration** **PY:** 5.63 **Comp. Rate($K/PY):** 68 **PoP:** 1/94-3/96

Assumes Engineering (nat. avg) oversight of stock/mat'l purchase activity: 1/4-time for 24 mos = .50 PY
Assumes Engineering (nat'l avg) oversight of machng & inspect activity: 1/2-time for 2.25 yrs = 1.13 PY
Assumes Sr. Tech (job shop) performing inspection activity: 1 tech, full-time for 2 yrs = 2.00 PY
Assumes Jr. Tech (job shop) performing inspection activity: 1 tech, full-time for 2 yrs = 2.00 PY
- estimate of $100K (approx. 2 PY) for inspection, from Weinstein/Osborne estimate, approx. doubled

---

**Procurement/Fabrication Material** **($K)** 15397

from Weinstein/Osborne estimate:

| | |
|---|---|
| aluminum enclosures: | $7280K |
| bridges: | $1450K |
| wire: | $298K |
| cathode planes: | $4300K |
| misc: | $80K |
| general M&S (nuts, screws, etc.) | $50K |
| Hexcell (top & bottom) | $1517K |
| capital equipment | $280K |
| tooling | $142K |

---

**Installation/Assembly** **PY:** 62.13 **Comp. Rate($K/PY):** 47 **PoP:** 1/94-12/95

from Weinstein/Osborne estimate:

Assumes physicist (job shop), 1.28 physt. full-time for 5 yr = 6.38 PY
Assumes machinist (job shop), 4.06 mchst. full-time for 2 yr = 8.12 PY
Assumes senior technician (job shop), 3.58 sr.tech. full-time for 5 yr = 17.87 PY
Assumes junior technician (job shop), 5.95 jr.tech. full-time for 5 yr = 29.76 PY

---

**Material: Installation/Assembly** **($K)** 75

Misc. office supplies for Installation/Assembly = $75K

---

**Contingency** **Total:** 30

| | | | |
|---|---|---|---|
| Technical: | 16 | Basis: | new design, some R&D required |
| Cost: | 6 | Basis: | in-house estimate, minimal experience |
| Schedule: | 8 | Basis: | delays completion of critical path item |

# MUON SYSTEM
# COST ESTIMATION WORKSHEET

**WBS Element Title:** Central Region Sector Assy; LSDTs; Off-Site; LSDT and Assy Fixt Final Design

**WBS Element No:** 03.2.1.2.3.1.6 **Date:**29 June 92 **Rev:** 0 **Estimator:** J. Kelsey

---

**Scope:** This element covers the labor and labor cost required for completing the final design of the LSDT chambers and chamber assembly fixturing, and modifying/generating drawings/specs.

---

**Engineering/Design** **PY:** 3.25 **Comp. Rate($K/PY):** 102 **PoP:** 7/93-12/93

Assumes Eng. (nat'l avg) complete LSDT final design: 2 eng, full-time for 6 mos = 1 PY
Assumes Eng. (nat'l avg) complete assy fixt final design: 1 eng, full-time for 3 mos = .25 PY
Assumes Eng. (nat'l avg) complete spec modification: 1 eng, full-time for 6 mos = .50 PY
Assumes Drafting (nat'l avg) complete LSDT & fixture drawings: 4 draftsman, full-time for 9 mos = 3.00 PY

---

**M&S: Engineering/Design and Inspection/Administration** **($K):** 20

| | |
|---|---|
| Misc. office supplies for Engineering/Design and Inspection/Administration: | $8K |
| PC/Mac/workstation charges: | $12K |

---

**Inspection/Administration** **PY:** .13 **Comp. Rate($K/PY):** 133 **PoP:** 7/93-12/93

Assumes Eng (nat'l avg) oversight of entire activity: 1 eng, 1/4-time for 6 mos = .13 PY

---

**Procurement/Fabrication Material** **($K)**

N/A

---

**Installation/Assembly** **PY:** **Comp. Rate($K/PY):** **PoP:**

N/A

---

**Material: Installation/Assembly** **($K)**

N/A

---

**Contingency** **Total:** 30

| | | | |
|---|---|---|---|
| Technical: | 16 | Basis: | new design, some R&D required |
| Cost: | 6 | Basis: | in-house estimate, minimal experience |
| Schedule: | 8 | Basis: | delays completion of critical path item |

---

**Comments**

# Appendix VII: Hardware Implementation of the Level 1 Trigger

The basic muon trigger is a local 4 layer coincidence of the 4 layers in a superlayer. When this occurs a small amount of dead time is incurred in that muon chamber only. The local coincidence is formed in hardware which is attached to each wire. The remainder of the trigger uses hardware which is shared among all wires in a muon chamber. For a valid track, the trigger output consists of the corrected beam crossing time, the bend angle of the track, and the Phi and Z coordinates of the local track segment. The global portion of the muon trigger must correlate the information from all muon chambers.

The basic trigger group is 16 drift cells, 4 in each of the 4 layers. The maximum drift time is 300 ns. The maximum signal transit time is 50 ns (for a 6 M long wire).

The output of each cell (drift wire) is input to a pipelined TDC similar to the precision TDC but with less resolution. This must be logically independent from the precision TDC. The resolution is 4 ns, so it divides the beam crossing interval into 4 parts. The pipeline is as long as the drift time in the drift cells plus the transit time. There is an OR output which is the OR of all of the pipeline stages, and indicates that there is a hit somewhere in the pipeline. Note that there is one pipeline for each wire in the chamber.

These pipeline ORs are then ORed with adjacent cells (in the same layer and same basic group) to form a layer OR. This is ANDed with the 3 other layers to form the local 4 fold coincidence. To avoid the problem of track sharing between 2 adjacent trigger groups, the adjacent groups are paired to form overlapping coincidence trigger groups of 32 cells, 8 in each of the 4 layers. The corresponding layer ORs are ORed together before the 4 fold AND.

When the 4 fold coincidence is detected the trigger system enters the second phase, and deadtime begins. The processing hardware cannot accept another 4 fold coincidence until this trigger is completed. The TDC data leaving the pipeline is extended (by adding a step count since the coincidence detection) and stored in a register at the end of the pipeline. After waiting the drift time (plus the wire transit time), the entire pipeline has been searched for data. All detected hits are now converted to time and are stored in local registers. The pairs of wires which are linked at the far end are examined to produce the cell struck and the Z position (1 M resolution). This logic is most naturally part of the TDC IC, and is not shared, but is replicated for each wire pair.

The 4 fold coincidence also triggers the rest of the trigger logic, which is shared by all wires in the chamber.

This hit cell pattern is now examined. Of the 4096 possible patterns of 1 hit per layer, only about 200 correspond to straight tracks within +- 17 degrees from the normal (10 Gev muon cutoff). The 12 bit pattern (3 bits per layer) is used as the input to a lookup table. If the pattern does not match, the trigger is aborted, and the dead time (less than 450 ns) is over. The 4 Z coordinates are simultaneously checked for consistency. The outputs of this stage are the Phi and Z coordinates of the track candidate.

If the pattern is valid, the time is examined, and a new pattern is formed using the time data to reduce the cell size. This new pattern (11 bits, a relative pattern, independent of Phi) is also used to enter a lookup table. There are only about 300 valid patterns out of the

2048 available. The presence of a delta ray will typically transform a valid pattern into an invalid one. There are three outputs, the track angle (with respect to the chamber), instructions for calculating the beam crossing time (which time pairs to use, and their polarity), and the beam crossing time correction (due to the angle).

The next step is to subtract the selected pairs of time measurements, and add the correction. This results in up 6 beam crossing times. Using either combinatorial logic, or a sequence of lookup tables, the times are compared, and a majority logic decision made. The Z correction (flight time from interaction point) is included in this step, as is the non linear drift characteristics of the chamber gas.

Simultaneously with the beam crossing calculation the Phi coordinate is used to extract the bend angle from the observed chamber angle (again, lookup tables). This bend angle will be known to 1 degree rms or better.

The final result from this trigger system is the beam crossing time, the bend angle, and the Phi and Z coordinates of the track.

A preliminary estimate of the trigger processing time. The drift and transit times cannot be reduced. The processing time estimates are an upper limit.

| | |
|---|---|
| drift time + transit time | 350 ns |
| cell pattern table lookup | 100 ns |
| time pattern table lookup | 100 ns |
| beam crossing calculation | 100 ns |
| beam crossing selection | 100 ns |
| total time | 750 ns |

This simple trigger scheme is not very robust. It does have some inherent rejection of delta rays, during the table lookup of the time pattern, but not enough redundancy to do much more than reject a trigger accompanied by a delat ray. The trigger can be made more robust by adding another layer to the superlayer (for a total of 5 layers). If the trigger uses the middle superlayer (which consists of 2 4 layer chambers), 8 layers would be available for the beam crossing calculation.

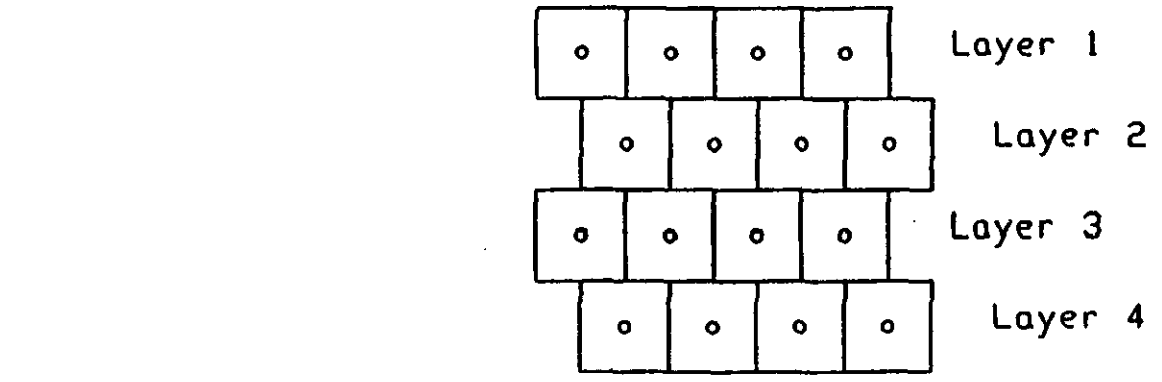


Basic Trigger Group

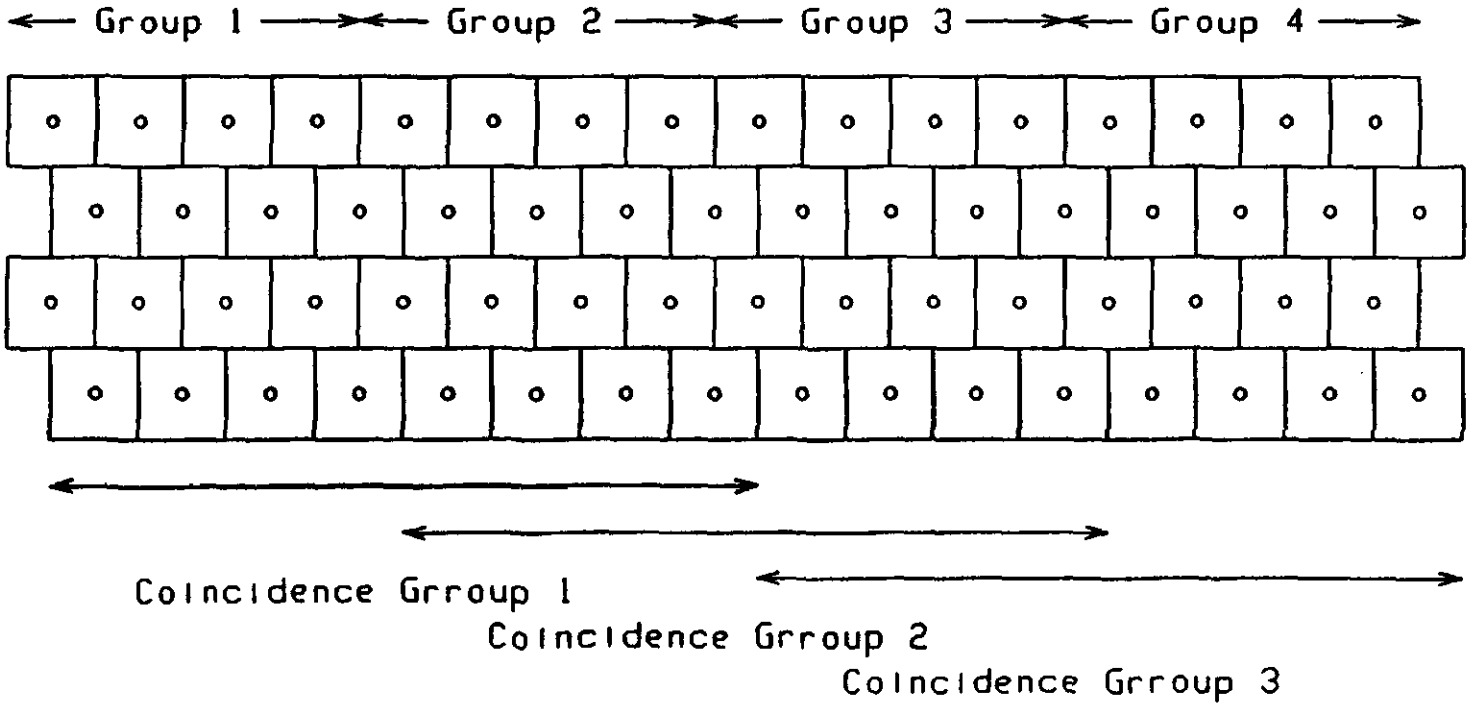


Fig.A.VII.1

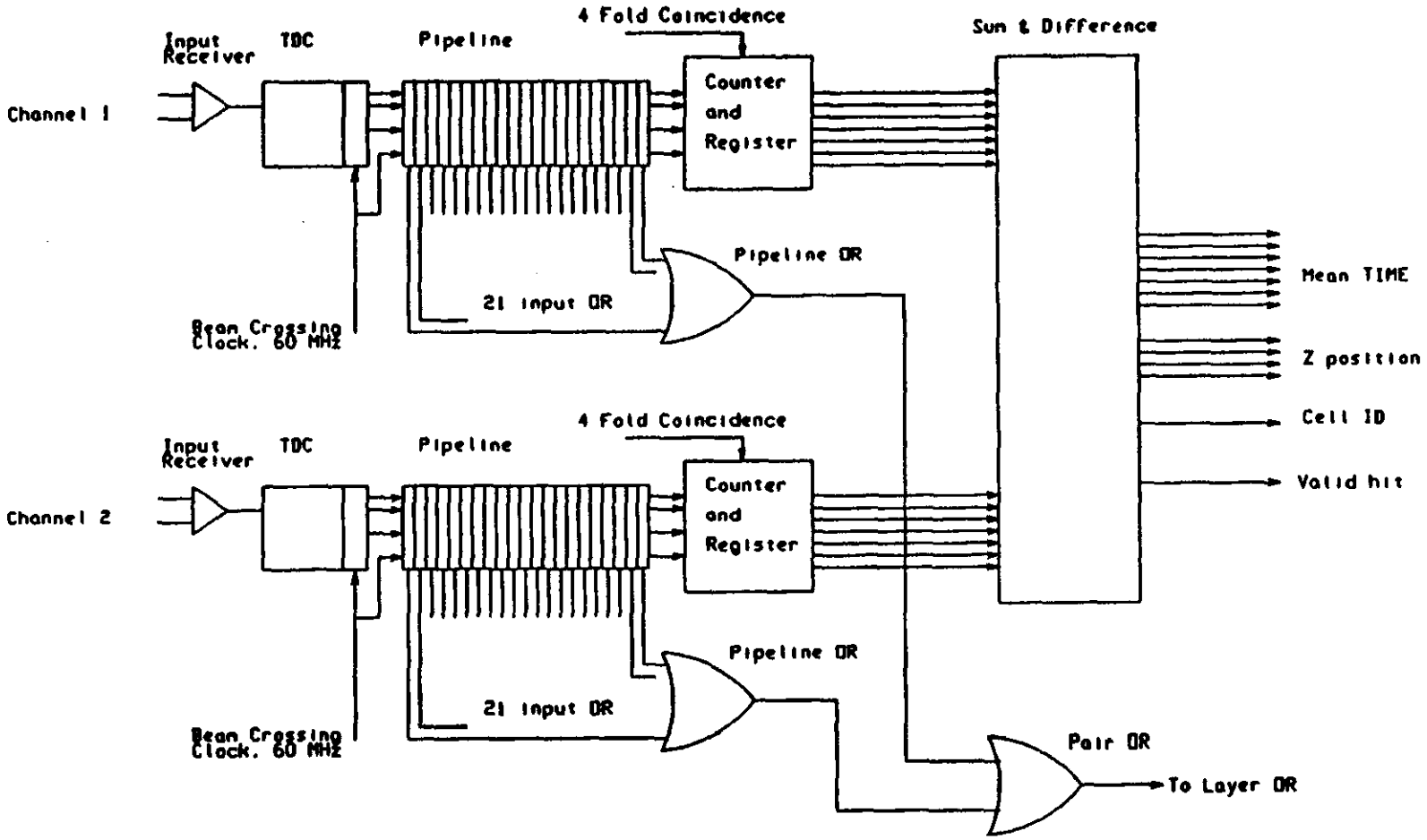


Muon Trigger TDC

Fig.A.VII.2

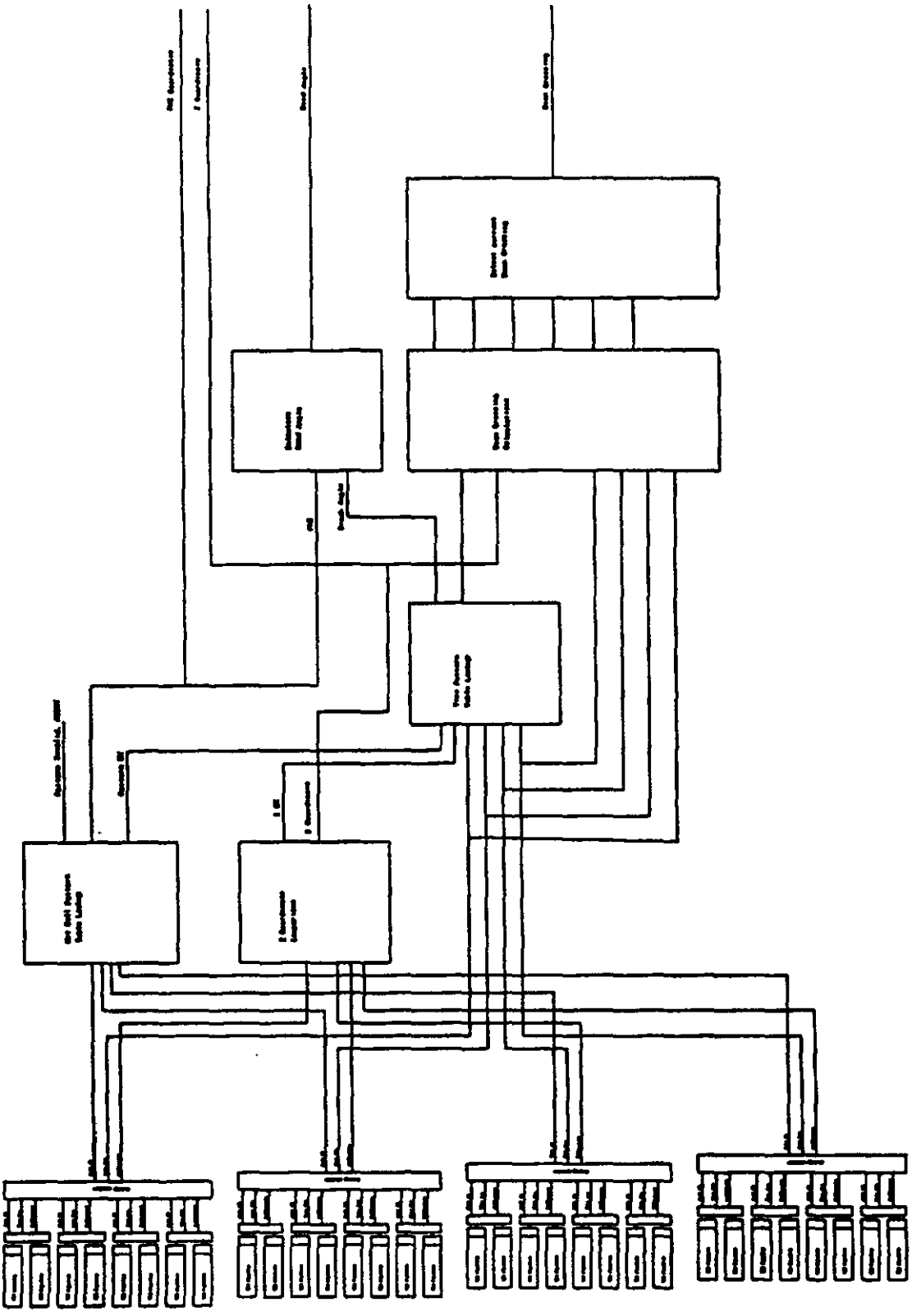

Fig.A.VII.3

Appendix VIII:

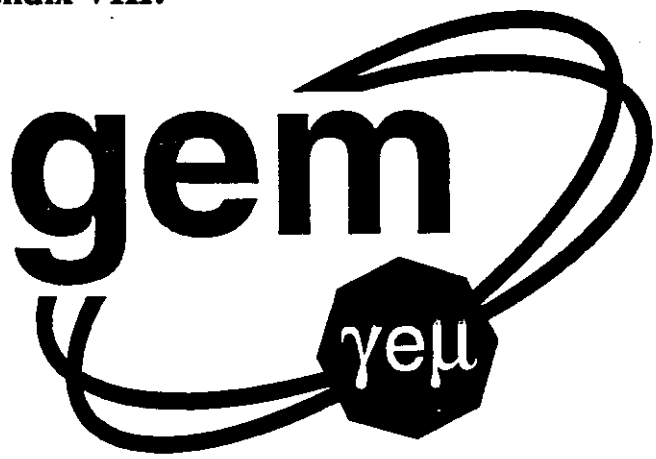


# Neutron Sensitivity of LSDT Chambers

A. Korytov, K. Linder, L.S. Osborne, F.E. Taylor
Massachusetts Institute of Technology

June 29, 1992

Abstract:

We have tested the sensitivity of the Limited Streamer Drift Tubes (LSDT) to neutrons using a $Cf^{252}$ spontaneous fission source. We obtain an "efficiency" for neutron detection of ~0.4% in either the direct beam from the source or from the moderated flux outside a 30 cm radius Boron loaded (5%) polyethylene can surrounding the source.

## I. Introduction

The hadronic showers in the calorimeters of the SSC detectors develop through successive collisions with the nuclei of the stopping material. Such collisions result in the production of spallation neutrons. The phenomenon is well known and gives rise, as an example, to the so-called $\pi/e$ energy ratio in calorimeters where the neutron component which is associated with a hadron shower is not efficiently detected[1]. This is a considerable effect ($\sim$ 5-10%). The spectrum of neutrons so produced has a distribution in energy characteristic of nuclear momenta and peaks in the 1 Mev region. One should expect that the number of neutrons so produced will be proportional to the energy dumped into the calorimeter by the hadronic showers and thus be dependent on the angle with respect to the beam; there will also be neutrons from small angle jets going into the up and downstream hardware adjacent to the detectors. By the same mechanism one might expect neutron sources from proton losses in the accelerator; for the time being we will not consider these.

The heavy nuclei in the calorimeter are not efficient in moderating the neutrons; however there are sufficient light nuclei and hydrogen in the other materials of the calorimeter e.g. G-10, scintillator, etc., that the neutrons are considerably moderated by the time they exit the calorimeter ( see Fig. 1).

It is important that we measure the sensitivity of the various detecting elements of the GEM detector to such neutron fluxes so that we may ascertain;

1.) the random counting rate and its contribution to chance coincidences for triggering purposes and its contribution to random "noise" in an event,

2.) the deterioration of the detector through excessive radiation and/or number of pulses,

3) what to do about it.

## II. Experimental Setup

Lacking a super collider at hand, we obtained a source, the spontaneous fissioner $Cf^{252}$, suitably stored in a Borated, polyethylene can. We also obtained from its author[3], the

calculated spectrum of neutrons and photons expected to emanate from the enclosing can. This spectrum was calculated for a 40 cm radius sphere of B-Poly with a Cf source; we have renormalized it to our 30 cm diameter can. This spectrum is plotted in Figure 1 along with a spectrum generated by L. Waters[2] which represents the neutron flux expected from just outside the GEM barrel calorimeter from one SSC event (actually, an average over 50 events) moderated by 10 cm of borated polyethylene placed outside the calorimeter. It is not surprising that the shape of the two spectra are similar; the sources are both "spallation" neutrons and the moderators are both Borated polyethylene plus the hydrogenic material present in the GEM calorimeter. Note also from the integral spectra (Fig. 1b) that the majority of neutrons are still "high" energy, > 20 kev. Measurements made outside the $Cf^{252}$ can should be a good representation of the expectations from the GEM environment. The normalizations are, of course, quite different, one being per SSC event, the other per Cf neutron.

The experimental setup for our measurements is shown in Figure 2. We could open the "cork" in the can and expose the LSDT tubes to the direct beam from the Cf source. We could also expose the tubes to the moderated beam by placing them at the side of the can.

In order to measure the "efficiency" for the tubes we require a measure of the neutron flux impinging on the tubes. We have two ways of doing this:

1.) We know the absolute neutron flux of the Cf source and can use the calculations of ref. 3 to get the flux outside the can,

2.) We have a neutron flux monitor, Nuclear Research Corporation Model NP-2,which, though it reads in Rem, it is provided with an energy response curve.

We had a NaI crystal operating into a LeCroy QVT to measure gamma ray spectra.

## III. Measurements

### A. Gamma Rays

Though the Boron-Poly case does indeed attenuate the neutrons it is ineffective with respect to gamma rays. Thus the calculations of reference 3 indicate that one gets 1.05 gammas outside the case for every Cf neutron; this gamma corresponds predominantly to the Boron capture gamma (0.42 Mev). Figure 3 shows the gamma spectrum observed outside the case with a comparison spectrum from $Na^{22}$ ( the 0.51 Mev annhilation gamma); the spectrum is consistent with the Compton spectrum from the Boron capture. In most of our measurements we protected the tubes from the gamma radiation with 5 cm of Pb.

B. Measurements in the direct Cf beam.

In all our measurements we used a 22 cm long, 2.2x2.2 cm cross section LSDT. Figure 4 shows an attenuation curve as a function of the thickness of interposed Pb with the tube over the open hole above the source. It shows an initial drop off characteristic of the Boron capture gamma followed by a drop off consistent with the scattering out cross section of neutrons on Pb.

We also varied the gas composition in the tube i.e. the relative amounts of Argon and Isobutane. If we assume that our pulses come from knock-ons on all the gas atoms with probability given by the tabulated cross sections then the Argon contributes little compared to the Isobutane ( 1 atom compared to 14 per molecule). The counting rate(CR) vs. gas composition is shown in Figure 5; the CR vs. % Isobutane shows a satisfactory linear dependence but the extrapolation to zero gives a finite contribution! This contribution is comparable with that from the gas. For the present we believe this may be due to some hydrogenic film or deposition due to lack of cleanliness in the original tube or from higher hydrocarbons in the flowing gas. Unfortunately, this effect was discovered after the Cf source was returned to its owner; the hypothesis has yet to be checked. Using the neutron monitor to measure the neutron flux we obtain an "efficiency" of $4.3 \times 10^{-3}$. If we consider the "efficiency" for the gas alone (see Fig. 5) we get $3.1 \times 10^{-3}$.

C. Measurements on the side

The tube was also placed on the side of the can where we have a moderated flux, again, behind 5 cm of Pb to partially eliminate the Boron capture gammas. In this case we obtain a gas efficiency of $4.0 \times 10^{-3}$. We have corrected the monitor flux measurement to eliminate the contribution from the thermalized component and the counting rate to eliminate the residual Boron capture gamma component. We also operated the tubes in the proportional region. Since the streamer mode will trigger on very small ionization such as might arise from the recoil of a heavy struck nucleus we wished to see if we were getting appreciable number of pulses from such sources. The "efficiency" in the proportional mode was only 20% less indicating this was not the main source of pulses.

D. Capture gammas

We have calculated the probability of counts from Al capture gammas in our tubes; this is small compared to the direct neutron counts, depending, as it does, on the product of two reaction probabilities. However, for a real array of chambers, where more mass is involved, the effect should be considered.

## IV. Conclusions

The experimental measurement of our sensitivity to neutrons is in relatively good agreement with expectations, namely, that we detect these neutrons from knock-ons in the gas.

In summary:

1.) The detection efficiency of our 1" cross section Aluminum tube is of the order of 0.4% per incident neutron.

2.) There remains a source of counts which is probably due to tube uncleanliness or deposition from the flowing gas. This remains to be checked.

3.) The calculated counting rates from the neutron fluxes expected outside the GEM calorimeter and in the barrel region coupled with these chamber efficiencies is accept-

able from either background counting or tube aging with the use of some moderator placed in or just out of the calorimeter.

4.) The use of polyethylene as a moderator should be followed by Pb to eliminate the capture gammas.

5.) The effects of capture gammas in the detectors themselves is not addressed by the above test since it depends more than linearly on the detector disposition.

## References


1.) R. Wigmans, NIM A259, 389 (1987); NIM A265, 273 (1988).

2.) D. M. Lee, R. E. Prael, L. Waters, GEM Note TN-92-91; L. Waters, private communication.

3.) E. Greenspan, private communication, Dept. of Nuclear Engineering, Univ. of California at Berkeley, Berekley, Calif.

## Figures

Fig. 1 Calculated neutron spectra for outside the GEM barrel calorimeter (ref.2) and for outside the can containing a $Cf^{252}$ source plotted; a) differentially, b) integrally.

Fig. 2 A schematic layout for the measurements made on LSDT tubes with the Cf source.

Fig. 3 The gamma ray spectrum observed outside the can(b) and a $Na^{22}$ refernce spectrum(a).

Fig. 4 The counting rate in the tube as a function of Pb thickness.

Fig. 5 Counting rate in the neutron beam as a function of gas composition-relative % of Argon and Isobutane.

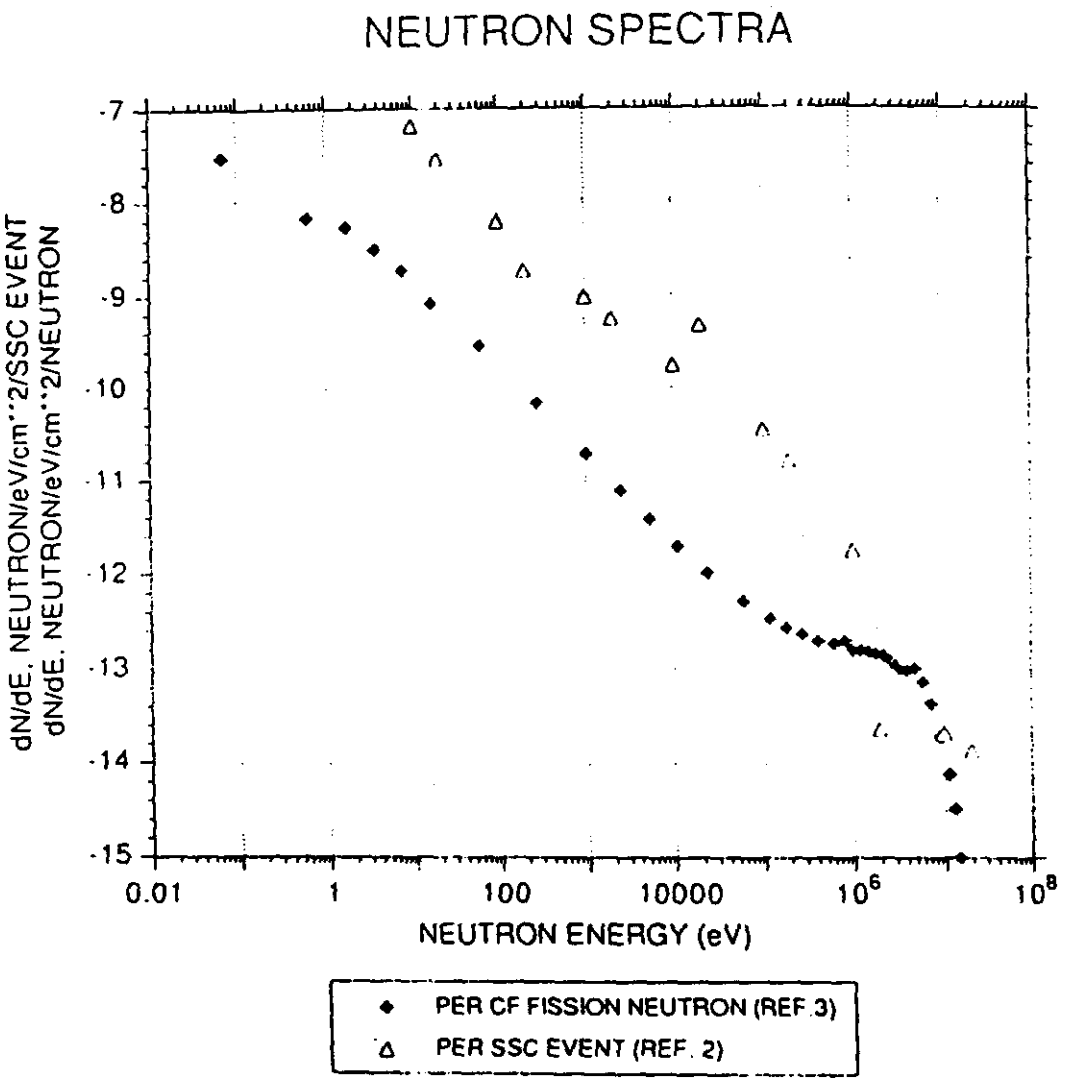


Fig. 1a Calculated neutron spectra for outside the GEM barrel calorimeter (ref.2) and for outside the can containing a $Cf^{252}$ source (ref 3).

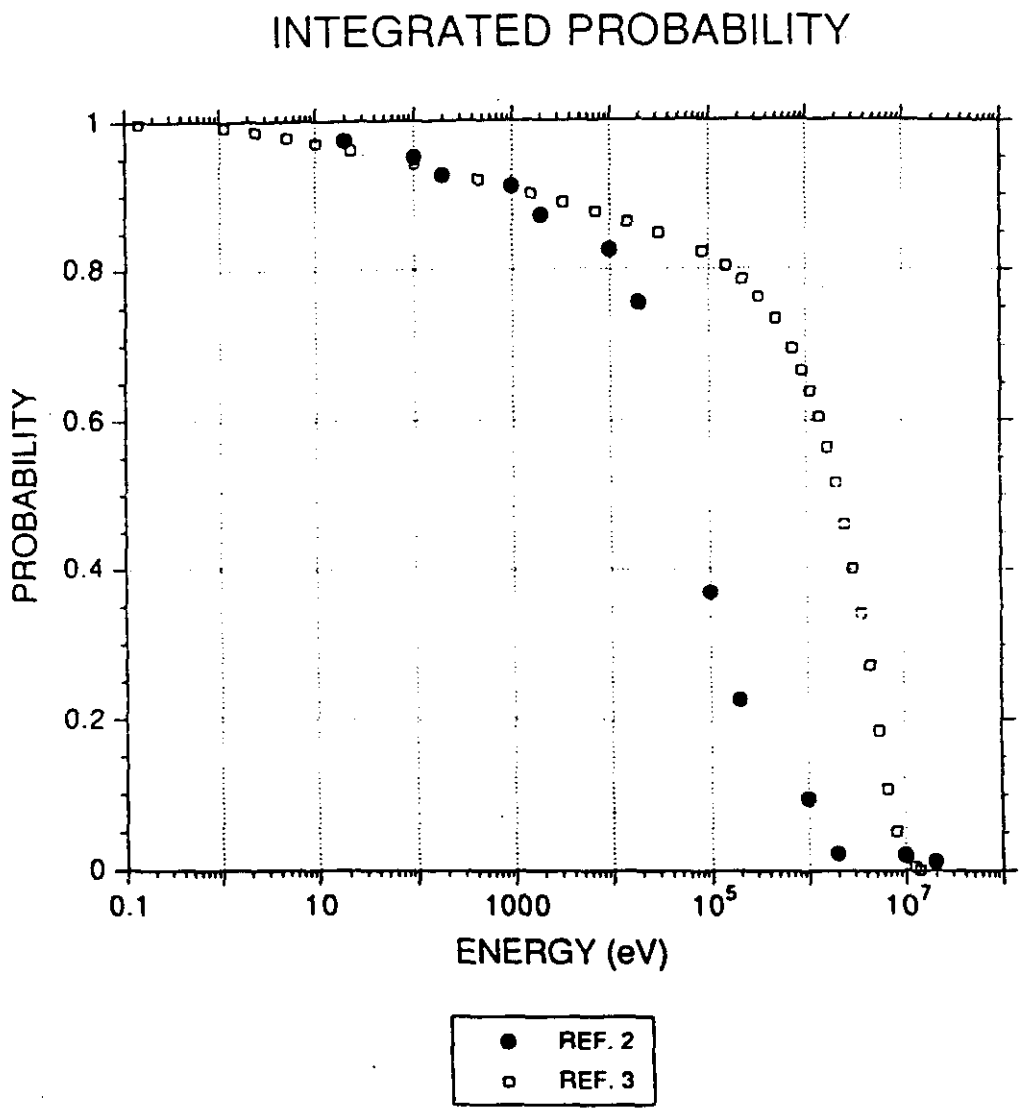


Fig. 1b The integral neutron spectra[2,3]. Note that these "moderated" fluxes are still primarily high energy neutrons.

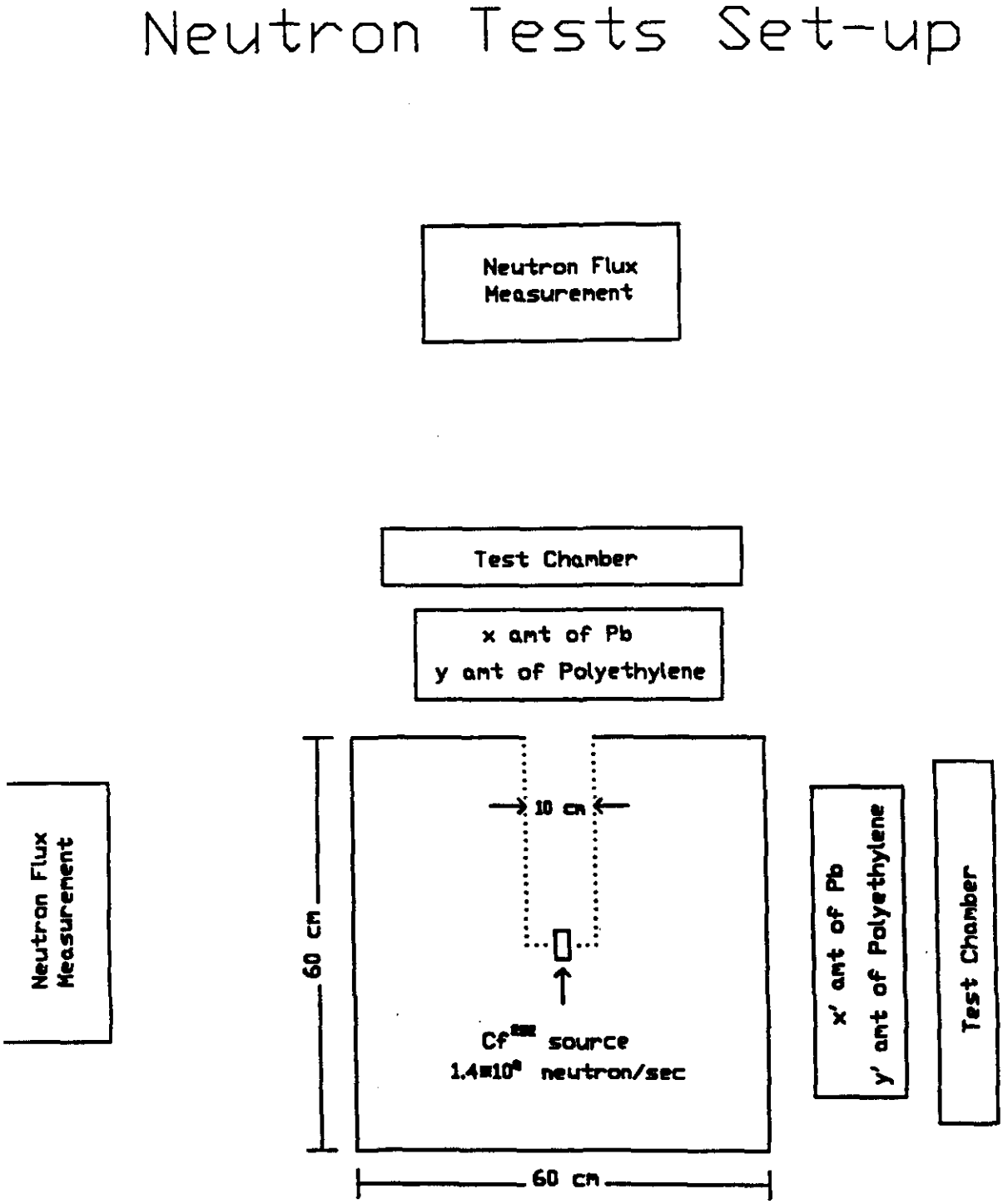


Fig. 2 A schematic layout for the measurements made on LSDT tubes with the Cf source.

a)

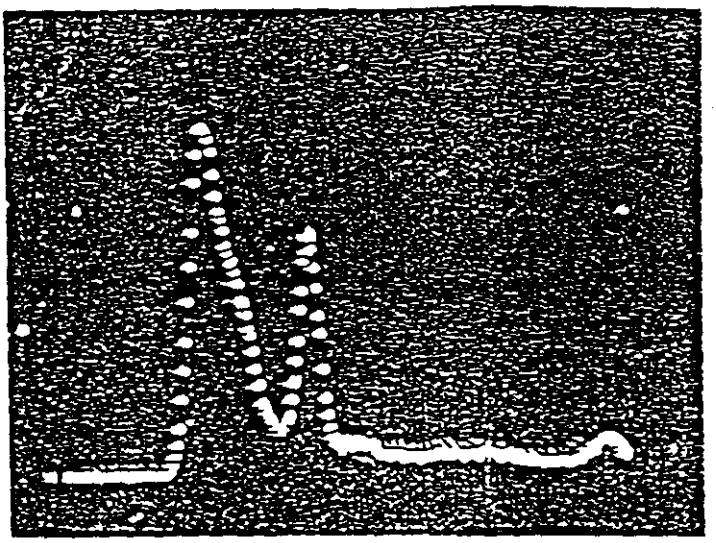

b)

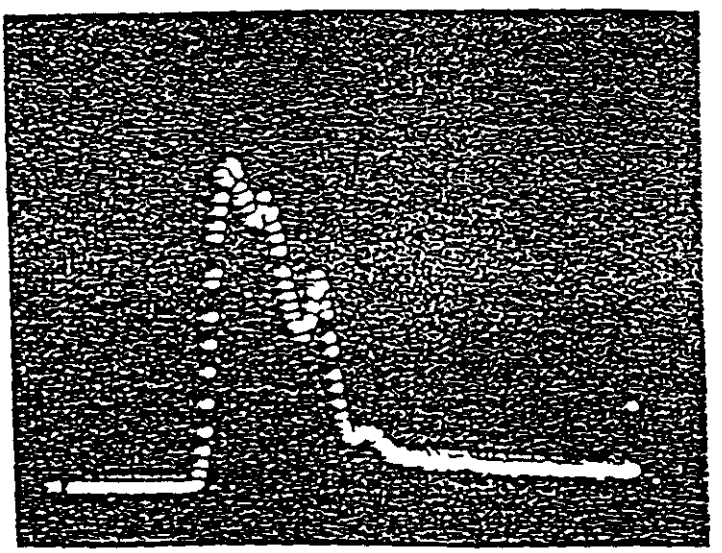

Fig. 3 The gamma ray spectrum observed outside the can(b) and a $Na^{22}$ reference spectrum(a).

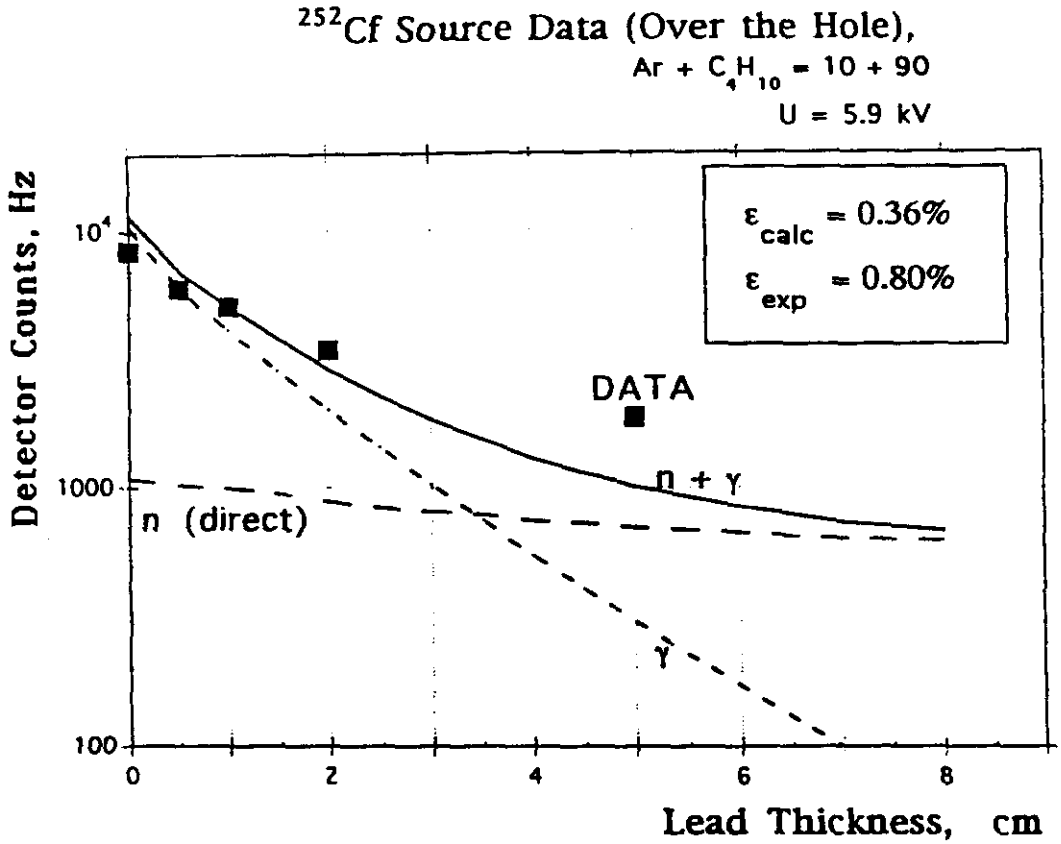


Fig. 4 The counting rate in the tube as a function of Pb thickness.

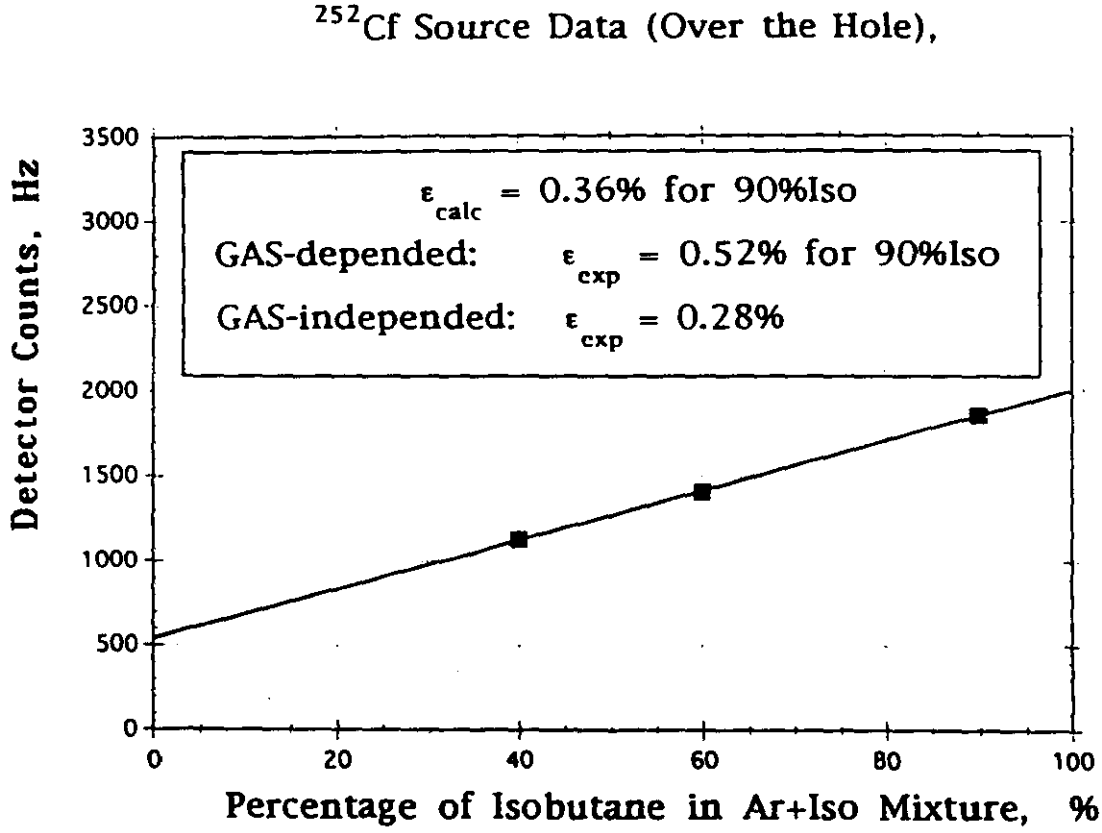


Fig. 5 Counting rate in the neutron beam as a function of gas composition-relative % of Argon and Isobutane.